Responses of herbivorous unicellular organisms to photosynthetic oxidative stress

Uzuka, Akihiro

Doctor of Philosophy

Department of Genetics
School of Life Science
SOKENDAI
(The Graduate University for Advanced Studies)

CONTENTS

Abstract.....1

Chapter 1. General introduction.....5

Figures.....10

Chapter 2. Toxicity of the photosynthetic prey to unicellular predators under illumination.....14

2.1. Introduction.....15

2.2. Materials and Methods.....17

2.2.1. Isolation of amoebae from a marsh.....17

2.2.2. Identification of amoebae by sequencing 18S rDNA.....17

2.2.3. Preparation of bacterial preys and quantification of photosynthetic pigments.....18

2.2.4. Cultivation and cryopreservation of amoebae.....19

2.2.5. Quantification of amoeba growth.....20

2.3. Results and discussion.....22

2.3.1. Preparation of herbivorous predators.....22

2.3.2. Preparation of bacterial preys and establishment of a system for co-cultivation of amoebae and bacterial preys.....24

2.3.3. Effect of predation of photosynthetic prey under illumination on amoeba growth.....26

2.4. Conclusions.....28

2.5. Figures.....30

Chapter 3. Responses of amoebae to the photosynthetic oxidative stress derived from photosynthetic preys.....34

3.1. Introduction.....35

3.2. Materials and Methods.....37

3.2.1. Preparation of RNA for transcriptome analyses.....37

3.2.2. RNA-seq analyses.....38

3.2.3. Comparison of mRNA level among amoebae or cultivation condition...39

3.2.4. GO enrichment analysis.....40

3.2.5. Quantification of phagocytic activity.....40

3.2.6. Quantification of digestion rate.....41

3.3. Results and discussion.....43

3.3.1. Transcriptome analyses to deduce the responses of three species of amoebae to phototoxicity of photosynthetic preys.....43

3.3.2. Decrease in phagocytic activity upon illumination in amoebae feeding on photosynthetic preys.....51

3.3.3. Acceleration of digestion of already-engulfed photosynthetic preys by amoebae upon illumination.....52

3.4. Conclusions.....54

3.5. Figures and tables.....56

Chapter 4. General discussion.....119

Figure.....128

Acknowledgements.....130

References.....133

Abstract

Chloroplasts in algae and plants were established by endosymbiotic events in which a cyanobacterium or unicellular eukaryotic alga was integrated into previously non-photosynthetic eukaryotes. It is believed that chloroplasts were established through multiple independent occurrences of predation, temporary retention, or permanent retention of a photosynthetic prey/endosymbiont by eukaryotic host cells. Photosynthesis in the chloroplast converts light to chemical energy and supports the life of algae and plants by providing photosynthetic products. However, photosystems also generate reactive oxygen species (ROS) which damage the cell. Thus, algae and plants have developed various mechanisms to reduce ROS generation, quench ROS, and repair biomolecules damaged by the oxidative stress, which are prerequisites for eukaryotic cells to perform photosynthesis. Although it has not been verified experimentally, when unicellular transparent organisms feed on phototrophs in the daytime, light reaches the photosystems of the engulfed prey. In addition, unregulated photosynthetic electron flow and excitation of chlorophyll molecules detached from photosystems probably occur during digestion, which in turn produce higher levels of ROS inside the predator cells. On the basis of this assumption, I attempted to understand whether feeding on phototrophs under illumination exposes unicellular predators to oxidative stress, and how the predators cope with the stress if they are exposed to oxidative stress. These studies will yield important insights that would help in gaining a better understanding of the evolutionary course in the establishment of photosynthetic eukaryotes as well as the impacts of photosynthesis in microbial communities in ecosystems.

I established a co-cultivation system of herbivorous predators and photosynthetic or non-photosynthetic bacterial prey to examine the effects of photosynthetic traits of prey on predators. I isolated three species of predatory amoebae

(*Naegleria* sp., *Acanthamoeba* sp., and *Vannella* sp.) that fed on both photosynthetic and non-photosynthetic bacterial prey from a sunny, shallow marsh. I chose the cyanobacterium *Synechococcus elongatus* as the prey. *S. elongatus* produced ample photosynthetic pigments (green prey) under normal conditions and had decreased photosynthetic pigments (pale prey) when reared under nitrogen-depleted conditions.

When the *Naegleria* sp. was illuminated (500 μE m^{-2} s^{-1}) when feeding on the green prey, about 30% of the amoeba cells burst but not the pale prey. Transcriptome analyses showed that genes related to oxidative stress responses, DNA repair, and carotenoid synthesis were upregulated upon illumination (200 μE m^{-2} s^{-1}) in all three amoeba species feeding on the green prey. Furthermore, most of the changes that occurred in the transcriptome upon illumination also occurred when the three amoeba species were treated with exogenous ROS. These results suggest that feeding on photosynthetic prey under illumination exposes the unicellular predators to photosynthetic oxidative stress.

The transcriptome analyses also indicated that genes related to phagocytosis, including actin and myosin, were downregulated upon illumination in the three amoeba species feeding on the green prey. Consistent with this result, a reduction of phagocytic activity upon illumination was observed in *Naegleria* sp. feeding on the green prey but not the pale prey. In contrast, digestion of already engulfed prey was accelerated upon illumination in *Naegleria* sp. feeding on the green prey. Both of these responses resulted in a reduction in the amount of photosynthetic prey in the amoeba cells, which may have caused a reduction of photosynthetic oxidative stress under light conditions.

In addition to these responses, several other changes, such as upregulation of genes that are related to respiration, genes encoding several monooxygenases, and genes

encoding components of v-ATPase, were observed in the transcriptome upon illumination in all the three amoeba species feeding on the green prey. These changes in transcriptome presumably resulted in the reduction of oxygen that is generated by photosystems of prey and a consequent reduction of ROS generation in amoeba cells. Acidification of phagosomes by v-ATPase is likely related to the acceleration of digestion of the green prey upon illumination. All the above mentioned changes in mRNA levels were shared by the three amoeba species which are distantly related to one another in terms of evolution, suggesting that these responses are probably prerequisites for unicellular amoebae to feed on phototrophs.

With regard to the low uptake and rapid digestion of the green prey by amoebae upon illumination, digestion/expulsion of facultative algal endosymbionts has been observed in other eukaryotes upon elevation of oxidative stress. Thus, reducing the number of phototrophs in the cells is probably a common strategy to reduce oxidative stress in eukaryotes accommodating/feeding on phototrophs. In contrast, it is known that algae and sessile land plants, which permanently possess chloroplasts, escape from high light and relocate their chloroplasts in the cells, respectively, to minimize light absorption under high light conditions. Such changes could possibly be prerequisites for eukaryotes to permanently possess chloroplasts.

Chapter 1. General introduction

The photosynthetic organelle chloroplast was established more than one billion years ago when a cyanobacterial ancestor was integrated into a previously non-photosynthetic eukaryotic host cell (called the primary endosymbiosis) (Rodriguez-Ezpeleta and Philippe 2006). The primitive eukaryotic alga established by the primary endosymbiotic event evolved into glaucophyte algae, red algae and green algae (evolved into land plants), all of which are grouped as Archaeplastida (Rodriguez-Ezpeleta *et al.* 2005) (Figure 1.1). The chloroplast established by the primary endosymbiotic event was further spread into other lineages of eukaryotes through secondary endosymbiotic events in which a primitive red or green algal cell was integrated into previously non-photosynthetic eukaryotes (Gould *et al.* 2008) (Figure 1.1). The secondary endosymbiotic events of red algae gave rise to chloroplasts in stramenopiles (diatoms, brown algae, etc.), haptophytes, cryptophytes, and dinoflagellates while the secondary endosymbiotic events of green algae gave rise to chloroplasts of euglenids and chlorarachniophytes (Keeling 2010) (Figure 1.1). In addition to chloroplasts, recent studies have shown that *Paulinella chromatophora* (phototrophic filose amoeba belongs to Rhizaria) possess photosynthetic organelle, which is called chromatophore, that was established more recently than chloroplasts by an independent primary endosymbiotic event of a cyanobacterium (Marin *et al.* 2005) (Figure 1.1). Thus, establishment of obligate photosynthetic organelles has occurred many times independently in distinct eukaryotic lineages.

Besides these photosynthetic organelles, there are several types of facultative endosymbiotic associations that support eukaryotic photosynthesis in nature. For example, the green amoeba (*Mayorella viridis*; Amoebozoa) and the green paramecium (*Paramecium bursaria*; Alveolata) accommodate facultative green alga (Figure 1.1).

Some species of dinoflagellates (e.g. *Gymnodinium acidotum*; Alveolata) and ciliates (e.g. *Mesodinium rubrum*; Alveolata) are known to engulf unicellular eukaryotic algae and retain their functional chloroplasts inside the cells to perform photosynthesis for days to weeks (Fields and Rhodes 1991; Lewitus *et al.* 1999; Johnson *et al.* 2006) (Figure 1.1). The phenomenon is called kleptoplasty. In the kleptoplasty, the engulfed algae are finally digested, and again these dinoflagellates and ciliates engulf new algal cells from environment.

Dinoflagellates also contain non-photosynthetic predatory species that feed on unicellular algae and photosynthetic species that possess chloroplasts of red algal or other algal secondary endosymbiotic origin (Stoecker 1999). In addition to dinoflagellates, non-photosynthetic predatory species feeding on algae have been found, which are evolutionally closely related to photosynthetic species that possess chloroplasts of secondary endosymbiotic origin in many other eukaryotic lineages. Based on above observations, it is generally believed that chloroplasts have been established through phagotrophic digestion of photosynthetic prey, temporary (kleptoplasty) and facultative retention of photosynthetic organisms in the cells, and ultimately obligate retention of photosynthetic endosymbionts by unicellular eukaryotes (Rodriguez-Ezpeleta and Philippe 2006) (Figure 1.2A).

Photosynthesis in the chloroplast converts light energy into chemical bond energy and provides photosynthetic products to eukaryotic host cells and further other non-photosynthetic eukaryotes in ecosystems (Ruban 2012). However, photosynthesis inevitably generates reactive oxygen species (ROS) as byproducts (Asada 2006; Szymanska and Strzalka 2010) which indiscriminately oxidize various types of biomolecules including DNA (called photosynthetic oxidative stress; Figure 1.2B). In

the photosystems, electrons extracted from water molecule by light energy flow through photosystems and are finally stored in NADPH as a reductant, which was consumed, for example, by fixation of carbon dioxide (Johnson 2016). In this process, leakage of electron to oxygen molecules also occur, which produces superoxide, hydrogen peroxide, and, hydroxyl radical. In addition, leakage of energy from photo-excited chlorophylls to oxygen molecule generates singlet oxygen (Asada 2006; Szymanska and Strzalka 2010). Thus, it is well known that algae and plants have developed various mechanisms to cope with the photosynthetic oxidative stresses during the course of evolution (Pospíšil 2012; Sharma *et al.* 2012). For examples, some unicellular algae exhibit negative phototaxis when they are exposed to high light (Witman 1993; Wakabayashi *et al.* 2011) (Figure 1.2B). In addition, algae and plant reduce levels of photosynthetic pigments to decrease light absorption by antenna pigments and hence energy flux to photosystems under high light condition (Smith *et al.* 1990) (Figure 1.2B). Photosystems themselves are constructed to dissipate excess light energy by discarding excess light energy as heat by non-photochemical quenching (NPQ) (Goss and Lepetit 2015), or by providing alternative routes to discard excess electron (Niyogi 2000) (Figure 1.2B). ROS that are generated by photosynthesis are deleted enzymatically or nonenzymatically by various types of antioxidants such as superoxide dismutase (SOD), ascorbate peroxidase (APX), catalase (CAT) and carotenoids, etc. (Ahmad *et al.* 2010) (Figure 1.2B).

In a similar manner to algae and plants, when unicellular transparent organisms feed on photosynthetic preys or accommodate photosynthetic facultative endosymbionts under light condition, photosystems of prey or endosymbionts absorb light energy and probably generate ROS inside the predator or host cells, which would damage the

predators or host cells (Figure 1.2B). In particular, unregulated photosynthetic electron transfer and/or excitation of unregulated photosynthetic pigment (such as chlorophyll) probably occur during the course of digestion in the daytime, which in turn produce higher levels of ROS. Thus, it is expected that unicellular herbivorous predators or host cells accommodating photosynthetic endosymbionts would have evolved mechanisms to cope with the photosynthetic oxidative stress. However, to date, there have been no studies about these issues. Understanding of the mechanisms should yield important insights into how organisms cope with the photosynthetic oxidative stresses in ecosystems, and also contribute to the understanding of evolution of photosynthetic endosymbiotic organelles.

As a first step, I decided to examine whether unicellular herbivorous predators are really exposed to the photosynthetic oxidative stress when they feed on algae under light condition, and, if that is the case, how herbivorous predators cope with the photosynthetic oxidative stress. To address these issues, I isolated three species of herbivorous amoebae from marsh and newly developed experimental system in which these amoebae and bacterial preys were co-cultured. Then, I examined behaviors of amoebae feeding on photosynthetic or non-photosynthetic preys under light or dark conditions. The results suggested that photosynthetic preys are phototoxic to amoebae by giving oxidative stress to them under light condition. In addition, it is suggested that similar mechanisms to cope with the photosynthetic oxidative stresses, such as reduction of uptake of photosynthetic preys while accelerating digestion of already engulfed preys upon illumination, developed in evolutionally distantly related herbivorous amoebae independently. Thus such mechanisms are probably required for unicellular and translucent predators to feed on photosynthetic preys in general.

Figures

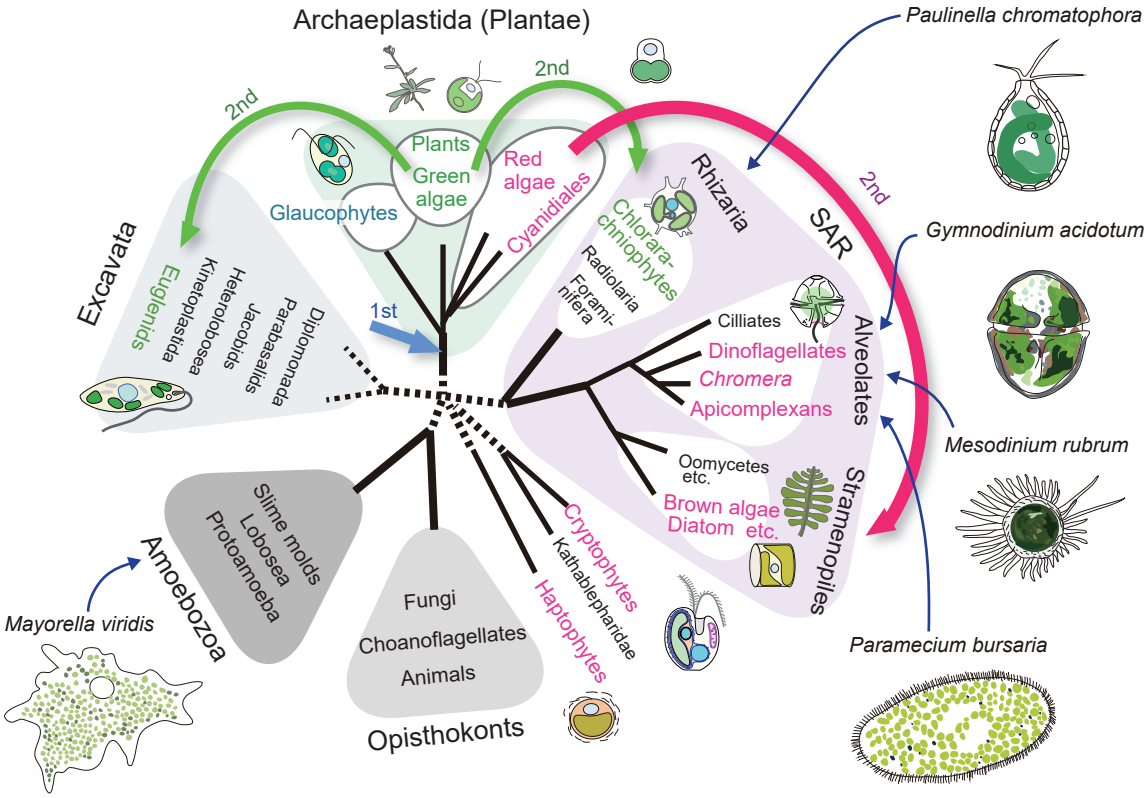

Figure 1.1. Phylogenic relationship in eukaryotes that possess obligate/facultative photosynthetic endosymbionts.

Eukaryotic algae in Archaeplastida (glaucophyte, red, and green algae) were established by the primary endosymbiotic event of a cyanobacterium into a previously nonphotosynthetic eukaryotic host (1st; light blue arrow). A primitive red or green algal cell was further integrated and spread into other lineages of eukaryotes through secondary endosymbiotic events (2nd; red arrow for red algal and green arrow for green algal secondary endosymbiotic events that eventually led to establishment of chloroplasts). Paulinella chromatophora, which belongs to Rhizaria, also possesses a photosynthetic organelle which was established more recently than chloroplasts in Archaeplastida through an independent primary endosymbiotic event of a cyanobacterium. Gymnodinium acidotum and Mesodinium rubrum, which belong to Alveolata, ingest free-living eukaryotic algae and utilize their chloroplasts as a photosynthetic apparatus temporally (kleptoplasty). Paramecium bursaria and Mayorella viridis, which belong to Alveolata and Amoebozoa, respectively, possess eukaryotic algal facultative endosymbionts in their cell (facultative endosymbiosis).

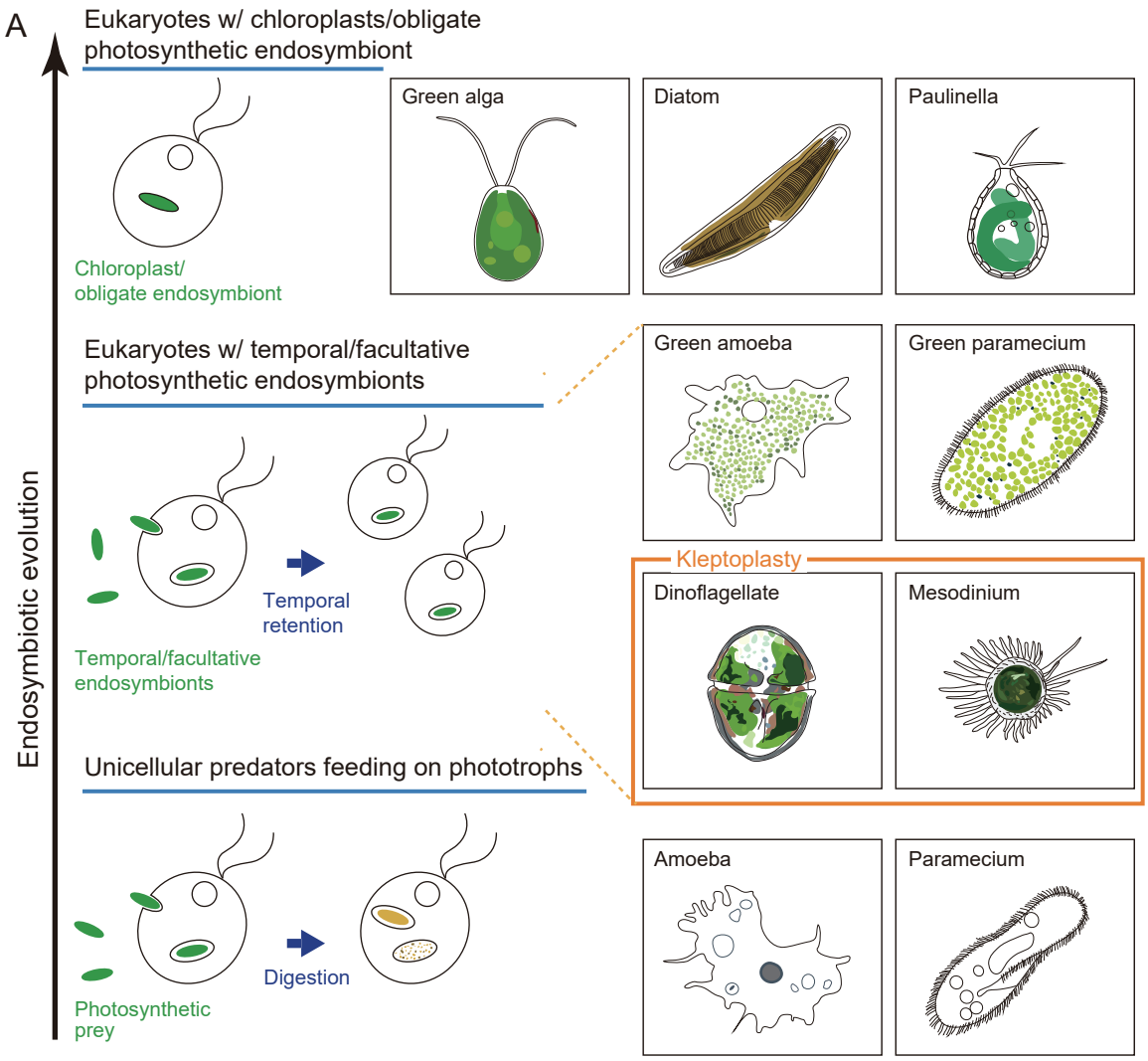
A
Eukaryotes w/ chloroplasts/obligate photosynthetic endosymbiont
Chloroplast/ obligate endosymbiont
Green alga
Diatom
Paulinella
Eukaryotes w/ temporal/facultative photosynthetic endosymbionts
Temporal retention
Temporal/facultative endosymbionts
Green amoeba
Green paramecium
Kleptoplasty
Dinoflagellate
Mesodinium
Unicellular predators feeding on phototrophs
Digestion
Photosynthetic prey
Amoeba
Paramecium
Endosymbiotic evolution

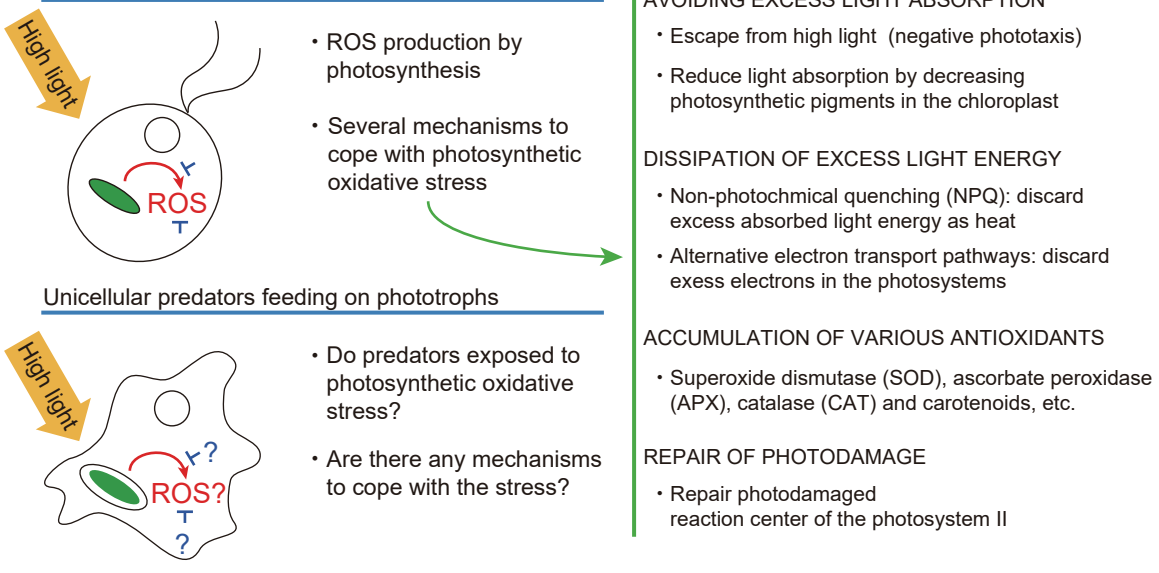
B
Photosynthetic eykaryotes
High light
ROS
• ROS production by photosynthesis
• Several mechanisms to cope with photosynthetic oxidative stress
Unicellular predators feeding on phototrophs
High light
ROS?
• Do predators exposed to photosynthetic oxidative stress?
• Are there any mechanisms to cope with the stress?
AVOIDING EXCESS LIGHT ABSORPTION
• Escape from high light (negative phototaxis)
• Reduce light absorption by decreasing photosynthetic pigments in the chloroplast
DISSIPATION OF EXCESS LIGHT ENERGY
• Non-photochmical quenching (NPQ): discard excess absorbed light energy as heat
• Alternative electron transport pathways: discard exess electrons in the photosystems
ACCUMULATION OF VARIOUS ANTIOXIDANTS
• Superoxide dismutase (SOD), ascorbate peroxidase (APX), catalase (CAT) and carotenoids, etc.
REPAIR OF PHOTODAMAGE
• Repair photodamaged reaction center of the photosystem II

Figure 1.2. Establishment of the chloroplast through endosymbiotic evolution and the mechanisms to cope with the photosynthetic oxidative stresses known in algae and plants.

(**A, left**) Chloroplast was established by an obligate endosymbiotic association between a previously nonphotosynthetic eukaryotic host and either a cyanobacterial (primary endosymbiosis) or eukaryotic (secondary endosymbiosis) photosynthetic endosymbiont. It is believed that the endosymbiotic association evolved in the order of the relationship between a unicellular eukaryotic predator and photosynthetic prey, that between a eukaryotic host and a temporal/facultative endosymbiont, and then that between a eukaryotic host and an obligate endosymbiont/chloroplast. (**A, right**) Examples of organisms that correspond to respective endosymbiotic stages are shown. Kleptoplasty is a phenomenon in which a host cell engulfs a eukaryotic alga, temporally retain the prey to perform photosynthesis, and then digest the alga. (**B**) Mechanisms to cope with the photosynthetic oxidative stress. Photosynthesis generates reactive oxygen species (ROS). It is well known that algae and plants have evolved several mechanisms to reduce the ROS production and cope with the photosynthetic oxidative stress. On the other hand, it has not been examined whether predators are also exposed to oxidative stress when they are feeding on photosynthetic prey under illumination.

Chapter 2. Toxicity of the photosynthetic prey to unicellular predators under illumination

2.1. Introduction

Plants and eukaryotic algae possess chloroplasts which were established either by primary or endosymbiotic events in which a cyanobacterial or eukaryotic algal ancestors, respectively, were integrated into previously non-photosynthetic eukaryotes (Rodriguez-Ezpeleta and Philippe 2006; Gould *et al.* 2008). It is believed that chloroplasts or other obligate photosynthetic organelles evolved through the predation and temporary retention of photosynthetic preys by eukaryotic unicellular predators and then facultative and obligate endosymbiotic associations with photosynthetic organisms by eukaryotic host cells (Rodriguez-Ezpeleta and Philippe 2006). The chloroplast benefits the eukaryotic host cells by performing photosynthesis and providing the products to the host cell (Johnson 2016). However, photosynthesis also inevitably generates reactive oxygen species (ROS) which damage the host cells (Asada 2006). Thus, algae and plants have developed various mechanisms to cope with the photosynthetic oxidative stresses (Pospíšil 2012; Sharma *et al.* 2012). In other words, development of such mechanisms to cope with the photosynthetic oxidative stresses was an important prerequisite for eukaryotic cells to acquire chloroplasts and photosynthetic abilities.

Although not examined and studied, when herbivorous unicellular predators feed on photosynthetic prey under illumination, engulfed preys are exposed to light, and thus would expose the predators to oxidative stress. If that is the case, herbivorous predators also probably have evolved some mechanisms to cope with the photosynthetic oxidative stresses that are derived from engulfed photosynthetic preys, in general. Such mechanisms must be required for predators to be herbivore, and will be the first step for

eukaryotes to develop facultative and then permanent endosymbiotic associations with photosynthetic organisms. The strategies that are required for predators and host cells accommodating photosynthetic organisms likely differ depending on the stages of endosymbiotic evolution (i.e. predation, temporary retention of prey, facultative and obligate endosymbiotic associations). Therefore, the understanding and the comparison of the mechanisms to cope with photosynthetic oxidative stress should give important insights into the understanding of endosymbiotic evolution and also understanding of how photosynthetic and non-photosynthetic organisms cope with the toxicity of photosynthesis in environments.

As a first step to address that issues, this study aimed to understand whether feeding on photosynthetic prey is really harmful to the unicellular herbivorous predators, and, if that is the case, how herbivorous predators cope with the photosynthetic oxidative stress in general. To this end, in this chapter, I established an experimental system in which herbivorous amoebae and photosynthetic and non-photosynthetic bacterial preys are co-cultured. Because it was unclear whether amoebae that had been kept in some stock centers were feeding on algae in nature and also the exact environment, in which they were sampled, were unclear; I newly isolated three species of evolutionally distantly related herbivorous amoebae from a sunny and shallow marsh where microalgae also thrived. In this chapter, I describe the detail of the co-cultivation system. In addition, by using the system, here I show that the photosynthetic prey exhibits phototoxicity to amoebae as expected.

2.2. Materials and Methods

2.2.1. Isolation of amoebae from a marsh

Water with microalgae was sampled from surface of mud and water plants at sunny points of Kodanuki marsh, Fujinomiya, Shizuoka, Japan (35˚ 22’ 8’’ N, 138˚ 33’ 5’’ E) in April 2013 (the water was at 20°C and approximately pH 7.0). For amoebae to proliferate dominantly, *Escherichia coli* DH-5α (this strain only used for this purpose in this study) was added to ~20 mL of the water samples as prey and incubated at 20˚C under illumination (20 μE m^{-2} s^{-1}) in 50 mL tubes for six days. As a result, several kinds of amoebae proliferated in some water samples. Then, for amoebae feeding on microalgae to proliferate dominantly, the mixture of amoebae was inoculated into BG11 liquid medium, an inorganic medium widely used for cultivation of fresh water cyanobacteria (Allen 1959; Allen 1968), supplemented with the cyanobacterium *Synechococcus elongatus* PCC 7942 at 20˚C under illumination for six days. To isolate respective amoeba cells, the culture was serially diluted with BG-11 medium supplemented with *S. elongatus* in 96-well plates and incubated at 20°C under illumination (20 μE m^{-2} s^{-1}). Amoebae proliferated in the most diluted wells were again subjected the dilution cloning as above. As a result, four kinds of amoebae (based on cellular shapes by microscopy) dominated in many wells independently but one grew very slowly. I isolated clones of the other three kinds of amoebae and used for further analyses.

2.2.2. Identification of amoebae by sequencing 18S rDNA

18S rRNA genes of the three species of amoebae were amplified by PCR with the primers MoonA and MoonB (Moon-van der Staay *et al.* 2000). The amplified products were cloned into the pGEM-T Easy Vector (Promega) and sequenced. In order to identify the linages to which three species of amoebae belong, the 18S rDNA sequences were subjected to BLASTN search against the nonredundant nucleotide sequence database of NCBI.

2.2.3. Preparation of bacterial preys and quantification of photosynthetic pigments

To prepare photosynthetic and non-photosynthetic prey, I chose the cyanobacterium *Synechococcus elongatus* PCC 7942, because *S. elongatus* (Green *S. elongatus*) reduces their photosynthetic pigments and thus reduces photosynthetic ability under a nitrogen-depleted condition (Pale *S. elongatus*). Green *S. elongatus* was cultured in BG-11 liquid medium in Erlenmeyer flasks at 30°C under continuous light (20 μE m^{-2} s^{-1}) on a rotary shaker. To prepare the pale *S. elongatus* in which chlorophyll *a* and phycobilin levels are reduced, *S. elongatus* was cultured under nitrogen-depleted condition as follows (Gorl *et al.* 1998). Exponentially growing cells in BG-11 was harvested by a centrifugation at 2,000 × *g* for 15 min and were washed twice with a nitrogen-depleted BG-11 (BG-11^{-N}). The washed cells were resuspended in 40 ml of BG-11^{-N} to give an OD_{750} of 0.25 and were cultured in 100 ml test tubes at 30°C under illumination (55 μE m^{-2} s^{-1}) with aeration (0.3 L ambient air/min) for a week.

E.coli hemA deletion mutant (Δ*hemA*) was obtained from the National BioResource Project. *E. coli* W3110 (the parental strain of Δ*hemA*) and Δ*hemA* was cultured in LB liquid medium in Erlenmeyer flasks at 37°C on a rotary shaker. For

Δ*hemA*, the medium was supplemented with 50 mM sodium pyruvate (Darie and Gunsalus 1994). To stain Δ*hemA* cells with chlorophyll *a*, 5×10^8 cells in 80 µl of distilled water were mixed with 400 µl of chlorophyll *a* dissolved in acetone (3.0 µl of 10 mg/ml chlorophyll *a* (034-21361, Wako, Japan) in DMSO was diluted with 397 µl of acetone). Then, acetone was evaporated in centrifugal evaporator (CVE-3100, EYELA) at 1,000 rpm at 30°C for 2 h. The stained cells in the residual water was washed with 1/16-strength BG-11 (BG-11^{-16}) and resuspended in BG-11^{-16}. As a negative control for the chlorophyll *a*-stained *E. coli,* acetone/DMSO-processed Δ*hemA* cells were prepared as above except that chlorophyll *a* was not added to the cells. Just before feeding the bacterial preys prepared as above to amoebae, preys were washed with BG-11^{-16} for three times.

To quantify chlorophyll *a* in bacterial preys, cell pellets from 1.0 ml of culture at OD_{600}=1.0 for *E. coli* or OD_{750}=1.0 for *S. elongatus* were resuspended in 1.0 ml of methanol. Cells were removed by centrifugation at 10,000 *g* for 10 min. A_{665} of the supernatant fractions were measured with a spectrophotometer and the chlorophyll *a* concentration was calculated (Grimme and Boardman 1972). To quantify phycocyanin in cyanobacterial preys, A_{678} and A_{620} of each culture were measured (Arnon *et al.* 1974) with a spectrophotometer (UV-2600, SHIMADZU) with integrating sphere attachment (ISR-2600PLUS, SHIMADZU).

2.2.4. Cultivation and cryopreservation of amoebae

To maintain amoeba cultures, amoebae were co-cultured cultured with *E. coli* W3110 as prey in BG-11^{-16} on a petri dish at 20°C under illumination (20 µE m^{-2} s^{-1}). For long-term preservation, three species of amoebae were suspended in BG-11

supplemented with 10% (v/v) DMSO (*Naegleria* sp. and *Acanthamoeba* sp.) or 10% (v/v) glycerol (*Vannella* sp.) and were preserved at -80°C.

To culture amoebae in a synthetic organic medium without bacterial prey, 1/10 strength Proteose Peptone Glucose Medium (PPG^{-10}; Culture Collection of Algae and Protozoa ; https://www.ccap.ac.uk/media/documents/PPG.pdf) was used. *Naegleria* sp. and *Acanthamoeba* sp. were able to grow in PPG^{-10} supplemented with 50 nM kanamycin at 20°C. Cysts of these amoebae were not formed in few days but the growth rates were very low compared with the cultures with bacterial prey.

In the co-cultivation system applied for the experiments, amoebae and bacterial preys were co-cultivated in petri dishes (35, 50, or 84.5 mm in diameter or 24-well plate). The dishes were put on a transparent acrylic box (35 cm × 25 cm × 5 cm) in which water at 20˚C was circulating. Dishes were illuminated from bottom by fluorescent lamps and aluminum foil was used to shade the dishes for the dark incubation. This system was constricted in a temperature controlled growth chamber. To perform the co-culture at 20˚C, the chamber was set at 20˚C. To perform the co-culture at 25˚C, the chamber was set at 31.5˚C (By the balance between 31.5˚C of the chamber and 20˚C of the circulating water, I confirmed that actual temperature of the medium in the dishes became 25˚C).

2.2.5. Quantification of amoeba growth

For preculture, *Naegleria* sp. and green *S. elongatus* (OD_{750}=0.4) or pale *S. elongatus* (OD_{750}=0.3) were co-cultured in 13ml of $BG\text{-}11^{-16}$ in 84.5 mm petri dishes at 25°C under dark for 2 h. To accelerate engulfment of bacterial prey by amoeba cells, *E. coli* W3110 (OD_{600}=0.1) was also added to respective co-culture. After the preculture, the

density of amoeba cells in the petri dish was determined based on pictures of bottom surface of the petri dish to which the amoebae adhered. Then a portion of the culture was transferred into 35 mm petri dishes to give a density of 400 amoeba cells/mm^2 and then incubated for 40 min under dark to let amoeba cells to adhere to the bottom of the petri dish. The liquid medium and free preys were removed by gentle rinse with BG-11^{-16}. Then, 3 ml of BG-11^{-16} supplemented with green (4.0×10^7 cells/dish) or pale (1.0×10^8 cells/dish) *S. elongatus* and *E. coli* (5.0×10^8 cells/dish) was added to amoebae in the petri dish. The co-cultures were incubated at 25°C under dark for 1 h and then (0 min) kept under dark or transferred to low light (200 μE m^{-2} s^{-1}) or high light (500 μE m^{-2} s^{-1}) condition. Micrographs were taken at 0, 90,180 and 360 min and the density of amoeba cells per area was determined.

2.3. Results and discussion

2.3.1. Preparation of herbivorous predators

The aim of this study is to examine whether feeding on photosynthetic preys under illumination give oxidative stress to unicellular predators (chapter 2), and if that is the case, how predators cope with the photosynthetic oxidative stress (chapter 3). To address these issues, I chose small amoebae as representatives of herbivorous unicellular organisms based on following reasons. Some amoebae are able to feed on both photosynthetic and non-photosynthetic organisms and thus it is feasible to compare behaviors of amoebae feeding on photosynthetic or non-photosynthetic preys. Amoebae do not swim and thus it is relatively easy to examine their behavior by microscopy. Amoebae are widespread in the eukaryotic phylogenetic tree and thus it is feasible to address the generality in the effects of photosynthetic traits of prey on predators.

In order to isolate amoebae that feed on both photosynthetic and non-photosynthetic preys, I collected water samples just above mud at Kodanuki marsh in Fujinomiya city, Japan (Figure 2.1A). The marsh was sunny and shallow and thus it was expected that habitats of the amoebae and the photosynthetic preys were overlapped. At first, only microalgae were predominantly found in the samples (Figure 2.1B) probably because the number of amoebae in the collected samples was relatively small in a natural condition. Then in order to increase the number of amoebae in the samples, *E. coli* was added to the samples as prey for amoebae. As a result, amoebae dominated in some samples six days after the addition of *E. coli*. Then, the mixture of amoebae was serially diluted with BG-11 medium (an autotrophic medium for fresh water algae) (Allen 1959; Allen 1968; Rippka *et al.* 1979) supplemented with the cyanobacterium

Synechococcus elongatus PCC 7942 as photosynthetic prey. As a result, three species of amoebae, which are relatively small in cell size (~20 μm), thus expected to be relatively small in the genome and transcriptome sizes, were isolated (Figure 2.1C). Given that these amoebae dominated by feeding on non-photosynthetic *E. coli* and then photosynthetic *S. elongatus*, these amoebae were expected to possess the ability to feed on both non-photosynthetic and photosynthetic preys. In addition, I confirmed that these amoebae engulfed and digested the microalgae in the original water samples. These traits of the three species of amoebae enabled further studies based on comparison of effects of photosynthetic and non-photosynthetic preys on amoebae.

In order to identify the phylogenetic positions of the isolated amoebae, 18S rDNA of each amoeba was sequenced. The sequence was subjected to BLASTN search against non-redundant database of NCBI. The BLASTN search showed that the isolated amoebae are most closely related to *Naegleria* spp. (Excavata), *Acanthamoeba* spp. (Amoebozoa) and *Vannella* spp. (Amoebozoa), respectively (Figure 2.1C). *Acanthamoeba* spp. and *Vannella* spp. belong to different orders of Amoebozoa and these two and *Naegleria* spp. belong to different eukaryotic supergroups. Thus, these three species are suitable to understand the generality among eukaryotes in mechanisms to cope with the photosynthetic oxidative stress that caused by photosynthetic preys.

These amoebae (hereafter, *Naegleria* sp., *Acanthamoeba* sp., and *Vannella* sp.) were cultivated in 16-times diluted BG-11 (BG-11^{-16}) medium with *E. coli* or *S. elongatus* as prey for short-term stock, and are cryopreserved in BG-11 supplemented with 10% DMSO (*Naegleria* sp. and *Acanthamoeba* sp.) or 10% glycerol (*Vannella* sp.) at -80˚C for long-term storage. In further experiments, the three species of amoebae were used for transcriptome analyses to gain insights into the generality in the responses

to the photosynthetic oxidative stress (chapter 3) and only *Naegleria* sp. were used for other assays (chapter 2 and 3), because growth of *Acanthamoeba* sp. and *Vannella* sp. became unstable after the long-term storage.

2.3.2. Preparation of bacterial preys and establishment of a system for co-cultivation of amoebae and bacterial preys

To examine effects of photosynthetic traits of prey on amoebae, comparison of behaviors of amoebae that feed on photosynthetic or non-photosynthetic prey was desired. In the process of amoeba isolation (2.3.1), *E. coli* as non-photosynthetic prey and *S. elongatus* as photosynthetic prey were used. However, the cell size, cellular composition, thickness of the cell wall, which affects the speed of digestion by amoebae, are largely different between *E. coli* and *S. elongatus.* In fact, amoebae digested *E. coli* faster than *S. elongatus* and, thus, growth of amoebae were much faster when *E. coli* was used as prey. Thus, even when differences in behavior of amoebae are detected between the culture with non-photosynthetic *E. coli* and that with photosynthetic *S. elongatus*, it is difficult to conclude that the differences are specifically resulted from the photosynthetic traits of *S. elongatus*. To overcome this issue, it is ideal to use the same species with or without photosynthetic ability as prey. To prepare *S. elongatus* prey with reduced photosynthetic capacity, I cultured *S. elongatus* under nitrogen-depleted condition, which is known to reduce the cellular levels of photosynthetic pigments, such as chlorophyll *a* and phycocyanin, and photosynthetic capacity in cyanobacteria (Gorl *et al.* 1998) (Figure 2.1D). In my cultivation condition, chlorophyll *a* and phycocyanin level in the cells under nitrogen-depleted condition (pale *S. elongatus*) became 8.6% and 2.6%, respectively, of cells under nitrogen-replete

condition (green *S. elongatus*) (Figure 2.1E). Consistent with these results, the level of autofluorescence of chlorophyll *a* almost disappeared in the pale *S. elongatus* (Figure 2.1F).

In addition to the green and pale *S. elongatus* preys, I prepared *E. coli* prey stained with chlorophyll *a* (Figure 2.1D) for the studies in the next chapter as the following reason. In normal cyanobacteria and chloroplasts, chlorophylls are bound to proteins so that the light energy absorbed by chlorophylls is properly transmitted to and through photosystems. However, once chlorophylls are detached from the proteins, the energy of free chlorophylls can be directly transferred to oxygen molecule, producing singlet oxygen (Triantaphylides and Havaux 2009; Krieger-Liszkay 2005). A heme, which is a complex of iron ion and porphyrin, is also known as generator of reactive oxygen species (Halliwell and Gutteridge 1990). To subtract the effects of the heme from chlorophyll *a*-stained *E. coli*, *E.coli hemA* deletion mutant (Δ*hemA*) was stained with chlorophyll *a* in acetone. For the negative control, *E.coli* Δ*hemA* was processed with acetone without chlorophyll *a* (Figure 2.1D, E, F).

Bacterial preys prepared as above and respective amoebae were co-cultured in the inorganic BG-11^{-16} liquid medium at 20˚C or 25˚C on a petri dish in a growth chamber. Dishes were illuminated by white fluorescent lamps from bottom and the dark condition was prepared by wrapping the dishes with an aluminum foil. To prevent elevation of temperature by the illumination, dishes were put on a transparent acrylic box in which cooled water at 20˚C was circulating (Figure 2.1G). All of the following experiments were performed by using this co-culturing system.

2.3.3. Effect of predation of photosynthetic prey under illumination on amoeba growth

Feeding on photosynthetic preys under illumination likely gives photosynthetic oxidative stress to unicellular predators because engulfed preys were exposed to light during digestion in transparent predator cells as discussed above. To test the possibility, growth rate of amoebae (*Naegleria* sp.) feeding on non-photosynthetic (pale *S. elongatus*) or photosynthetic prey (green *S. elongatus*) under dark, low light (200 μE m^{-2} s^{-1}) or high light condition (500 μE m^{-2} s^{-1}) was compared (Figure 2.2). The high light condition should naturally occur in shallow marsh. For example, the water surface around noon in summer is ~2,000 μE m^{-2} s^{-1}.

The amoeba cells were pre-cultured with respective preys under dark for 4 h and then kept under dark or transferred to low or high light condition. As a result, amoebae proliferated in a similar manner regardless of photosynthetic trait of the *S. elongatus* prey (green or pale) under dark or low light condition (Figure 2.2B, C). In contrast, under high light condition, the number of amoeba cells decreased by 28.3% in 90 min upon the exposure to high light only when amoebae fed on green *S. elongatus* (Figure 2.2A, D). Although I failed to take pictures or movies, burst of the amoeba cells were observed when the cells were feeding on the green prey under high light condition. Above results suggest that feeding on photosynthetic preys under illumination is harmful to amoebae.

The decrease in the number of amoeba cells feeding on the green prey from 0 min to 90 min under high light condition was only 28.3% and remaining amoebae grew slowly from 90 min to 360 min (Figure 2.2D). In my observation, the amoebae that were still alive tended to contain fewer green preys compared with amebae that burst

under high light condition. Thus, the toxicity of preys to respective amoeba cells probably varied depending on the number of photosynthetic preys that existed in the cells. In addition, the amoebae that were still alive under high light condition tended to contain fewer green preys compared with amebae under low light or dark condition. Thus, especially under high light condition, the major population of the amoeba cells feeding on green prey probably stopped or decreased the speed of uptake of preys to reduce the phototoxicity of the preys (this phenomenon was examined in chapter 3 in detail).

Under high light condition, the growth of amoebae feeding on the pale prey was delayed compared to that under dark or low light condition during the first 90 min (Figure 2.2D). This delay in the growth was likely caused by the incomplete removal of photosynthetic pigments in the pale prey (Figure 2.1E, F) or high light itself, which requires amoebae to cope with the residual phototoxicity of the pale preys or high light by delaying the cellular growth.

2.4. Conclusions

The aim of this chapter was to establish an experimental system to examine effects of photosynthetic preys on unicellular and transparent predators especially focusing on the phototoxicity related to photosynthesis. As predators, three species of amoebae, *Naegleria* sp., *Acanthamoeba* sp. and *Vannella* sp., were isolated from a sunny and shallow marsh. These three species of amoebae feed on both photosynthetic and non-photosynthetic preys, thus are suitable for studies based on comparison of effects of photosynthetic and non-photosynthetic preys on them. In addition, the three species are evolutionally distantly related and thus suitable to gain insights into the generality and diversity of the effects of photosynthesis of preys on predators.

As preys for amoebae, the green and the pale (reduced photosynthetic ability) *S. elongatus* preys were prepared. The preparation of these two types of preys facilitated the study in this chapter and contributed to show that photosynthetic preys are toxic to unicellular predators under light condition as predicted. In addition to these two bacterial preys, I prepared *E. coli* prey stained with or without chlorophyll *a*, which is known to produce singlet oxygen upon illumination (Krieger-Liszkay 2005), for studies in chapter 3.

By developing a system for co-cultivation of amoebae and bacterial preys, I found that feeding on photosynthetic preys under high light condition causes cell death of amoebae. However, I also found that majority of amoebae likely cope with the lethality by decreasing uptake of prey under high light condition (this point is further examined in chapter 3). Based on the results of this chapter, I conclude that photosynthetic prey is toxic to the amoebae under light condition. However, it is still

unclear whether the phototoxicity results from photosynthetic oxidative stress of the prey at this point. Thus, this issue was addressed in chapter 3.

2.5. Figures

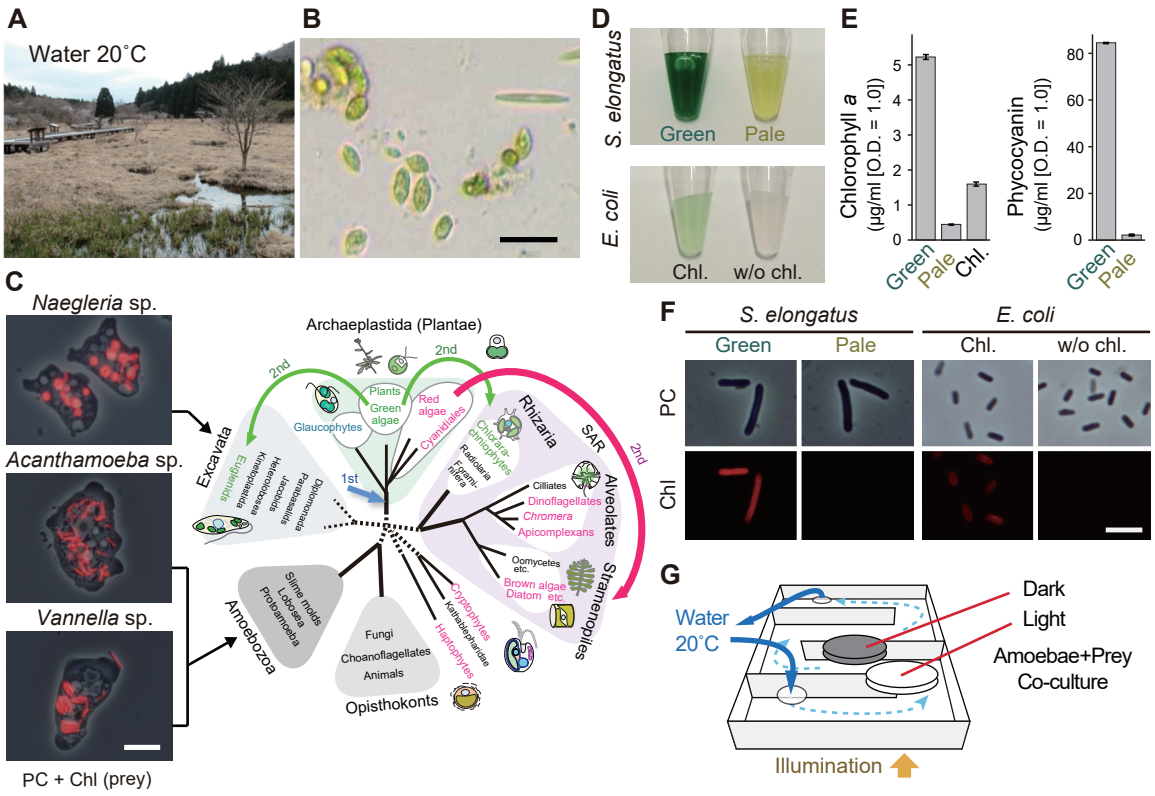

Figure 2.1. Habitat and isolation of amoebae, preparation of bacterial preys, and conditions for their co-cultivation.

(**A**) The Kodanuki marsh in Shizuoka Prefecture, Japan, where water and soil samples were collected to isolate amoebae. (**B**) A micrograph of the collected samples showing existence of unicellular algae. Scale bar = 50 μm. (**C**) After cultivation of the isolated samples with *E. coli* and then *S. elongatus*, three species of amoebae dominated in the sample and are isolated. PC, phase-contrast; Chl, chlorophyll *a* autofluorescence of *S. elongatus* prey engulfed by amoebae. Scale bar = 10 μm. (**D**) To compare effects of photosynthetic trait of prey on amoebae, normal (green) and pale *S. elongatus* were prepared. The pale prey was prepared by cultivating the cells under a nitrogen-depleted medium to reduce the levels of photosynthetic pigments (chlorophyll *a* and phycocyanin). To examine the effect of chlorophyll on amoebae, *E. coli* cells were incubated in acetone with (Chl) or without (w/o chl) chlorophyll *a*, dried, and then resuspended in an inorganic medium. (**E**) Chlorophyll *a* and phycocyanin levels of respective bacterial prey. The error bar represents the standard deviation of three biological replicates. (**F**) Micrographs of respective bacterial prey. Images of chlorophyll *a* autofluorescence were obtained in following conditions. Strength of excitation for *E. coli* was 66.7 times stronger than that

for *S. elongatus*. Exposure time was 1.0 sec for *E. coli* and 0.1 sec for *S. elongatus*. (**G**) The co-cultivation system. Amoebae and bacterial prey were co-cultivated in petri dishes. The dishes were put on a transparent box in which water at 20˚C was circulating. Dishes were illuminated from bottom of the box and aluminum foil was used to shade the dishes (dark condition).

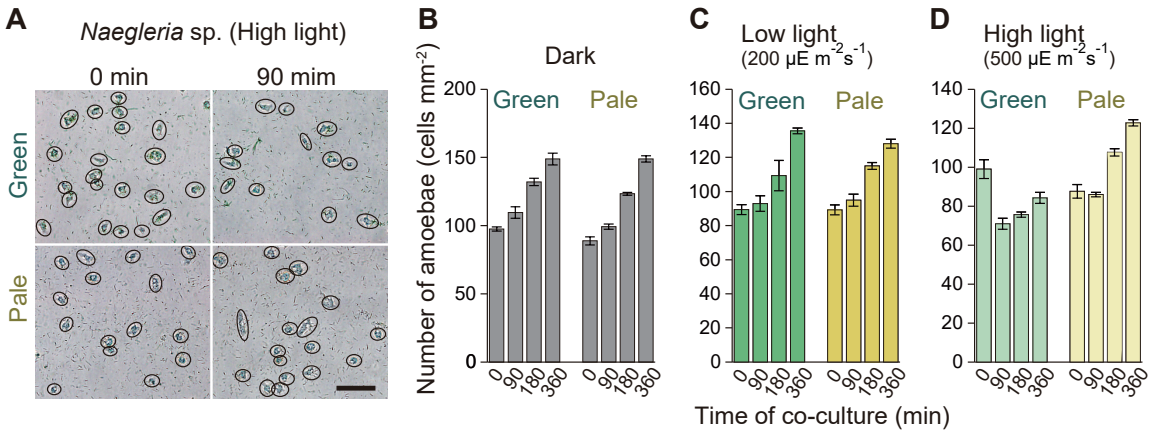

Figure 2.2. Effects of the photosynthetic trait and light on growth of amoebae. *Naegleria* sp. feeding on green or pale *S. elongatus* under dark condition was either cultivated under dark or transferred to low (200 µE m^{-2} s^{-1}) or high light condition (500 µE m^{-2} s^{-1}). (**A**) Microscopic images of amoebae and bacterial prey just before 0 min and 90 min after the transfer to the high light. Amoeba cells are indicated by circles. Scale bar = 100 µm. (**B**) Changes in number of amoeba cells in respective conditions. The error bar represents the standard deviation of three biological replicates.

Chapter 3. Responses of amoebae to the photosynthetic oxidative stress derived from photosynthetic preys

3.1. Introduction

Although algae and plants were inevitably exposed to the photosynthetic oxidative stresses in the daytime, they have developed several mechanisms to cope with the photosynthetic oxidative stresses (Pospíšil 2012; Sharma *et al.* 2012). These are, for example, mechanisms to avoid absorption of excess light energy by photosystems (Smith *et al.* 1990), to dissipate excess absorbed energy as heat (Goss and Lepetit 2015), and to enzymatically and nonenzymatically scavenge produced ROS (Ahmad *et al.* 2010). Development of such mechanisms was a prerequisite for algae and plants to possess chloroplasts (described in general introduction).

I hypothesized that herbivorous unicellular predators are also exposed to the photosynthetic oxidative stress when they feed on photosynthetic preys upon illumination and have evolved mechanisms to cope with the photosynthetic oxidative stress which are prerequisites for the predator to be herbivore. In chapter 2 (2.3.3), it was shown that feeding on photosynthetic prey (green *S. elongatus*) is really harmful to amoebae (*Naegleria* sp.) at least under high light condition (500 μE m^{-2} s^{-1}) (Figure 2.2A, D). The aim of this chapter is to understand whether the phototoxicity results from photosynthetic oxidative stresses and how herbivorous unicellular predators respond to the oxidative stresses from the prey. To deduce the oxidative stress and mechanisms to cope with the phototoxicity of prey, changes in transcriptome of three species of amoebae (*Naegleria* sp., Excavata; *Acanthamoeba* sp. and *Vannella* sp., Amoebozoa) upon illumination when they fed on photosynthetic prey (green *S. elongatus*) were examined. In addition, to assess whether changes in respective mRNA levels upon illumination were caused by photosynthetic traits of prey (e.g. ROS

generated by the prey) and/or light stimuli, experiments with non-photosynthetic prey (pale *S. elongatus*), *E. coli* stained with or without chlorophyll *a* (prepared in chapter 2), and experiments without bacterial prey and with exogenous ROS were also performed. Because a certain population of *Naegleria* sp. died under high light condition (500 μE m^{-2} s^{-1}), the transcriptome analyses were performed under low light condition (200 μE m^{-2} s^{-1}).

Based on the data of transcriptome analyses and subsequent GO enrichment analyses, here I show that amoebae are exposed to photosynthetic oxidative stresses that caused by photosynthetic preys. In addition, it is shown that the three species of amoebae exhibit similar changes in transcriptome in terms of functions and GO terms to cope with the photosynthetic oxidative stress. In addition, however, it is also shown that the responses of respective mRNAs and the responsive mechanism differ among the three species, suggesting that the similar responses to oxidative stresses were evolved independently in the three species of amoebae.

Further, I show that phagocytic activity is decreased while digestion rate of already engulfed photosynthetic prey is increased in *Naegleria* sp. upon illumination when they feed on photosynthetic preys. Based on the transcriptome data, it is suggested that these strategies to reduce ROS production by preys inside amoebae also operate in *Acanthamoeba* sp. and *Vannella* sp.

3.2. Materials and Methods

3.2.1. Preparation of RNA for transcriptome analyses

Three species of predatory amoebae, *Naegleria* sp., *Acanthamoeba* sp. and *Vannella* sp., were used as predators. Four types of bacteria, green and pale *S. elongatus*, *E. coli* with or without chlorophyll *a*-staining, were used as preys (2.2.3). The co-culture of respective amoebae and respective bacterial preys started at the following cellular density. Concentration of an amoeba was 9.8×10^5 cells per 50 mm petri dish (500 cells/mm^2). Concentration of a bacterial prey was 3.0×10^8 cells per 50 mm petri dish (300 cells/amoeba cell) for *S. elongatus* and 1.0×10^9 cells per 50 mm petri dish (1,200 cells/amoeba cell) for *E. coli*. The difference in the density of bacterial prey between *S. elongatus* and *E. coli* was because *E. coli* prey was consumed faster by amoebae than *S. elongatus* prey. The co-culture was incubated at 20˚C under dark for 12 h and then illuminated (200 μE m^{-2} s^{-1}) for 1 h. Total RNA of amoebae was extracted from cultures just before the illumination (dark) or 1 h after the illumination (light).

Naegleria sp. and *Acanthamoeba* sp. were also cultured without bacterial preys in the organic PPG^{-10} supplemented with 50 μg/ml kanamycin (2.2.4). The starting cell density was 9.8×10^5 cells per 50 mm petri dish (500 cells/mm^2) for respective amoebae. Amoebae were cultured under dark for 12 h and then illuminated (200 μE m^{-2} s^{-1}) for 1 h (w/o prey). For the Rose Bengal (RB) treatment condition, amoebae were cultured with 30 nM RB under dark for 12 h and then illuminated (200 μE m^{-2} s^{-1}) for 1 h. For the hydrogen peroxide (H_2O_2) treatment condition, amoebae were cultured without any treatment under dark for 12 h, and then treated with 4 μM H_2O_2 and further incubated under dark for 1 h. Total RNA of amoebae was extracted from cultures just after 12 h

dark incubation (dark) and just after the extra 1 h incubation (w/o prey under light, RB exposed to light, or H_2O_2 treatment under dark). The H_2O_2 and RB treatment were applied only for *Naegleria* sp. In each condition, one of two dishes was illuminated or treated with H_2O_2 after 12 h, and the other was harvested at 12 h for the negative control.

To extract total RNA of amoebae, liquid medium and bacterial preys were removed as much as possible by gentle wash with fresh medium, and then amoebae adhering to the bottom of the petri dish were suspended in 400 μl of TRIzol reagent (Invitrogen). The total RNA of amoebae was purified by RNeasy Mini Kit (QIAGEN).

3.2.2. RNA-seq analyses

mRNA of respective samples was purified from 0.6-14.8 μg of total RNA with Dynabeads Oligo(dT)25 (Life Technologies), according to Yoon and Brem (2010). The purified mRNA was fragmented into small pieces using divalent cations under elevated temperature. The cleaved RNA fragments were used for first strand cDNA synthesis using SuperScript II Reverse Transcriptase (Invitrogen) and random primers. Then, second strand cDNA synthesis was conducted. These cDNA fragments then went through an end repair process and ligation of adapters. These products were purified and enriched by PCR to create the final cDNA library. Sequencing was performed by HiSeq 2000 with 100 base-paired end format with TruSeq SBS kit v3 (Illumina). The reads were cleaned up using the cutadapt program version 1.81 (Tanabe 2011) by trimming low-quality ends (<QV30) and adapter sequences and by discarding reads shorter than 50 bp.

For *de novo* assembly of the RNA-seq reads, reads from *S. elongatus* and *E. coli* (W3110) prey were removed by Bowtie 2 ver. 2.1.0 (Langmead and Salzberg 2012). The *De novo* assembly of amoeba reads was conducted by Trinity ver. 2.0.6 (Grabherr *et al.* 2011) using DDBJ pipeline (Kaminuma *et al.* 2010; Nagasaki *et al.* 2013) with the paired-end mode with an option: --min_contig_length 200. When splicing variants of a gene were found, the longest transcript was selected as a representative mRNA sequence.

The assembled mRNA contigs were subjected to BLASTX and BLASTP (query mRNA sequence was translated to amino acid sequences using TransDecoder ver. 2.0.1, http://transdecoder.github.io) search against the Uniprot Swiss-Prot protein database. The results of BLAST searches were processed by Trinotate ver. 2.0.2 comprehensive annotation suite (https://trinotate.github.io) to obtain the annotation database of mRNA contigs.

3.2.3. Comparison of mRNA level among amoebae or cultivation condition

The RNA-seq reads were mapped to the *de novo* assembled mRNA contigs of respective amoeba species by Bowtie2 ver. 2.1.0 (Langmead and Salzberg 2012). The *De novo* assembly of amoeba reads was conducted by Trinity ver. 2.0.6 (Grabherr *et al.* 2011). The Fragments Per Kilobase of exon per Million mapped fragments (FPKM) values, which are expression levels of each contig normalized by length of transcripts and number of mapped reads, of respective contigs under respective conditions were estimated by RSEM ver. 1.2.21 (Li and Dewey 2011).

In Figure 3.1A, B, contigs in which FPKM was 0 in any culture condition were omitted from further analyses. In addition, contigs which exhibited FPKM value less

than 1.0 both under two comparative conditions (i.e. light versus dark; with or without H_2O_2 under dark) were also omitted from further analyses. In the comparison of FPKM values (two-fold change threshold) between light and dark condition with the green *S. elongatus* prey, contigs that exhibited two or more fold changes both in two independent cultures were evaluated as up- or downregulated contigs.

In Figure 3.1D, 3.3, 3.4, the FPKM values of respective contigs were compared only when the total of values of two comparative conditions were ≥20. Otherwise, the data were defied as not detected (ND).

3.2.4. GO enrichment analysis

The GO enrichment analysis was performed for RNA-seq reads of *Naegleria* sp., *Acanthamoeba* sp. and *Vannella* sp. feeding on the green *S. elongatus* prey under dark and light condition by using GOseq ver1.22.0 (Young *et al.* 2010). Differential expression genes were defined by using edgeR ver. 3.21.1 (Robinson *et al.* 2010) (*P*-value ≤ 0.05 based on the results of two independent cultures).

By using the GO terms in the Trinotate annotation, terms that are significantly (*P*-value ≤ 0.05) enriched in the up- and downregulated contigs upon illumination compared with the entire transcriptome were determined by GOseq.

To facilitate the interpretation of the results, some GO terms were further categorized manually into 10 categories: “actomyosin”, “carotene”, “cytoskeleton”, “DNA repair”, “motion”, “oxidative stress responses”, “phagocytosis”, “proteolysis”, “respiration”, and “v-ATPase”.

3.2.5. Quantification of phagocytic activity

Naegleria sp. (500 cells/mm^2) and *S. elongatus* (green or pale, 6.0×10^4 cells/mm^2) were co-cultured in 1 ml of BG-11^{-16} in 24-well culture plate (surface area of each well was 1.86 cm^2) at 25 ˚C for 4 h under dark. Then, the plate was kept under dark or transferred to light (200 μE m^{-2} s^{-1}) condition and further incubated for 1 h. Then fluorescent beads of 1.0 μm in diameter (Fluoresbrite® YG Microspheres 1.00μm; Polysciences, Inc.) was added to culture to give a concentration of 8,889 beads/mm^2 (2 beads in 15×15 μm^2), and further incubated for 1 h under dark or light. Then the number of beads engulfed amoeba cells during the 1 h incubation was determined.

3.2.6. Quantification of digestion rate

To label green and pale *S. elongatus* preys fluorescently, *S. elongatus* cells were suspended in 25 μg/ml of FM1-43 (Invitrogen) dissolved in BG-11^{-16} and incubated at room temperature under dark for 12 h. Then, the stained preys were washed with BG-11^{-16} for three times.

Naegleria sp. (1,500 cells/mm^2) and the preys stained with FM1-43 (9.0×10^4 cells/mm^2) were co-cultured in 1 ml of BG-11^{-16} in the 24-well culture plates at 25˚C for 4 h under dark for amoeba cells to engulf the prey stained with FM1-43. Then, the liquid medium was removed. Then, free bacterial preys were removed from the well as much as possible by gentle rinse with BG-11^{-16} and then *Naegleria* sp. adhering to the bottom of the plate was resuspended in 300 μl of BG-11^{-16}. Then, the samples were put on MAS-coated slide glass (#S9115, Matsunami) and incubated at 25˚C under dark for 30 min to immobilize amoebae not to newly engulf bacterial prey. Then (hour 0) the glass, on which amoebae were immobilized, were incubated in a sealed petri dish with a moist filter paper at 25˚C under dark or light (200 μE m^{-2} s^{-1}). Micrographs by

fluorescence microscopy were taken at 0, 1, 2.5 and 4 h. The fluorescence intensity of preys in amoeba cells (per area of amoeba cells) was determined with ImageJ software (Abramoff *et al.* 2004).

3.3. Results and discussion

3.3.1. Transcriptome analyses to deduce the responses of three species of amoebae to phototoxicity of photosynthetic preys

I previously demonstrated that feeding on photosynthetic preys is harmful to *Naegleria* sp. under high light condition (2.3.3). To understand how the unicellular herbivorous predators cope with the phototoxicity of photosynthetic preys, change in transcriptome in the three species of amoebae (*Naegleria* sp., *Acanthamoeba* sp., and *Vannella* sp.) feeding on photosynthetic prey upon illumination were examined. Because changes in mRNA levels of some genes are likely caused by the light stimulus regardless of photosynthetic trait of the prey, I also examined the changes in transcriptome upon illumination in all the three species of amoebae feeding on non-photosynthetic prey, or in *Naegleria* sp. and *Acanthamoeba* sp. which were grown in an organic medium without bacterial prey. In addition, to examine whether the changes in respective mRNA levels in amoeba feeding on the green *S. elongatus* are resulted from photosynthetic oxidative stress, I also examined the effect of chlorophyll *a*, exogenous H_2O_2, and a singlet oxygen producer (Rose Bengal) on the transcriptome.

To this end, I prepared four kinds of bacterial preys: green *S. elongatus* (green) as the photosynthetic prey, pale *S. elongatus* (pale) as the non-photosynthetic prey, *E. coli* with (chl.) or without (w/o chl.) chlorophyll *a*-staining (Figure 2.1D,E and G). To grow amoebae without any bacterial preys, 1/10 strength of Proteose Peptone Glucose Medium (PPG^{-10}) was used (w/o prey). To examine the effect of singlet oxygen, 30 nM Rose Bengal (RB), a hydrophilic photosensitive dye generating singlet oxygen upon illumination (Kochevar and Redmond 2000), was added to the culture without bacterial

preys. To examine the effect of H_2O_2, amoebae cells cultured without bacterial preys were treated with 4 μM H_2O_2 under dark condition.

Four conditions, Chl., w/o chl., RB and H_2O_2 were applied only for *Naegleria* sp.; and the condition w/o prey was applied only for *Naegleria* sp. and *Acanthamoeba* sp. because *Vannella* sp. without bacterial preys did not exhibit any growth in the organic medium. Respective amoebae were cultured at 20˚C under dark for 12 h in respective conditions and then illuminated (200 μE m^{-2} s^{-1}) except for H_2O_2 treatment. Samples for dark condition were harvested just after the 12 h dark incubation and samples for light condition were harvested 1 h after the onset of illumination. For H_2O_2 treatment, 4 μM H_2O_2 was added just after 12 h dark incubation and further incubated under dark for 1 h and then harvested. To assess the reproducibility, the transcriptome analysis of amoebae with the green prey was performed twice in three species of amoebae by using two independent cultures at different times. To determine the transcriptome, RNA-seq was performed by Illumina HiSeq 2000.

By *de novo* assembly of RNA-seq reads with Trinity ver. 2.0.6 (Grabherr *et al.* 2011), total 32,128 (*Naegleria* sp.), 44,273 (*Acanthamoeba* sp.) and 33,493 (*Vannella* sp.) mRNA contigs were obtained. As representative mRNA contigs for isoforms transcribed from the identical genomic loci, the longest contigs of *Naegleria* sp. (21,376 contigs), *Acanthamoeba* sp. (21,513 contigs) and *Vannella* sp. (19,779 contigs) were selected. By the prediction of protein-coding regions with TransDecoder ver. 2.0.1 (implemented in the Trinity software, http://transdecoder.github.io), total 19,827 (*Naegleria* sp.), 20,264 (*Acanthamoeba* sp.) and 15,302 (*Vannella* sp.) protein-coding mRNA contigs were obtained (Figure 3.1A). Respective contigs were annotated by

Trinotate ver. 2.0.2, an annotation protocol and toolkit for *de novo* assembled transcriptomes (available at http://trinotate.github.io).

First, up- and downregulated mRNA contigs upon illumination in amoebae feeding on the green prey were extracted based on comparison of FPKM values (>2-fold changes). Percentages of upregulated contigs (genes) were 2.6% (*Naegleria* sp.), 2.8% (*Acanthamoeba* sp.), and 1.3% (*Vannella* sp.), while percentages of downregulated genes were 2.8% (*Naegleria* sp.), 2.9% (*Acanthamoeba* sp.) and 0.8% (*Vannella* sp.) (Figure 3.1A). Then, contigs, whose magnitude in the change upon illumination was compromised in the amoebae feeding on the pale prey or amoebae cultured without prey were extracted as "specific to Green" (Figure 3.1A). Percentages of genes upregulated specific to green were 0.5% (*Naegleria* sp.), 0.9% (*Acanthamoeba* sp.), and 1.2% (*Vannella* sp.) while percentages of genes downregulated specific to green were 1.2% (*Naegleria* sp.), 1.3% (*Acanthamoeba* sp.) and 0.5% (*Vannella* sp.). These changes are probably directly caused the photosynthetic trait of the green prey. However, the changes upon illumination regardless of the photosynthetic trait of preys (i.e. pale or w/o prey) would also be important for amoebae to cope with the phototoxicity of the preys because some of these changes would be programmed upon illumination to cope with "expected" phototoxicity of the preys in nature.

To assess what extent of the changes in the transcriptome observed upon illumination in amoebae feeding on the green prey are related to possible photosynthetic oxidative stress, the results of the green prey were compared with the effect of chlorophyll-stained *E. coli* prey and exogenous RB and H_2O_2 treatments (Figure 3.1B; area-weighted Venn diagrams). 93.5% (477/510) and 85.3% (474/556) of contigs, which were up- and downregulated (>2-fold changes) upon illumination in amoeba feeding on

the green prey, were also up- and downregulated in amoebae feeding on chlorophyll-*a*-stained *E. coli* upon illumination, RB treatment upon illumination or H_2O_2 treatment under dark, respectively. These results suggest that most of the changes in mRNA levels in amoebae feeding on the green prey under illumination results from photosynthetic oxidative stress even though some changes were also observed upon illumination regardless of the photosynthetic trait of preys (Figure 3.1A) as above.

To assess what kinds of functions were upregulated or downregulated upon illumination in amoebae feeding on the green prey, GO enrichment analyses were performed by GO-seq (Young *et al.* 2010) (P-value $\leq$ 0.05). In the analyses, differentially expressed genes were defined based on the differential expression analyses using edgeR (Robinson *et al.* 2010) (P-value $\leq$ 0.05). To facilitate the interpretation of the results, some GO terms were further categorized manually into 10 categories: “actomyosin”, “carotene”, “cytoskeleton”, “DNA repair”, “motion”, “oxidative stress responses”, “phagocytosis”, “proteolysis”, “respiration”, and “v-ATPase” (Figure 3.1C).

GO terms that were categorized into oxidative stress responses, DNA repair, proteolysis, and respiration were enriched only or predominantly in upregulated contigs in all the three species of amoebae (Figure 3.1C; Table 3.1, *Naegleria* sp.; Table 3.3, *Acanthamoeba* sp.; Table 3.5, *Vannella* sp.). In addition, GO terms that were categorized into carotene and v-ATPase were enriched only in upregulated contigs in the two species of amoebae (Figure 3.1C; Table 3.1, *Naegleria* sp.; Table 3.3, *Acanthamoeba* sp.). On the other hand, GO terms that were categorized into actomyosin, motion, and phagocytosis were enriched only or predominantly in downregulated contigs in all the three species of amoebae (Figure 3.1C; Table 3.2, *Naegleria* sp.; Table 3.4,

Acanthamoeba sp.; Table 3.6, *Vannella* sp.). The upregulation of GO terms related to oxidative stress responses and DNA repair suggest that the amoebae were exposed to oxidative stress when they fed on the green prey under light condition. In addition, carotenoids are known to be very efficient physical and chemical quenchers of singlet oxygen, as well as potent scavengers of other reactive oxygen species (Bartley and Scolnik 1995; Ramel *et al.* 2012). The upregulation of GO terms related to respiration is likely to consume oxygen that is generated by photosystems in the green prey. The upregulation of proteolysis and v-ATPase, which acidify lysosomes and phagosomes, likely led to acceleration of digestion of the green prey under light condition (this was further examined below.). The downregulation of GO terms related to actomyosin, motion, and phagocytosis likely led to deceleration of uptake of the green prey under light condition, because actomyosin is known to be involved in phagocytosis (Buss *et al.* 2002; Smythe and Ayscough 2006; Chandrasekar *et al.* 2014; Mooren *et al.* 2012; Hasson 2003; Olazabal *et al.* 2002) (this was also further examined below.).

Then I further examined changes in respective mRNA levels that are related to GO terms discussed above based on the FPKM values (Figure 3.1D, 3.3, 3.4). With regard to oxidative stress responses, for example, there are four mRNAs encoding glutathione peroxidase in *Naegleria* sp. while only one mRNA in *Acanthamoeba* sp. and *Vannella* sp. (Figure 3.1D). This gene is known to reduce oxidative damage (Arthur 2000), and the mRNAs were reproducibly upregulated in all the three species of amoebae feeding on the green prey upon illumination (Figure 3.1D). The genes were also upregulated upon illumination in *Naegleria* sp. and *Acanthamoeba* sp. feeding on the pale prey and cultured without prey (Figure 3.1D). In contrast, the gene was not upregulated upon illumination in *Vannella* sp. feeding on the pale prey. Thus it is

suggested that the mechanism for the upregulation of glutathione peroxidase is different among species of amoebae (Figure 3.1D).

With regard to mRNAs that are related to proteolysis, I examined the changes in levels of mRNAs that are likely involved in digestion of preys in phagosomes [putative lysosomal/phagosomal proteases (Bohley and Seglen 1992; Miao *et al.* 2008; Guha and Padh 2008); Figure 3.3, Proteolysis]. However, there were marginal differences in respective mRNA levels between light and dark conditions in the three species of amoebae feeding on green prey. Only the exception was that cathepsin A mRNA in *Naegleria* sp., which were upregulated upon illumination when the cells fed on green or pale prey (Figure 3.3, Proteolysis). Thus, to interpret the upregulation of the GO term related to proteolysis, further analyses will be required.

With regard to mRNAs that are related to respiration and protein import from cytosol to mitochondria (TIC and TOC proteins), majority of mRNAs was upregulated upon illumination in the three species of amebae when they fed on the green prey (Figure 3.3, Respiration). For example, *COX15* is involved in heme A synthesis (Barros *et al.* 2001), and the mRNA (the three species of amoebae possess single copy of the gene) was upregulated upon illumination in the three species of amebae when they fed on the green prey (Figure 3.1D). *COX15* was also upregulated upon illumination in *Naegleria* sp. and *Acanthamoeba* sp. when they fed on the pale prey or cultured without prey, thus the upregulation is triggered by the light stimulus regardless of photosynthetic traits of preys (Figure 3.1D). In contrast, *COX15* was not upregulated upon illumination in *Vannella* sp. feeding the pale prey, thus the upregulation was specific to photosynthetic traits of the green prey for *Vannella* sp.

Prohibitin 1 and prohibitin 2 have been suggested to function as chaperone for respiratory chain proteins or a general structuring scaffold required for optimal mitochondrial morphology (Artal-Sanz and Tavernarakis 2009). TIM14 and TIM44 are components of the translocon that import mitochondrial protein precursors translated in the cytosol into mitochondria (Schiller *et al.* 2008; Mokranjac *et al.* 2003). These mRNAs were upregulated upon illumination in *Naegleria* sp. and *Acanthamoeba* sp. when they fed on the green prey while were not upregulated when they fed on the pale prey or are grown without prey (Figure 3.3, Respiration 2). These mRNAs were also upregulated by RB (plus illumination) and H_2O_2 (under dark) treatment in *Naegleria* sp., suggesting that the upregulation was triggered by oxidative stresses (Figure 3.4, Respiration 1, 2).

GO terms categorized into carotene were enriched in upregulated contigs of *Naegleria* sp. (Table 3.1) and *Acanthamoeba* sp. (Table 3.3). In addition, in the contig level, mRNA encoding zeaxanthin epoxidase, which is involved in carotenoid synthesis (DellaPenna and Pogson 2006), was upregulated upon illumination in *Vannella* sp. feeding on the green but not the pale prey (Figure 3.3, Carotenoid synthesis). However, the mRNAs encoding phytoene desaturase (Bartley *et al.* 1999) in *Naegleria* sp. and *Acanthamoeba* sp. and bifunctional lycopene cyclase/phytoene synthase (Velayos *et al.* 2000) in *Acanthamoeba* sp. that are related to carotenoid synthesis were also upregulated upon illumination regardless of photosynthetic traits of preys (i.e. upregulated also in pale and w/o prey). In addition, mRNA encoding phytoene desaturase was also upregulated by H_2O_2 treatment under dark condition in *Naegleria* sp. (Figure 3.4, Carotenoid synthesis). Thus, this gene is able to be upregulated by either the light stimulus or oxidative stress.

GO terms categorized into v-ATPase, which acidify lysosomes and phagosomes (Toei *et al.* 2010), were enriched in upregulated contigs of *Naegleria* sp. (Table 3.1). Additionally, a related GO term, endosomal lumen acidification (GO:0048388, *P*-value = 1.5E-02), was enriched in upregulated contigs of *Acanthamoeba* sp. (Table 3.3). In addition to *Naegleria* sp. and *Acanthamoeba* sp., mRNAs encoding v-ATPase subunits were also upregulated upon illumination when *Vannella* sp. fed on the green prey, although the differences in FPKM values between light and dark were relatively small compared to the other two species of amoebae (Figure 3.3, Vacuolar-type H^+-ATPase). The upregulation of these mRNAs upon illumination was specific to amoebae feeding on the green prey and was not observed in amoebae feeding on the pale prey or grown without prey. These results suggest that the upregulation of v-ATPase mRNAs was specific to photosynthetic traits of prey (Figure 3.4, Vacuolar-type H^+-ATPase).

With regard to myosin, type II myosin is known to be involved in phagocytosis (Olazabal *et al.* 2002; Chandrasekar *et al.* 2014). There are two mRNAs of type II myosin in *Naegleria* sp. and one in *Acanthamoeba* sp. and *Vannella* sp., and these mRNAs were downregulated upon illumination in the three species of amoebae when they fed on the green prey but not when they fed on the pale prey or were grown without prey (Figure 3.1D). In addition, type II myosin mRNA was downregulated in *Naegleria* sp. when they fed on *E. coli* stained with chlorophyll *a* or they were treated with RB (under illumination) or H_2O_2 (under dark) (Figure 3.1D). Thus, the dawn-regulation of type II myosin mRNA was specific to the photosynthetic oxidative stresses.

As observed above, although *Naegleria* sp., *Acanthamoeba* sp. and *Vannella* sp. are evolutionally distantly related, many functional categories of genes upregulated and downregulated upon illumination were shared by these three species of amoebae feeding on the photosynthetic prey. However, as observed at the contig level, the responses of respective mRNAs (repertories of genes in which mRNA level changed and mechanisms that trigger the change of mRNA level) were different among three species of amoebae. These results suggest that these responses were important for unicellular predators to feed on photosynthetic preys under illumination safely but developed in these amoebae independently during evolution.

In this study, ROS generation in amoeba cells upon illumination was not able to be directly quantified by using CellRox Green Reagent (Molecular Probes®), Amplex Red Reagent (Molecular Probes®) or Singlet Oxygen Sensor Green Reagent (Invitrogen). However, genes that are related to oxidative stress responses were upregulated upon illumination in the three species of amoebae feeding on the green prey, and the transcriptome changes were mostly shared with changes by effects of chlorophyll *a*, H_2O_2, and RB, indicating that these amoebae were exposed to oxidative stresses derived from engulfed photosynthetic preys under illumination.

3.3.2. Decrease in phagocytic activity upon illumination in amoebae feeding on photosynthetic preys

In chapter 2 (2.3.3), it was suggested that major population of ameba cells likely avoid the lethal photo toxicity of photosynthetic prey by reducing uptake of preys under high light condition (Figure 2.2D). In addition, genes encoding actin and several types of myosin, which are known to be involved in phagocytosis (Buss *et al.* 2002; Smythe and

Ayscough 2006; Chandrasekar *et al.* 2014; Mooren *et al.* 2012; Hasson 2003; Olazabal *et al.* 2002), were downregulated upon illumination in the three species of amoebae feeding on the green prey (Figure 3.3, Myosin and actin). In a similar manner, phagocytosis-related GO terms were enriched in the downregulated genes in three species of amoebae (Table 3.2, 3.4 and 3.6). These results suggest that the phagocytic activity is downregulated when amoebae feeding on photosynthetic preys under illumination.

In order to test this possibility, effect of the photosynthetic trait of prey on phagocytic activity on *Naegleria* sp. was examined. To this end, *Naegleria* sp. was pre-cultivated with green or pale *S. elongatus* prey under dark for 4 h and then further incubated under dark or light (200 μE m^{-2} s^{-1}) for 1 h. Then, fluorescent latex beads of 1 μm in diameter were added to the culture to quantify phagocytic activity. In this assay, *Naegleria* sp. cell was able to engulf up to four beads within 1 h (Figure 3.2A). When amoebae fed on the pale prey, number of beads that were engulfed by amoeba cells was similar between light and dark condition (Figure 3.2B). In contrast, when amoebae fed on the green prey, the number of beads that were engulfed by amoeba cells under light condition was significantly lower than that under dark condition. These results suggest that the phagocytic activity decreases when amoebae fed on photosynthetic preys under illumination as expected.

3.3.3. Acceleration of digestion of already-engulfed photosynthetic preys by amoebae upon illumination

Above results suggest that phagocytic activity decreases upon illumination in amoebae feeding on the green prey probably to reduce the number of preys inside amoeba cells to

reduce photosynthetic oxidative stresses. The results also raised the question of how amoebae cope with photosynthetic preys that have been engulfed under dark condition but have not been digested when they are illuminated.

In order to address this issue, digestion rate of engulfed prey was compared in *Naegleria* sp. feeding on the green or pale prey under light or dark condition. To quantify the digestion, plasma membrane of intact green and pale *S. elongatus* preys were stained with the fluorescent dye, FM1-43. *Naegleria* sp. cells were pre-cultured under dark with the green or pale preys stained with FM1-43 for amoebae to engulf the prey. Then, the co-culture was immobilized onto the MAS-coated slide glass to inhibit amoebae to newly engulf bacterial prey and the glass was further incubated under dark or light (200 μE m^{-2} s^{-1}) condition for 4 h. Decrease in fluorescence intensity of the prey in amoeba cells during the incubation were quantified as the digestion rate.

The digestion rate was larger under light than dark condition regardless of photosynthetic trait of the prey. However, the difference in the digestion speed between light and dark when feeding on the green prey [1.92 = light (-2.73 intensity/h) / dark (-1.42 intensity/h)] was much larger than that when feeding on the pale prey [1.17 = light (-5.28 intensity/h) / dark (-4.49 intensity/h)] (Figure 3.2C-F). These results suggest that amoebae digest already-engulfed photosynthetic preys faster under light than dark probably to decrease photosynthetic oxidative stress.

3.4. Conclusions

The aim of this chapter was to examine whether the phototoxicity of photosynthetic preys to amoebae results from photosynthetic oxidative stress and how amoebae responses to the phototoxicity. To this end, I examined changes in transcriptome of the three species of amoebae (*Naegleria* sp., *Acanthamoeba* sp. and *Vannella* sp.) upon illumination when they fed on photosynthetic or non-photosynthetic prey. When amoebae feeding on photosynthetic preys were illuminated, genes related to oxidative stress responses and DNA repair were upregulated in respective amoebae. These results suggest that the phototoxicity of the prey is at least results from photosynthetic oxidative stress, although I failed to directly detect generation of ROS in amoeba cells. The detection of ROS is often difficult because half-life of ROS are very short and their reactivities are immediately transmitted other molecules (e.g. lipids) sequentially.

In chapter 2, toxicity of feeding on photosynthetic preys under illumination was shown experimentally only in *Naegleria* sp. However, up-regulation of genes related to oxidative stress responses and DNA repair in all the three species of amoebae examined suggest that the amoebae suffer from phototoxicity of photosynthetic prey in general regardless of their phylogenetic positions.

GO terms that are related to phagocytosis were enriched in downregulated contigs and genes encoding actin and several types of myosin proteins were downregulated upon illumination in all the three species of amoebae. As suggested by these results, decrease in phagocytic activity upon illumination was demonstrated in *Naegleria* sp. when they fed on the photosynthetic prey (Figure 3.2A, B). In contrast, digestion of already-engulfed photosynthetic prey was accelerated upon illumination in

Naegleria sp. (Figure 3.2C, D). Both the reduction in phagocytic uptake of the prey and acceleration of digestion result in decrease in the amount of photosynthetic preys inside amoeba cell thus should reduce ROS production in amoeba cells.

The transcriptome analyses also showed that genes that are related to respiration, carotenoid synthesis, v-ATPase were upregulated. The upregulation of respiration likely contributes to reduce the level of oxygen that is generated by photosystems of prey. Carotenoid likely dissipates ROS, and v-ATPase likely accelerates acidification of phagosomes to digest prey rapidly. With regard to these assumptions, further studies will be required.

Finally, the transcriptome analyses in this chapter suggested that the three species of amoebae possess very similar strategies to cope with the photosynthetic oxidative stress in terms of functions and GO terms. However, the mode of responses of respective mRNA differs among the three species, suggesting that the mechanisms were evolved independently in the three species of amoebae. Thus it is suggested that these responses are probably prerequisites for predators to feed on photosynthetic preys.

3.5. Figures and tables

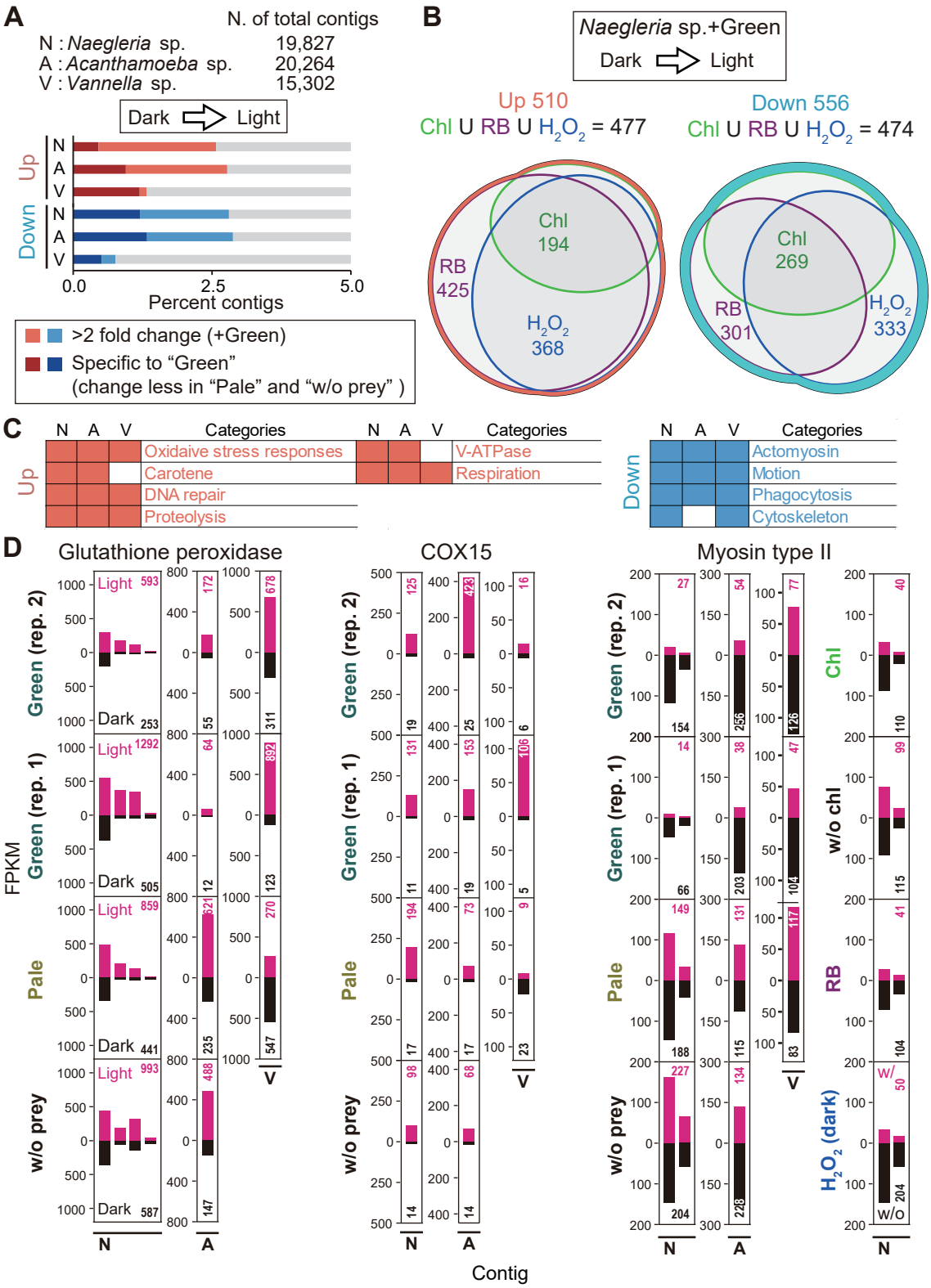

Figure 3.1. Effects of the photosynthetic traits of bacterial prey, chlorophyll, and ROS on transcriptome in *Naegleria* sp., *Acanthamoeba* sp. and *Vannella* sp.

Respective amoebae were co-cultured with green or pale *S. elongatus* or *E. coli* with or

without chlorophyll *a* under dark for 12 h (dark) and then transferred to light (200 μE m^{-2} s^{-1}) for 1 h (light). To examine the effect of illumination that is independent of prey, respective amoebae were cultured in an organic growth medium without prey under dark for 12 h (dark) and then transferred to light for 1 h (light). To examine the effects of singlet oxygen, *Naegleria* sp. was cultured without prey and with 30 nM Rose Bengal (RB), which produces singlet oxygen by illumination, under dark for 12 h (dark) was transferred to light for 1 h (light). To examine the effects of H_2O_2, *Naegleria* sp. was cultured without prey for 12 h under dark (w/o H_2O_2) was treated with 4 μM H_2O_2 under dark for 1 h (w/ H_2O_2). (**A**) Percentage of up (orange and red bars)/down-regulated (light blue and blue bars) (≥2-fold change) contigs when amoebae feeding on green under dark were transferred to light. The results shown are based on reproduction in two independent cultures and experiments (rep. 1 and rep. 2). Red and blue bars indicate contigs in which the magnitude of change upon illumination was compromised (the light/dark ration became less than the half of amoebae feeding on green *S. elongatus*) when feeding on pale *S. elongatus* or without prey. Thus changes in these contigs upon illumination are caused by photosynthetic trait of the green *S. elongatus* prey. (**B**) Area-weighted Venn diagrams showing the contents of up/down-regulated contigs in *Naegleria* sp. feeding on green *S. elongatus* upon illumination that are shared with Chl., RB, or H_2O_2. Up/down-regulation in RB indicates contigs that exhibited ≥2-fold change in the presence of 30 nM RB only under illumination. Up/down-regulation in H_2O_2 indicates contigs that exhibited ≥2-fold change under dark when 4 μM H_2O_2 was added to the culture. Up/down-regulation in Chl. indicates contigs that exhibited ≥2-fold change upon illumination when feeding on *E. coli* with chlorophyll *a* but exhibited a compromised change (the light/dark ration became less than the half of amoebae feeding on *E. coli* with chlorophyll) when feeding on *E. coli* without chlorophyll. (**C**) Categorization of GO terms into 10 categories based on their functions. Categories highlighted in orange are enriched in upregulated contigs while categories highlighted in light blue are enriched in downregulated contigs when amoebae feeding on green prey were illuminated. Colored squares beside each category indicate enrichment of GO terms of respective categories in respective amoeba species. N, *Naegleria* sp.; A, *Acanthamoeba* sp.; V, *Vannella* sp. (**D**) Examples of changes in the mRNA levels (FPKM values) of contigs. Each bar

corresponds to one contig. For example, there are five contigs encoding glutathione peroxidase in *Naegleria* sp. (N) while only one contig in *Acanthamoeba* sp. (A) and *Vannella* sp. (V). Numbers in the graph indicates total of the FPKM values in respective conditions.

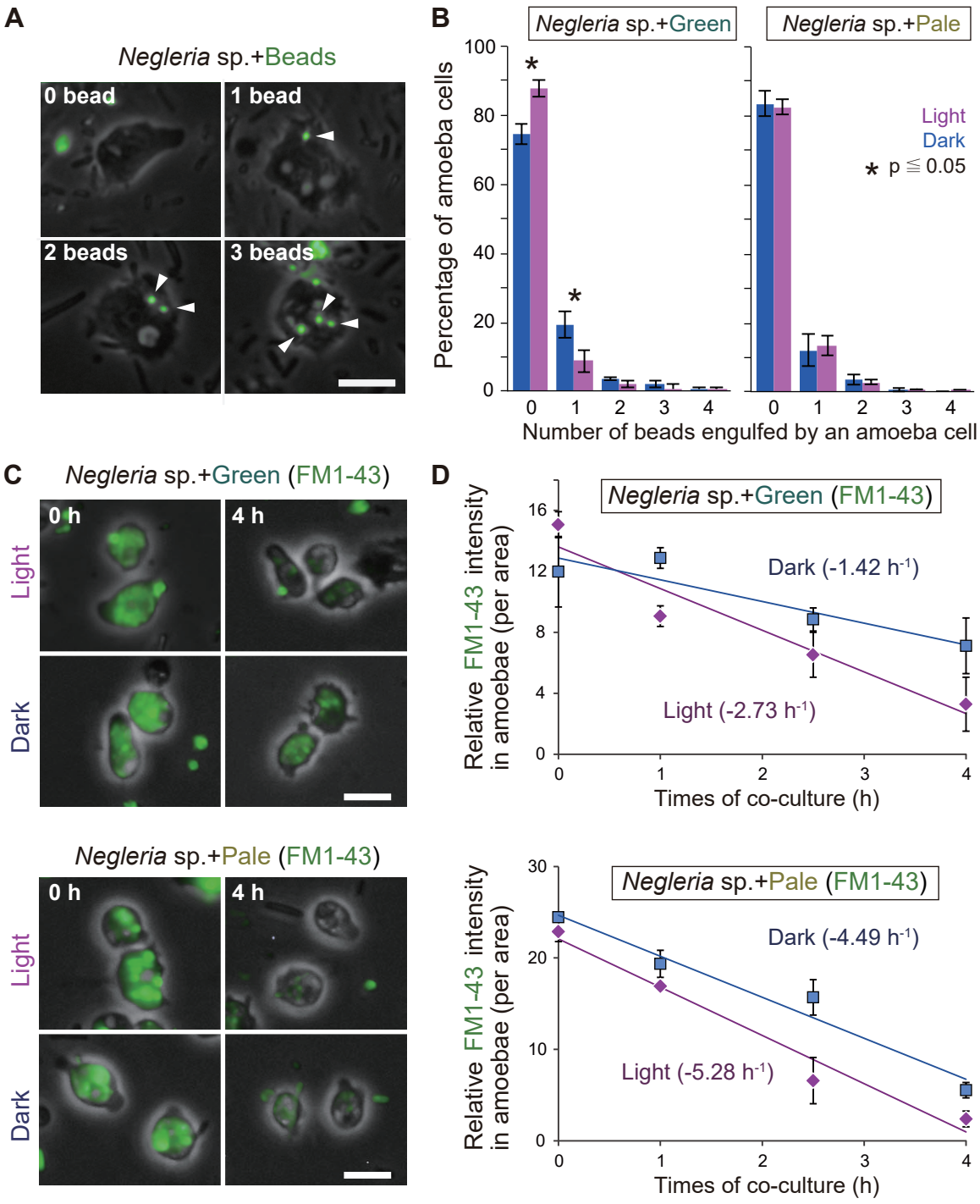

Figure 3.2. Effects of the photosynthetic trait of bacterial prey on engulfment and digestion of prey by *Naegleria* sp.

(**A, B**) *Naegleria* sp. was co-cultured with green or pale *S. elongatus* prey under dark and then kept under dark or transferred to light (200 μE m^{-2} s^{-1}) for 1 h. Just after the 1 h incubation, the green fluorescent beads were added and then further incubated under dark or light for 1 h. (A) Micrographs of amoeba cells (phase-contrast) that engulfed 0 to 3

beads (green fluorescence). (B) Comparison of number of fluorescent beads engulfed by amoeba cells in respective co-cultures. The error bar represents the standard deviation of three biological replicates. (**C, D**) *Naegleria* sp. was co-cultured with green or pale *S. elongatus* prey that was stained with the green fluorescent dye FM1-43 under dark, and then cells and preys were stuck on MAS-coated cover glass to inhibit amoebae to newly engulf bacterial prey. Then (hour 0) the cells were kept under dark or transferred to light (200 μE m^{-2} s^{-1}) for 4 h. (C) Micrographs showing amoeba cells (phase-contrast) digesting green or pale *S. elongatus* prey (FM1-43 green fluorescence) under dark or light condition. Images at hour 0 and 4 are shown. (D) Quantification of decrease in FM1-43 fluorescence from prey that had been engulfed by amoebae by hour 0 (rate of digestion) in respective conditions. The error bar represents the standard deviation of three biological replicates. Scale bars = 20 μm (A, C).

Oxidative stress response 1

Superoxide dismutase

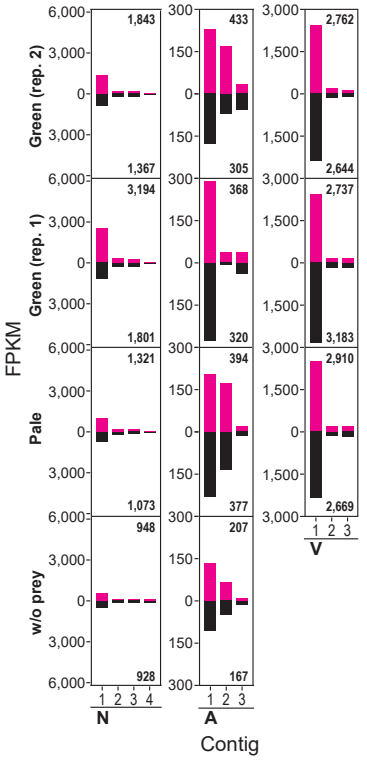

N1 comp160733_c0_seq1|m.20402
N2 comp197010_c0_seq1|m.19572
N3 comp197010_c1_seq1|m.19300
N4 comp218227_c0_seq1|m.7624

A1 comp188230_c0_seq1|m.40801
A2 comp188346_c0_seq1|m.30103
A3 comp132351_c0_seq1|m.39071

V1 comp121193_c0_seq2|m.27450
V2 comp117429_c0_seq1|m.23863
V3 comp122599_c0_seq1|m.22457

Catalase

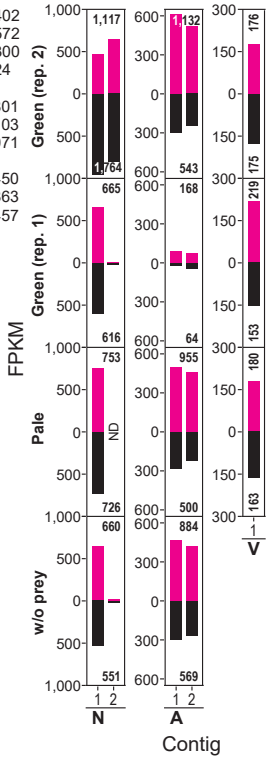

N1 comp192408_c0_seq1|m.4650
N2 comp174950_c0_seq1|m.10133

A1 comp188885_c0_seq1|m.25786
A2 comp188885_c0_seq1|m.25787

V1 comp123359_c0_seq1|m.13841

Thioredoxin

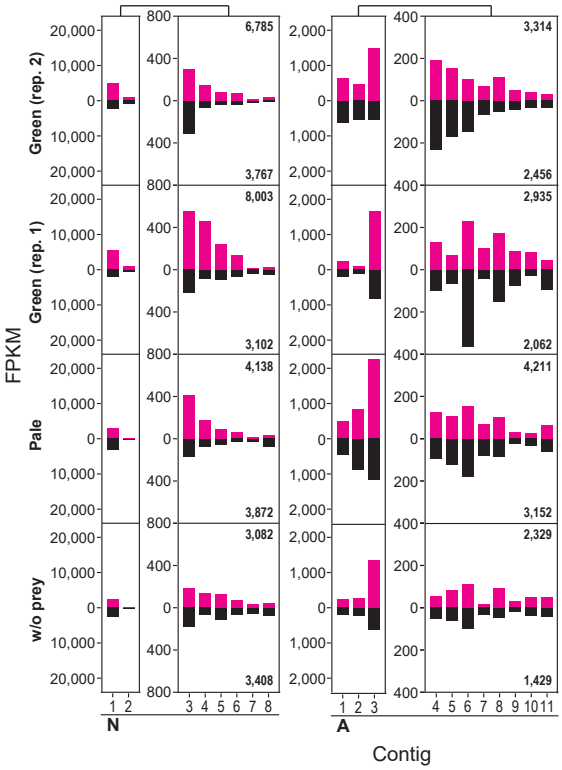

N1 comp222740_c10_seq1|m.26011
N2 comp215338_c0_seq1|m.23334
N3 comp218001_c0_seq1|m.3573
N4 comp217802_c0_seq1|m.12789
N5 comp214336_c0_seq1|m.23096
N6 comp223805_c0_seq1|m.9397
N7 comp212182_c0_seq1|m.21773
N8 comp229501_c0_seq1|m.21674

A1 comp191596_c1_seq2|m.42213
A2 comp191030_c0_seq1|m.46136
A3 comp188618_c0_seq1|m.31761
A4 comp197048_c0_seq1|m.7755
A5 comp192368_c0_seq1|m.33075
A6 comp194676_c0_seq1|m.19143
A7 comp190977_c1_seq1|m.39093
A8 comp191774_c0_seq1|m.37757
A9 comp195144_c0_seq1|m.32433
A10 comp193291_c1_seq4|m.35492
A11 comp193004_c0_seq1|m.19663

V1 comp122719_c0_seq1|m.34782
V2 comp118199_c0_seq1|m.31505
V3 comp121352_c1_seq1|m.29457
V4 comp124849_c0_seq1|m.14768
V5 comp124069_c0_seq1|m.31318
V6 comp129006_c3_seq1|m.23320

Oxidative stress response 2

Ascorbate peroxidase

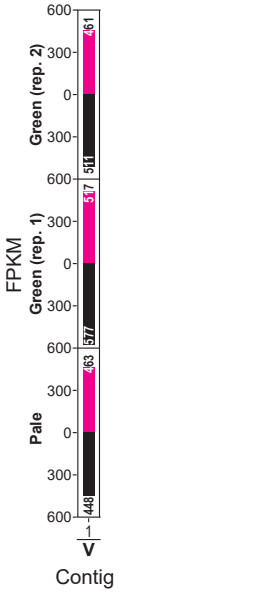

V1 comp122783_c0_seq1|m.3926

Peroxiredoxin

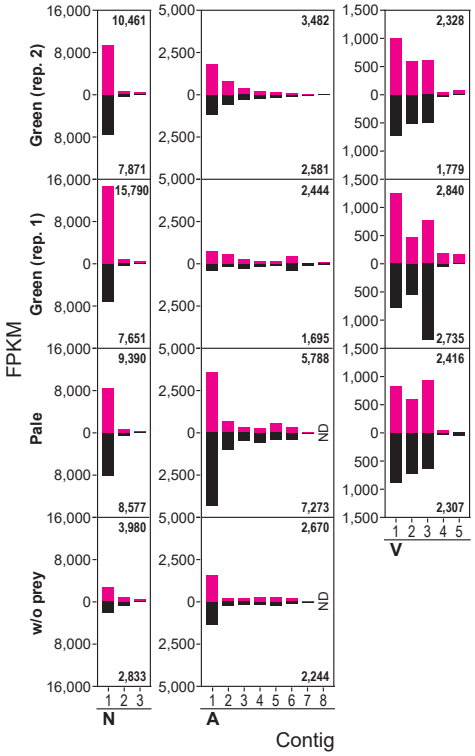

N1 comp161327_c0_seq1|m.21473
N2 comp196746_c0_seq1|m.16621
N3 comp225147_c1_seq1|m.3590

A1 comp190305_c0_seq1|m.42848
A2 comp191074_c1_seq1|m.50692
A3 comp197629_c1_seq1|m.44286
A4 comp184213_c1_seq1|m.49637
A5 comp193391_c0_seq4|m.23221
A6 comp189344_c0_seq2|m.39712
A7 comp193418_c0_seq1|m.21148
A8 comp193037_c0_seq1|m.37269

V1 comp118373_c0_seq1|m.26901
V2 comp123133_c0_seq1|m.25027
V3 comp118911_c0_seq1|m.29873
V4 comp126377_c0_seq2|m.11535
V5 comp127697_c0_seq2|m.5968

Glutaredoxin

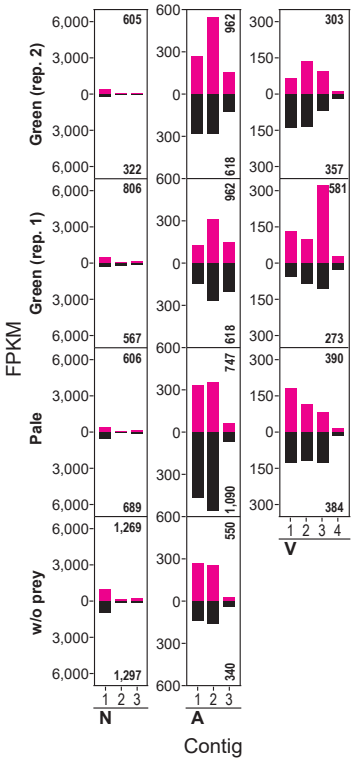

N1 comp197043_c0_seq1|m.26229
N2 comp196883_c0_seq1|m.24409
N3 comp221174_c0_seq1|m.16477

A1 comp199540_c0_seq1|m.12891
A2 comp127545_c0_seq1|m.49958
A3 comp189732_c0_seq1|m.39341

V1 comp117553_c0_seq1|m.45875
V2 comp122551_c0_seq1|m.17789
V3 comp120750_c0_seq1|m.35507
V4 comp129187_c1_seq1|m.1393

Glutathione peroxidase

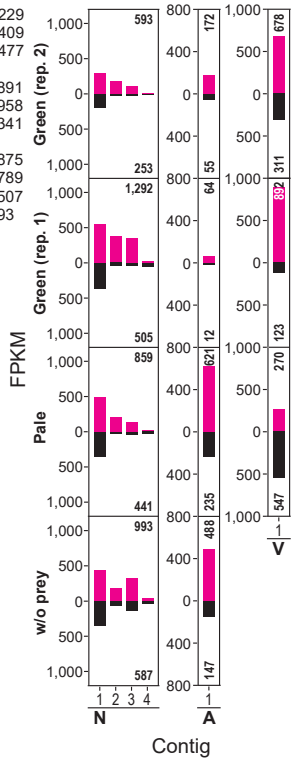

N1 comp197051_c1_seq2|m.22797
N2 comp227059_c0_seq3|m.1915
N3 comp226183_c1_seq1|m.3708
N4 comp230203_c0_seq1|m.20301

A1 comp190730_c0_seq1|m.38776

V1 comp118319_c0_seq2|m.24239

Oxidative stress response 3

Glutathione synthetase

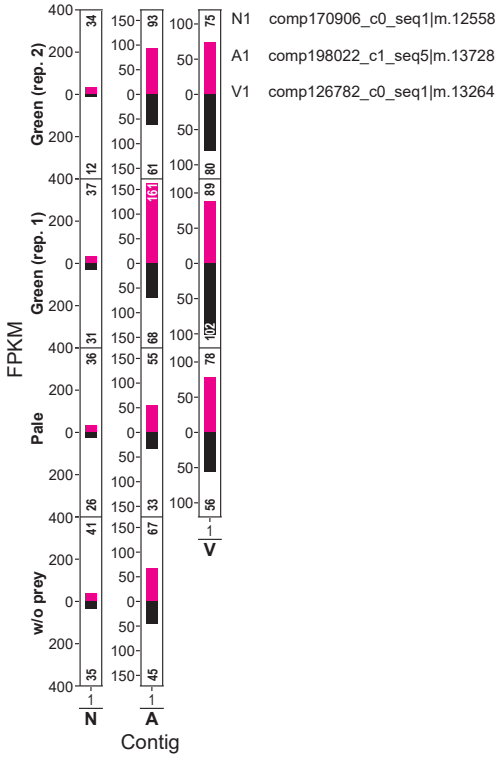

N1 comp170906_c0_seq1|m.12558

A1 comp198022_c1_seq5|m.13728

V1 comp126782_c0_seq1|m.13264

Carbonyl reductase

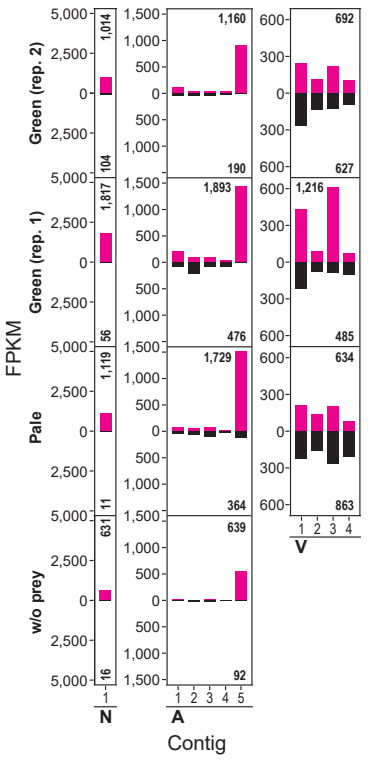

N1 comp222757_c0_seq1|m.17440

A1 comp193008_c0_seq1|m.24805
A2 comp195979_c0_seq1|m.27346
A3 comp192631_c0_seq2|m.37586
A4 comp190819_c0_seq1|m.38965
A5 comp193008_c0_seq1|m.24804

V1 comp126764_c0_seq1|m.31102
V2 comp121793_c0_seq1|m.35963
V3 comp122682_c0_seq2|m.16871
V4 comp121793_c1_seq1|m.39085

Glutathion S-transferase

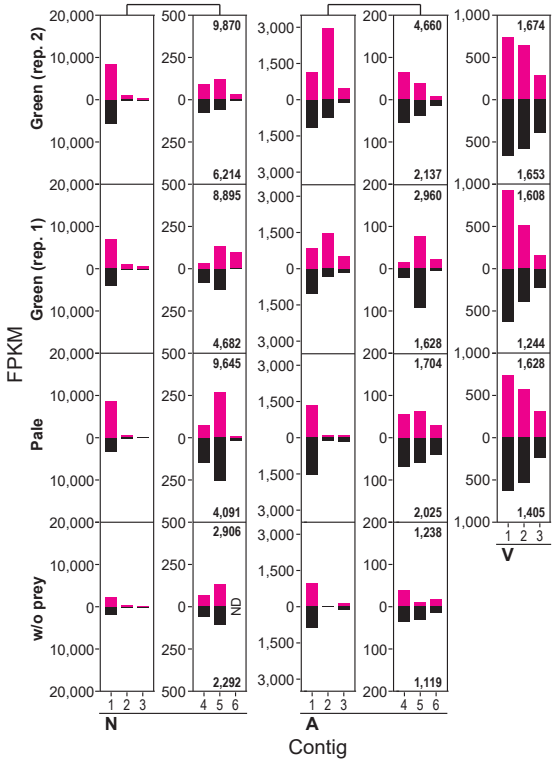

N1 comp222120_c0_seq1|m.19841
N2 comp215852_c0_seq1|m.19804
N3 comp220161_c1_seq1|m.17653
N4 comp219327_c0_seq1|m.18450
N5 comp171992_c0_seq1|m.19016
N6 comp219524_c0_seq1|m.20621

A1 comp188728_c0_seq1|m.30477
A2 comp190111_c0_seq1|m.44542
A3 comp193211_c0_seq1|m.42968
A4 comp191147_c0_seq2|m.40291
A5 comp190522_c0_seq1|m.39396
A6 comp191234_c0_seq2|m.34399

V1 comp98094_c0_seq1|m.26854
V2 comp106525_c0_seq1|m.37532
V3 comp125662_c0_seq1|m.37473

Oxidative stress response 4

Apolipoprotein D

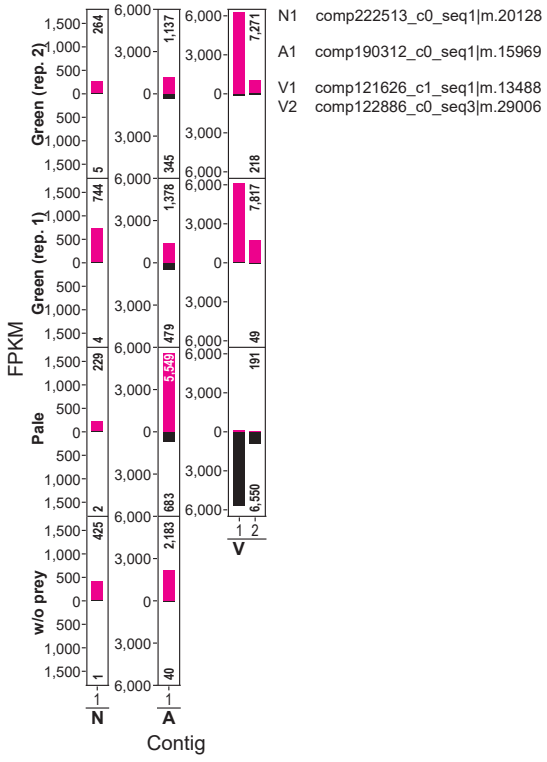

Cob(I)yrinic acid a,c-diamide adenosyltransferase

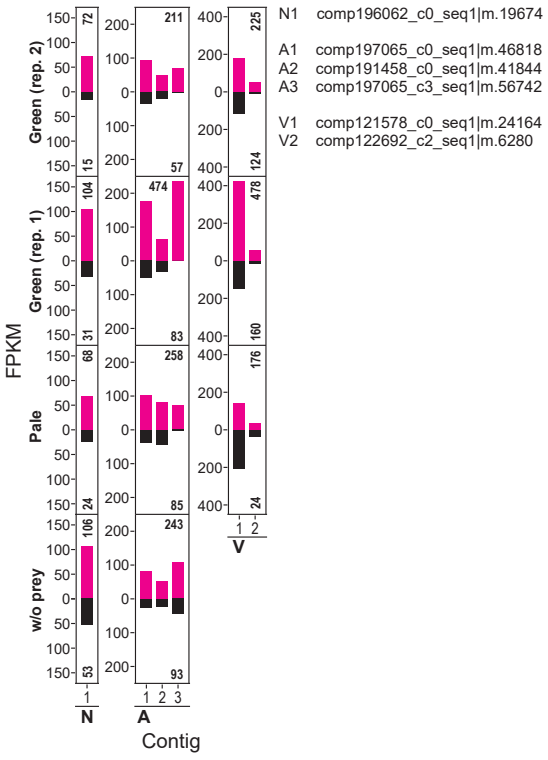

NADP-reducing hydrogenase subunit HndC

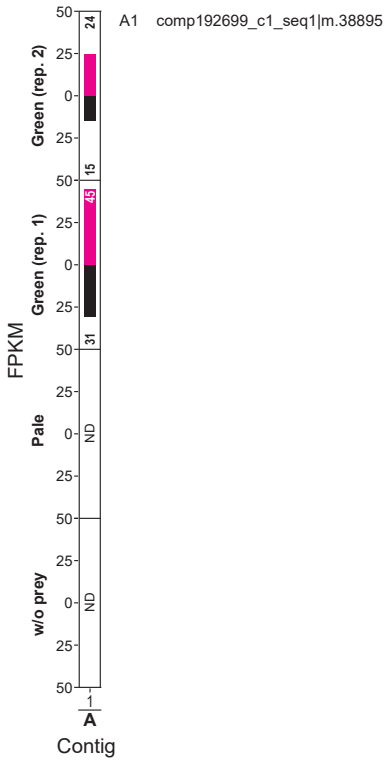

Peptide methionine sulfoxide reductase

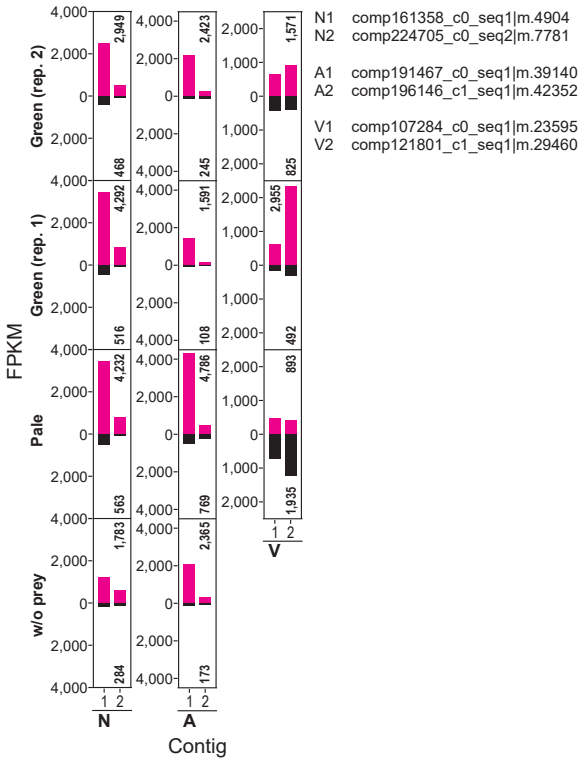

Carotenoid synthesis

Carotene epsilon-monooxygenase

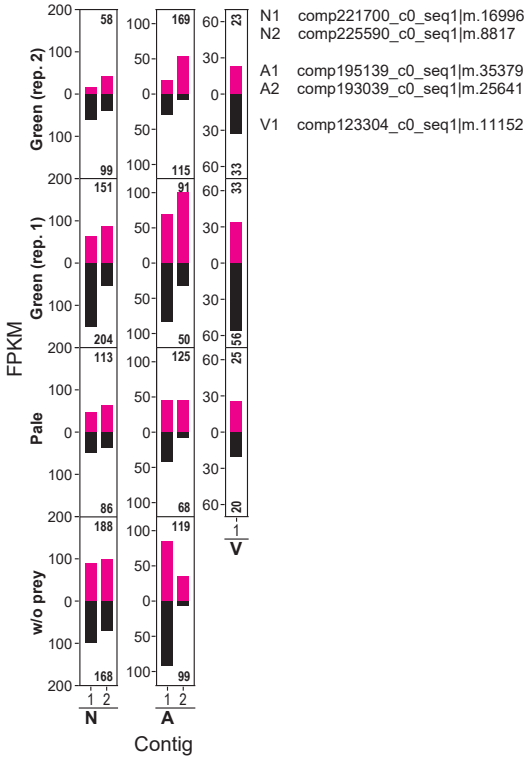

N1 comp221700_c0_seq1|m.16996
N2 comp225590_c0_seq1|m.8817

A1 comp195139_c0_seq1|m.35379
A2 comp193039_c0_seq1|m.25641

V1 comp123304_c0_seq1|m.11152

Phytoene desaturase

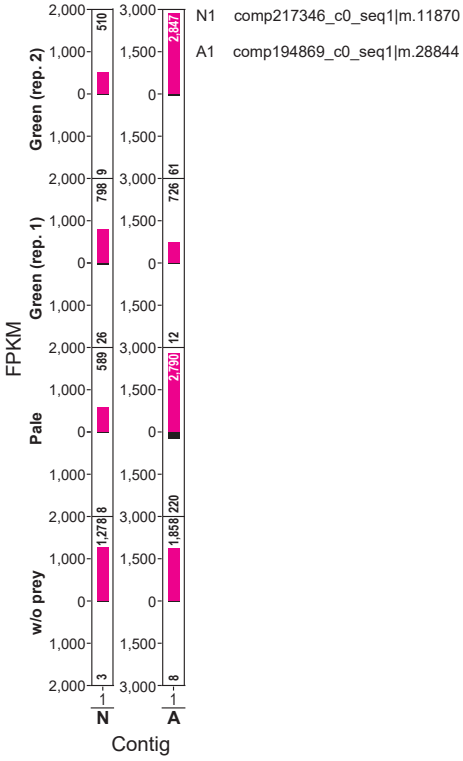

N1 comp217346_c0_seq1|m.11870

A1 comp194869_c0_seq1|m.28844

Bifunctional lycopene cyclase/phytoene synthase

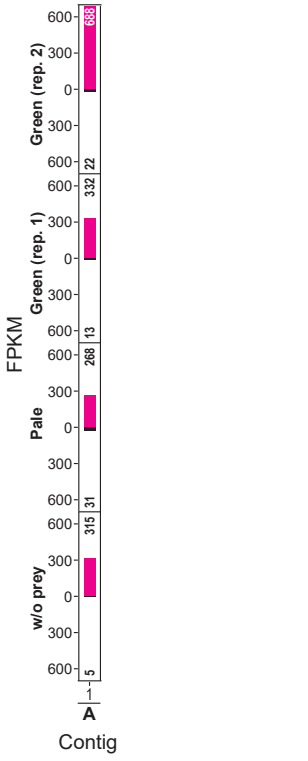

A1 comp195533_c0_seq1|m.19074

Zeaxanthin epoxidase

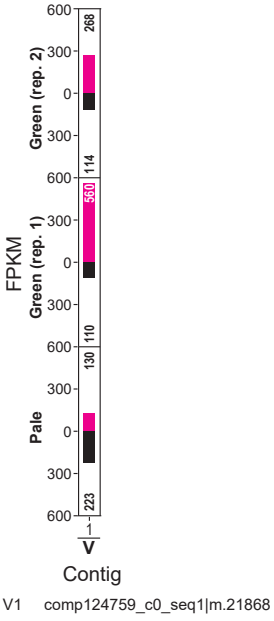

V1 comp124759_c0_seq1|m.21868

Geranylgeranyl pyrophosphate synthase

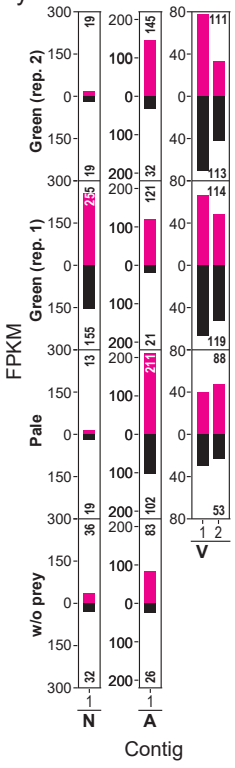

N1 comp213578_c0_seq1|m.14664

A1 comp194723_c0_seq1|m.21777

V1 comp124726_c1_seq1|m.28171
V2 comp124726_c0_seq1|m.31417

DNA repair 1

ALKB

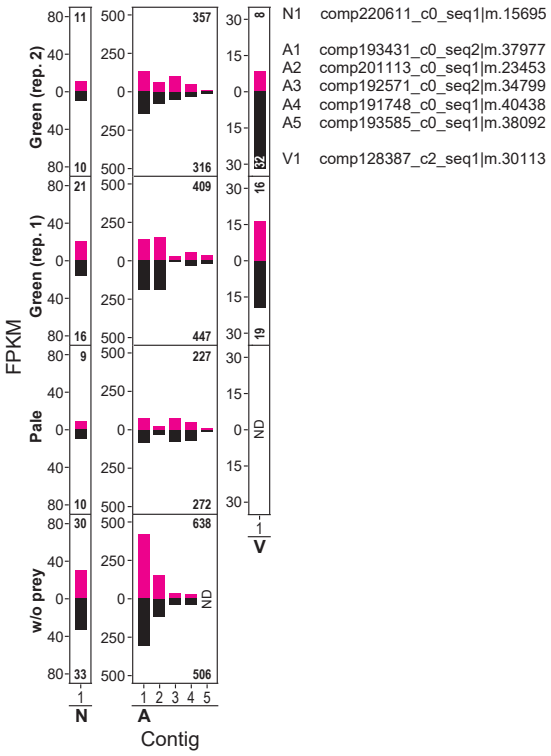

DNA-(apurinic or apyrimidinic site) lyase

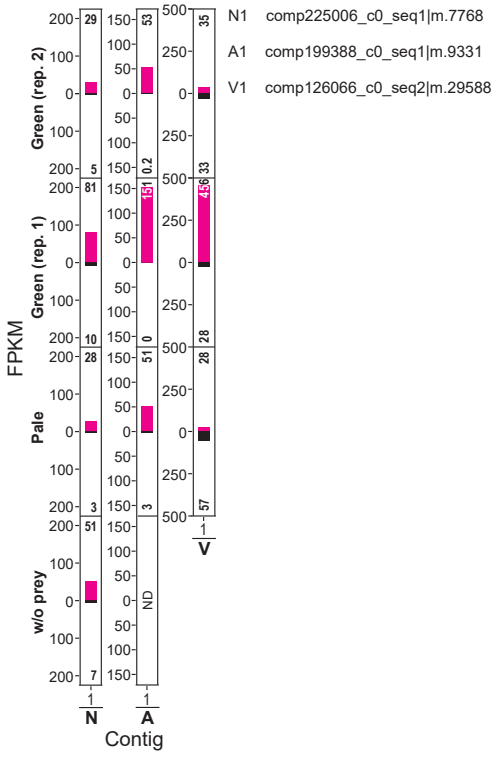

Deoxyribodipyrimidine photo-lyase

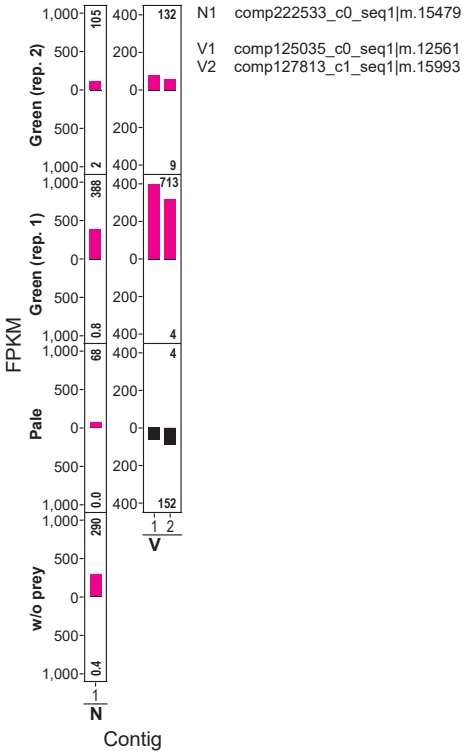

GT -mismatch-specific thymine DNA glycosylase

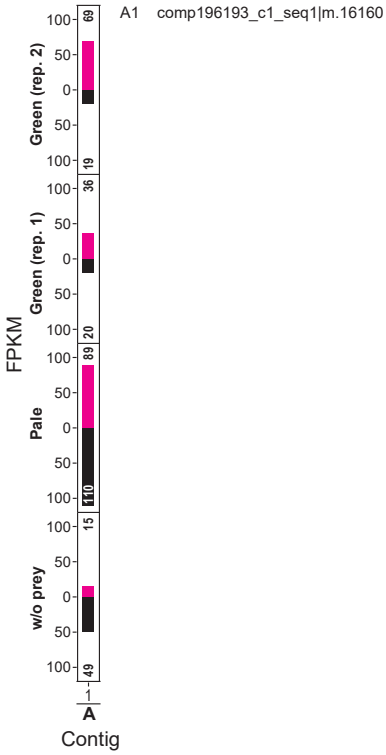

DNA repair 2

MCM8

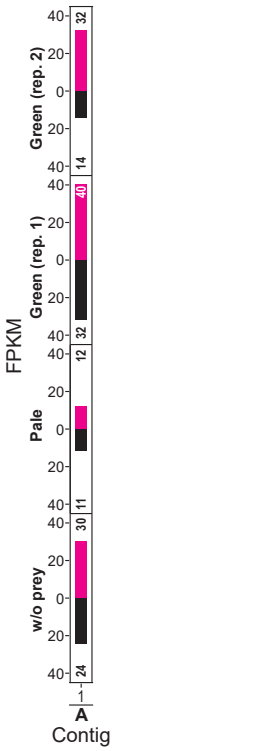

A1 comp197416_c1_seq3|m.39014

Msh2

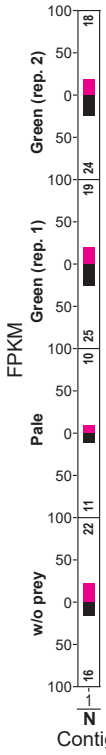

N1 comp225420_c0_seq1|m.4740

RHP23

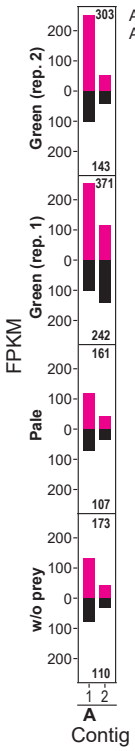

A1 comp191210_c0_seq1|m.31519
A2 comp193102_c0_seq1|m.31176

RHP26

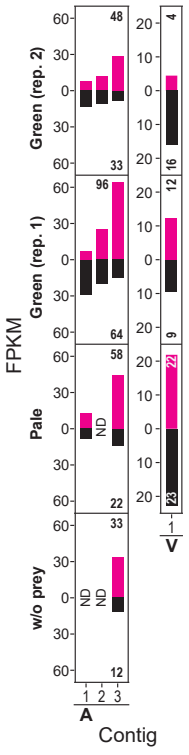

A1 comp198392_c1_seq1|m.38884
A2 comp198240_c0_seq1|m.8513
A3 comp198384_c0_seq1|m.21338

V1 comp127772_c1_seq3|m.15332

RAD5

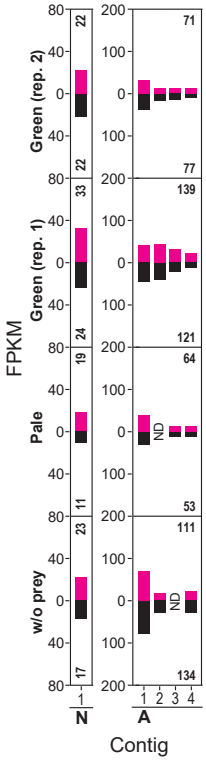

N1 comp218612_c0_seq1|m.4221

A1 comp198679_c3_seq1|m.9138
A2 comp198190_c0_seq1|m.23434
A3 comp198158_c0_seq2|m.16420
A4 comp199095_c1_seq2|m.895

DNA repair 3

RAD16

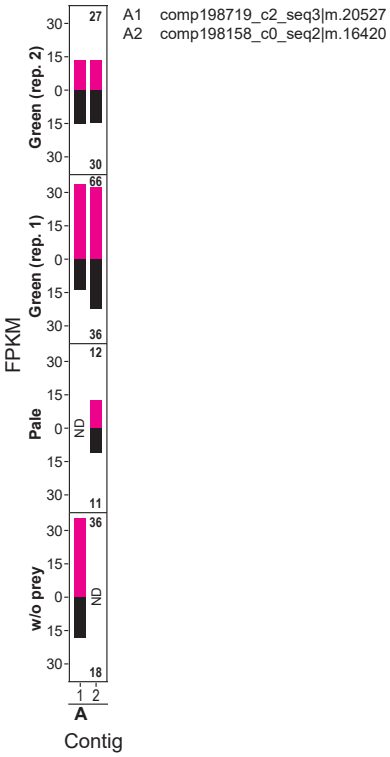

RAD23

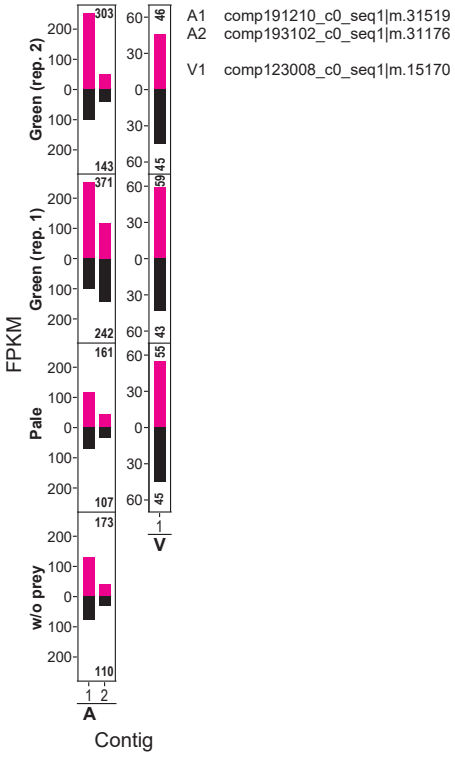

RAD51

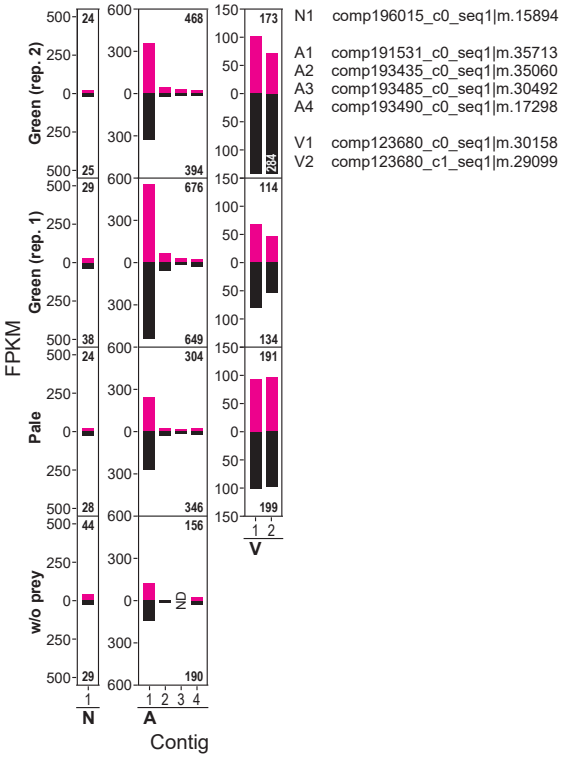

XRCC

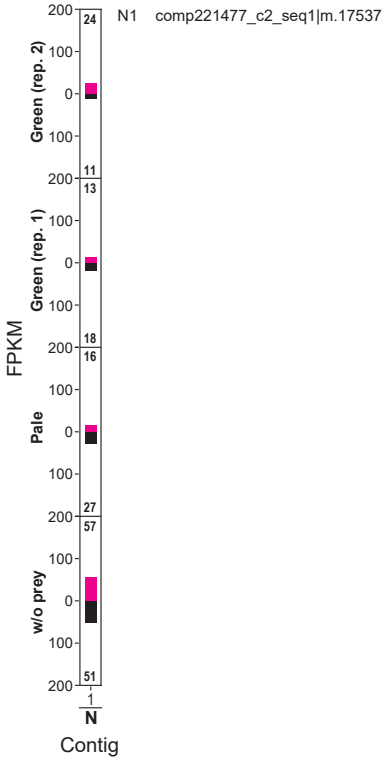

Respiration 1

ATP/ADP translocase

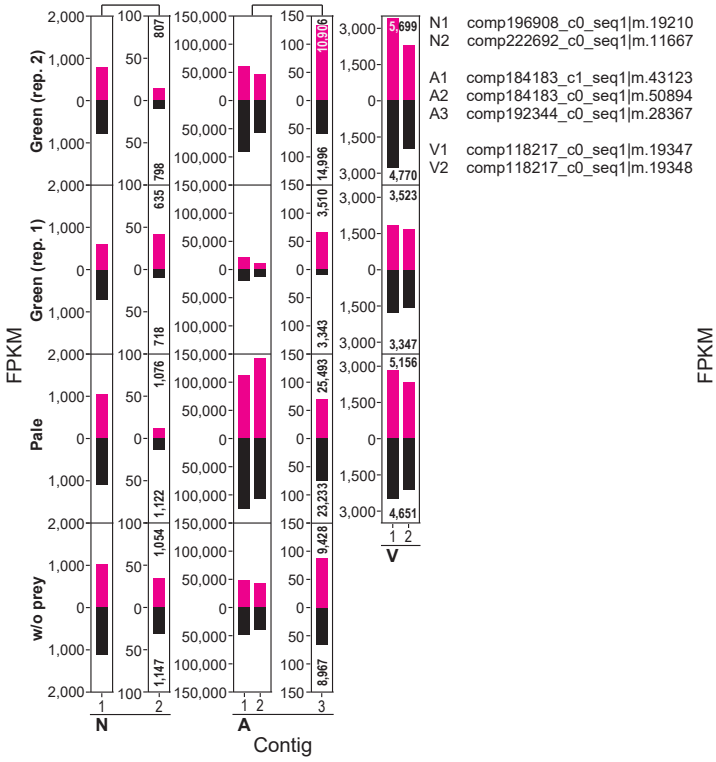

COX11

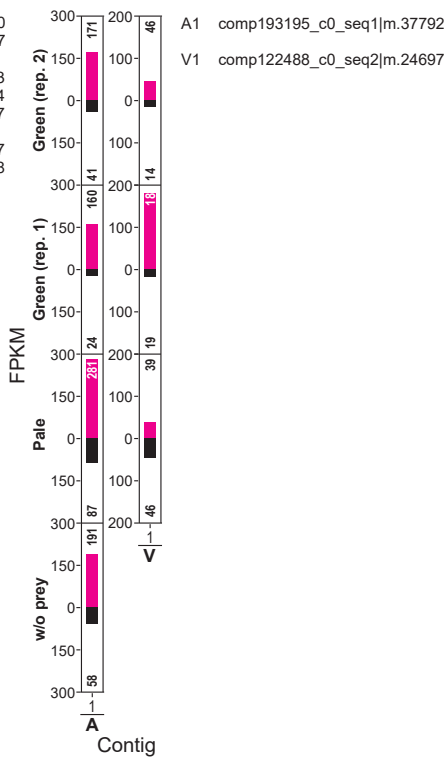

COX15

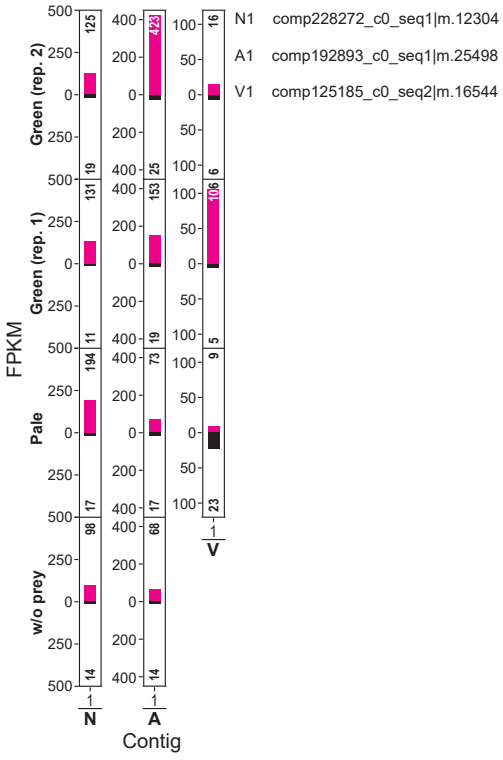

COX19

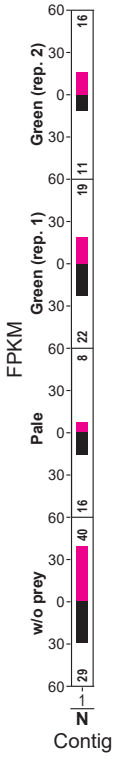

SCO1

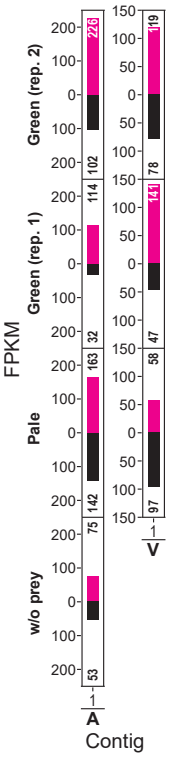

N1 comp169334_c0_seq1|m.12493

Respiration 2

Prohibitin 1

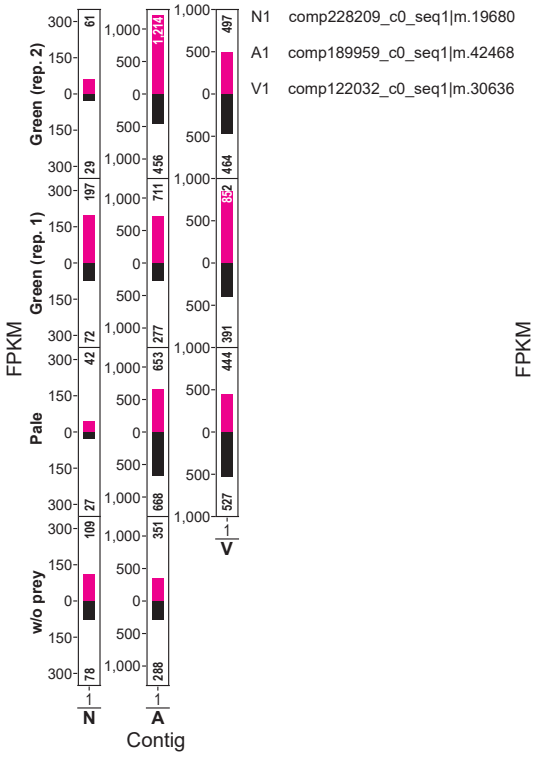

Prohibitin 2

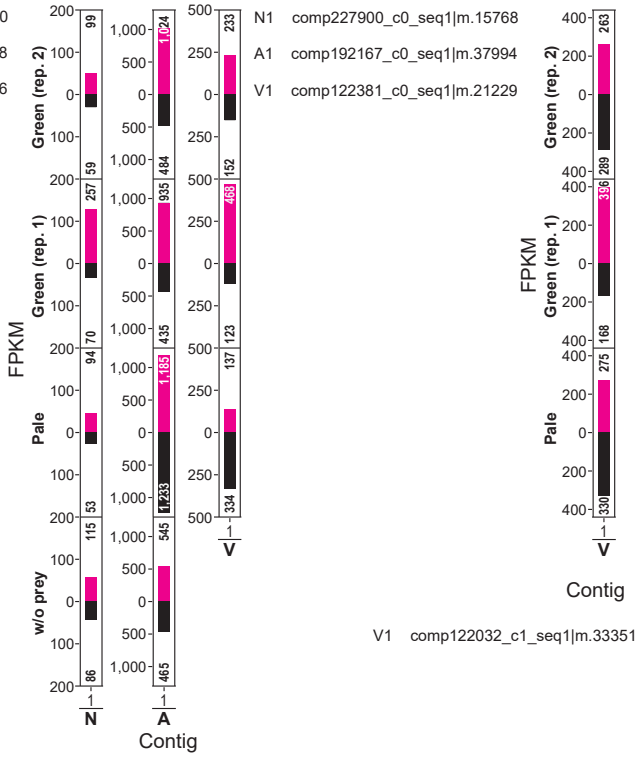

Prohibitin 3

V1 comp122032_c1_seq1|m.33351

TIM10

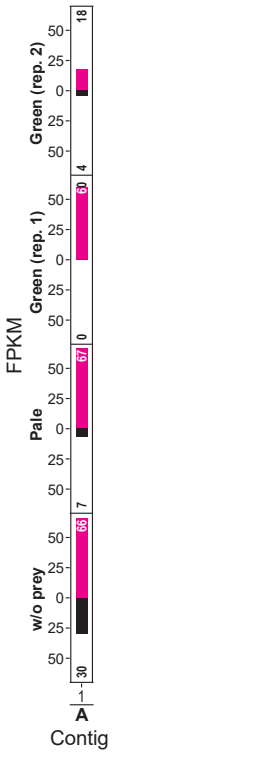

TIM14

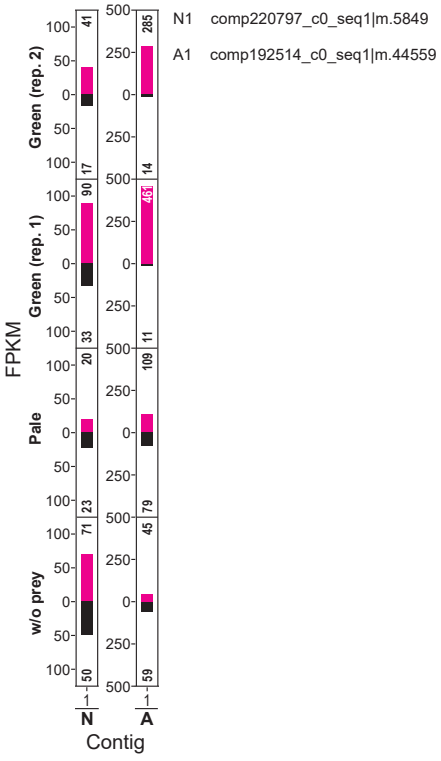

TIM16

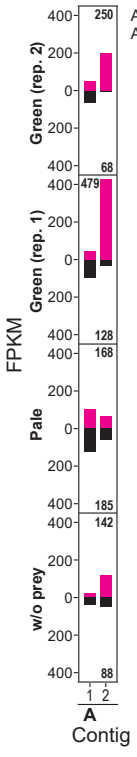

A1 comp190184_c0_seq3|m.41328

Respiration 3

TIM17

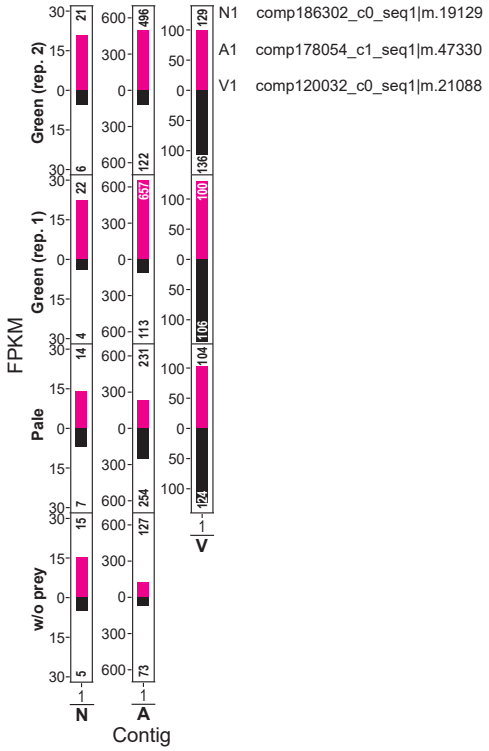

N1 comp186302_c0_seq1|m.19129
A1 comp178054_c1_seq1|m.47330
V1 comp120032_c0_seq1|m.21088

TIM21

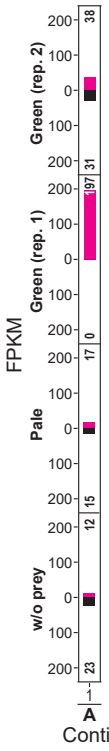

TIM22

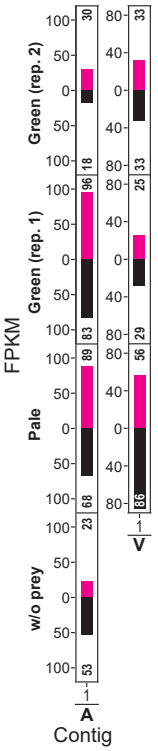

A1 comp195111_c0_seq1|m.20430
V1 comp122494_c0_seq1|m.24138

A1 comp190408_c0_seq1|m.49523

TIM23

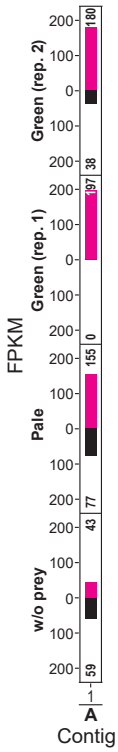

A1 comp190408_c0_seq1|m.49523

TIM44

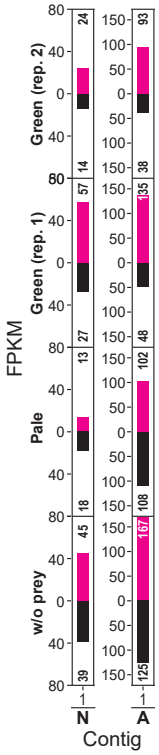

N1 comp182943_c0_seq1|m.12522
A1 comp192049_c0_seq1|m.28999

TIM50

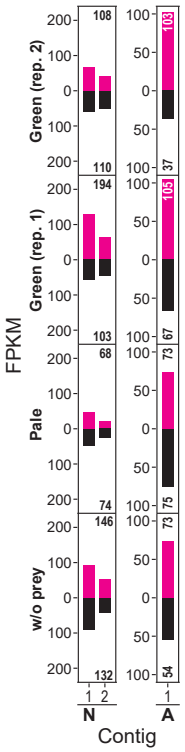

N1 comp168559_c0_seq1|m.14233
N2 comp221198_c0_seq1|m.14508
A1 comp191345_c0_seq1|m.34823

TOM40

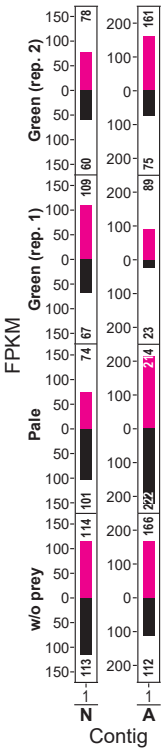

N1 comp227996_c0_seq1|m.16805
A1 comp190840_c0_seq1|m.33776

Vacuolar-type H⁺-ATPase 1

V-ATPase subunit A

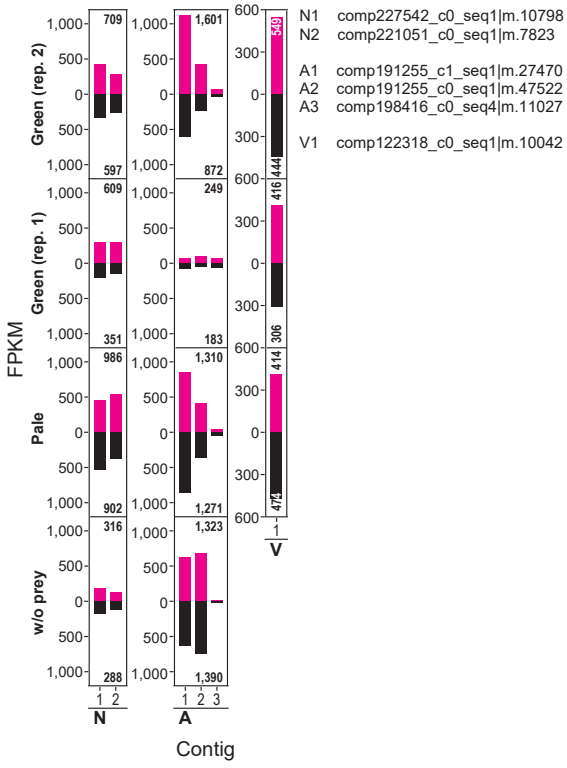

V-ATPase subunit B

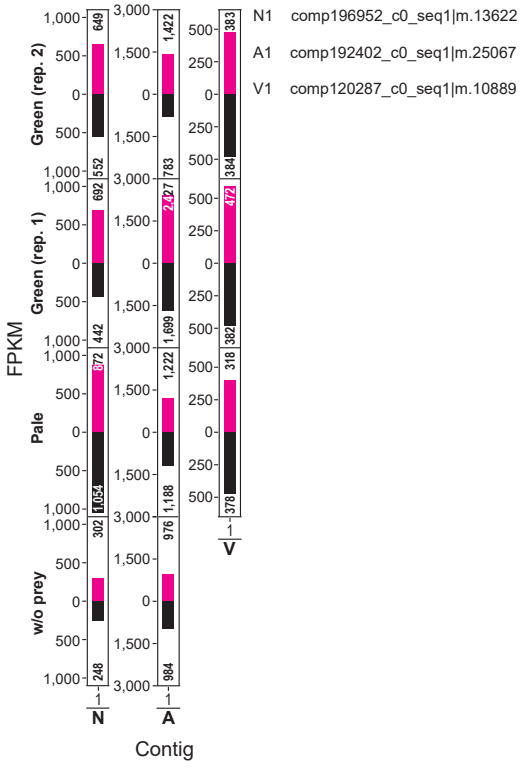

V-ATPase subunit C

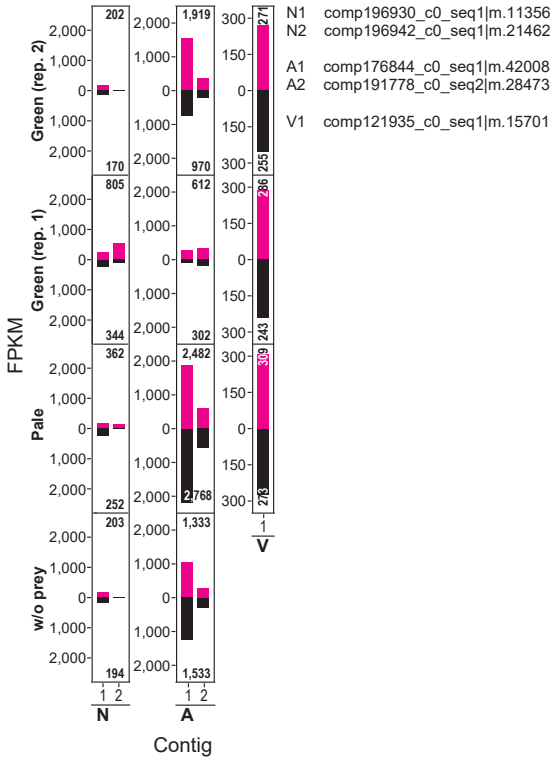

V-ATPase subunit D

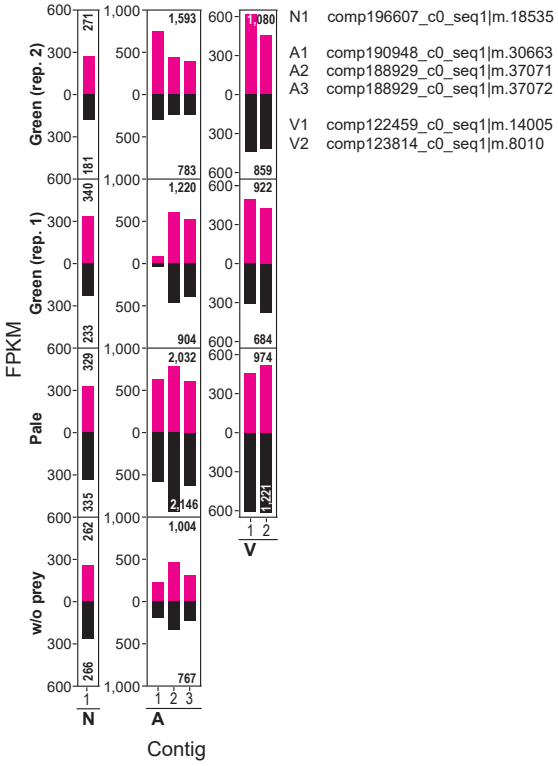

Vacuolar-type H⁺-ATPase 2

V-ATPase subunit E

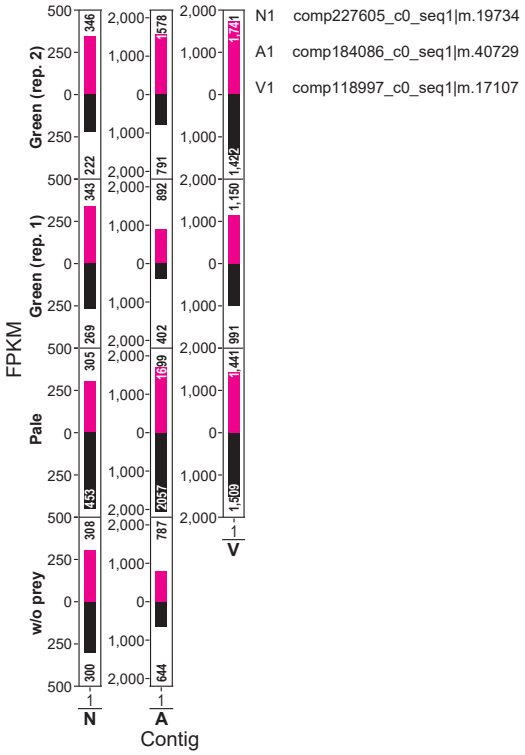

N1 comp227605_c0_seq1|m.19734
A1 comp184086_c0_seq1|m.40729
V1 comp118997_c0_seq1|m.17107

V-ATPase subunit F

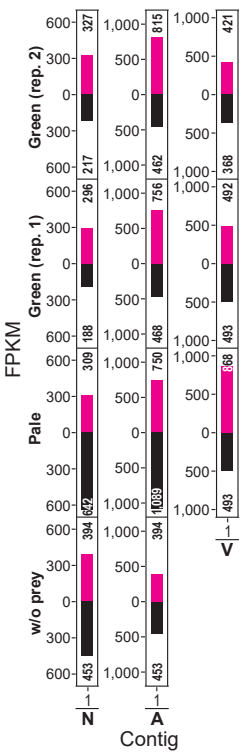

N1 comp227723_c0_seq1|m.25000
A1 comp188094_c0_seq1|m.44297
V1 comp125494_c0_seq1|m.33170

V-ATPase subunit G

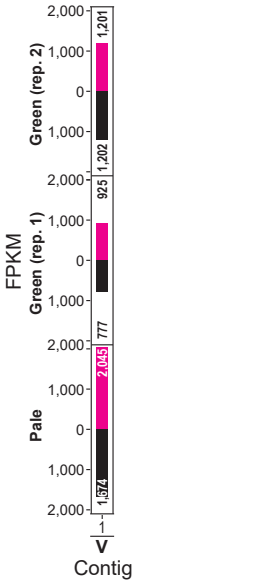

V1 comp120889_c0_seq1|m.32212

V-ATPase subunit H

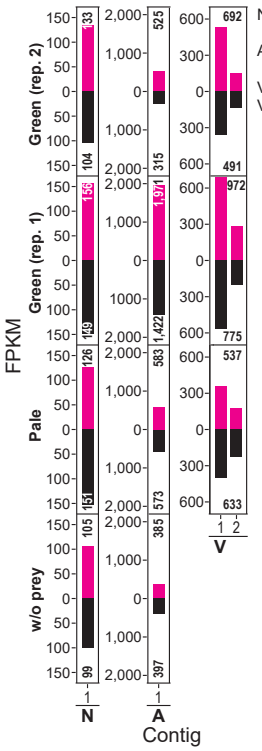

N1 comp158917_c0_seq1|m.13351
A1 comp192911_c0_seq1|m.9326
V1 comp120946_c0_seq1|m.43677
V2 comp120946_c1_seq1|m.18228

V-ATPase subunit a

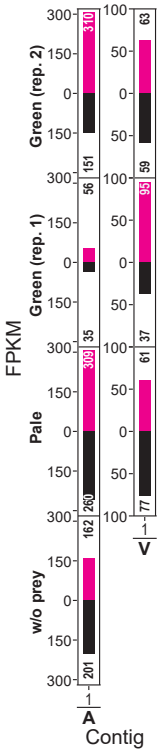

A1 comp194101_c0_seq1|m.13631
V1 comp127080_c1_seq1|m.5035

Vacuolar-type H⁺-ATPase 3

V-ATPase subunit c''

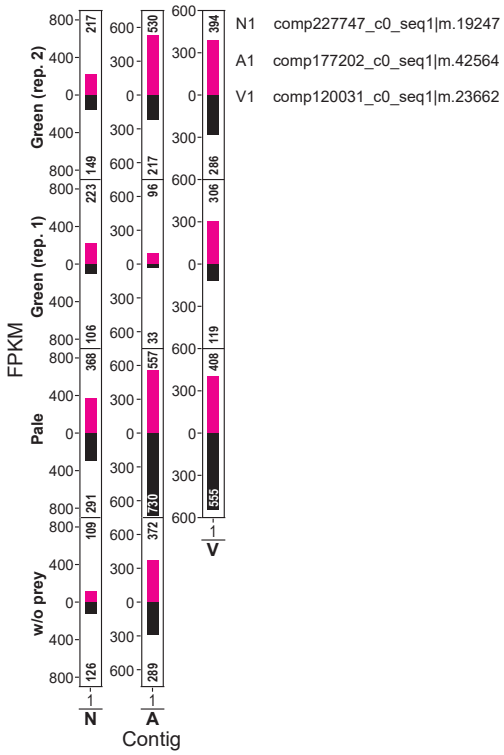

Proteolysis 1

Cathepsin A

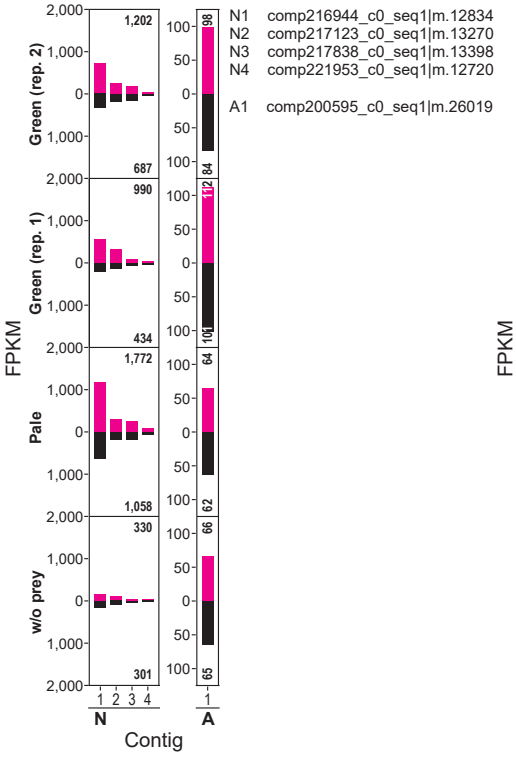

N1 comp216944_c0_seq1|m.12834
N2 comp217123_c0_seq1|m.13270
N3 comp217838_c0_seq1|m.13398
N4 comp221953_c0_seq1|m.12720

A1 comp200595_c0_seq1|m.26019

Cathepsin C

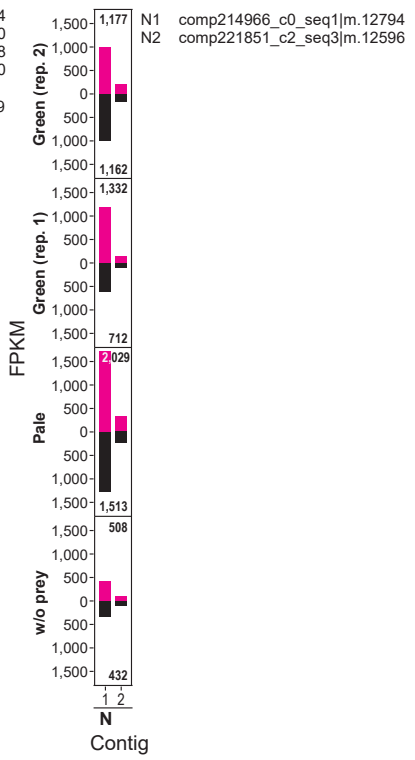

N1 comp214966_c0_seq1|m.12794
N2 comp221851_c2_seq3|m.12596

Cathepsin F

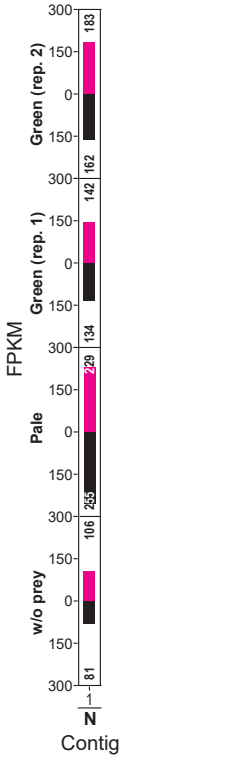

N1 comp221740_c0_seq1|m.7856

Cathepsin B

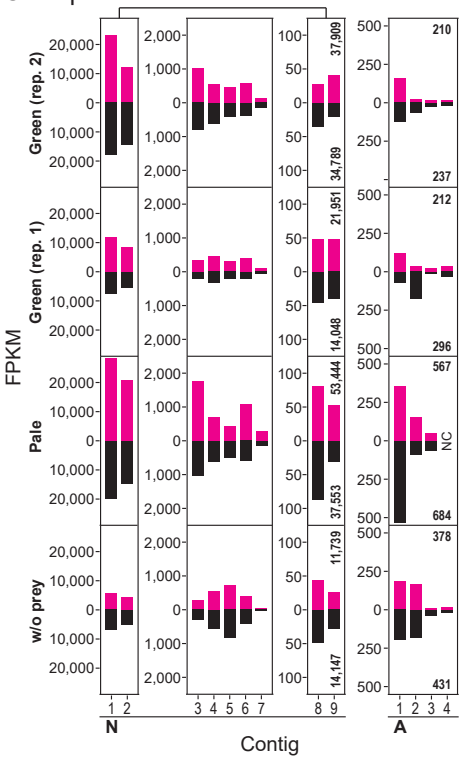

N1 comp222264_c1_seq2|m.24062
N2 comp222264_c0_seq2|m.18254
N3 comp161120_c0_seq1|m.21113
N4 comp196690_c1_seq1|m.20318
N5 comp196690_c0_seq1|m.25763
N6 comp161120_c1_seq1|m.24792
N7 comp222291_c0_seq1|m.19331
N8 comp219614_c1_seq1|m.18120
N9 comp224223_c0_seq1|m.11597

A1 comp192370_c0_seq1|m.36718
A2 comp197700_c0_seq1|m.9917
A3 comp195746_c1_seq1|m.28322
A4 comp196648_c0_seq6|m.14151

Proteolysis 2

Cathepsin L

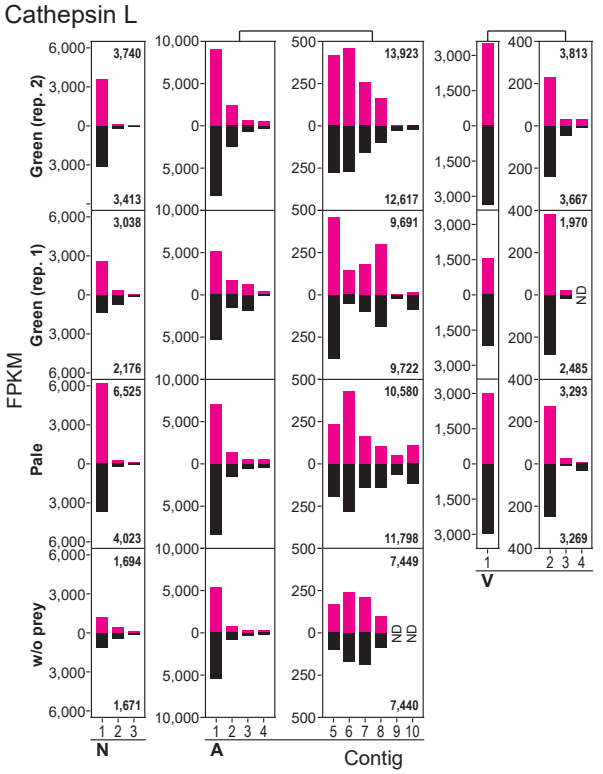

N1 comp227258_c0_seq1|m.16318
N2 comp196035_c1_seq1|m.18909
N3 comp217656_c0_seq1|m.16225

A1 comp184181_c0_seq1|m.37815
A2 comp191394_c1_seq1|m.40371
A3 comp194227_c1_seq2|m.37440
A4 comp192259_c1_seq1|m.47635
A5 comp192261_c1_seq1|m.50689
A6 comp192259_c0_seq1|m.39127
A7 comp193323_c1_seq1|m.26742
A8 comp192261_c2_seq1|m.48742
A9 comp196286_c2_seq2|m.23901
A10 comp198110_c0_seq1|m.2200

V1 comp122919_c1_seq1|m.20448
V2 comp122872_c0_seq1|m.10793
V3 comp124629_c0_seq1|m.18255
V4 comp121275_c0_seq2|m.23570

Cathepsin Z

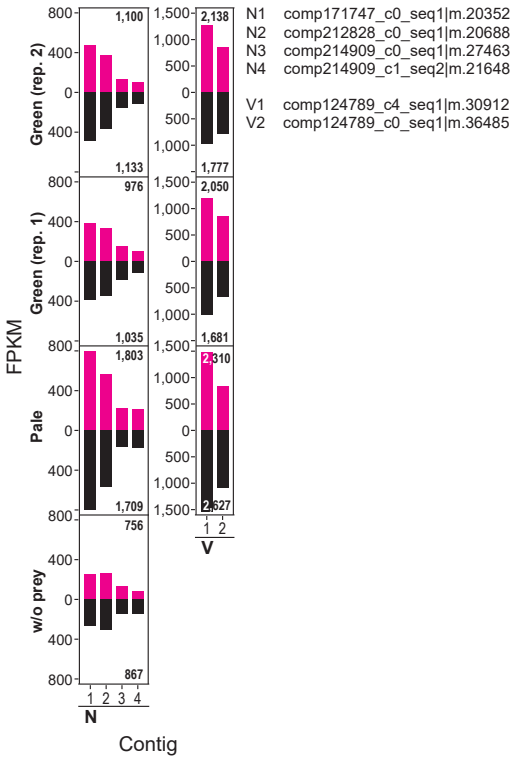

N1 comp171747_c0_seq1|m.20352
N2 comp212828_c0_seq1|m.20688
N3 comp214909_c0_seq1|m.27463
N4 comp214909_c1_seq2|m.21648

V1 comp124789_c4_seq1|m.30912
V2 comp124789_c0_seq1|m.36485

Chymotrypsin

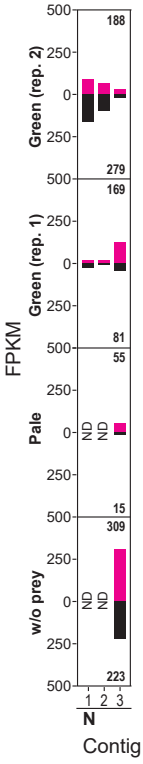

N1 comp227093_c0_seq1|m.4050
N2 comp224595_c1_seq1|m.18363
N3 comp224121_c0_seq1|m.5208

Oxygen reducing metabolisms

Methylsterol monooxygenase

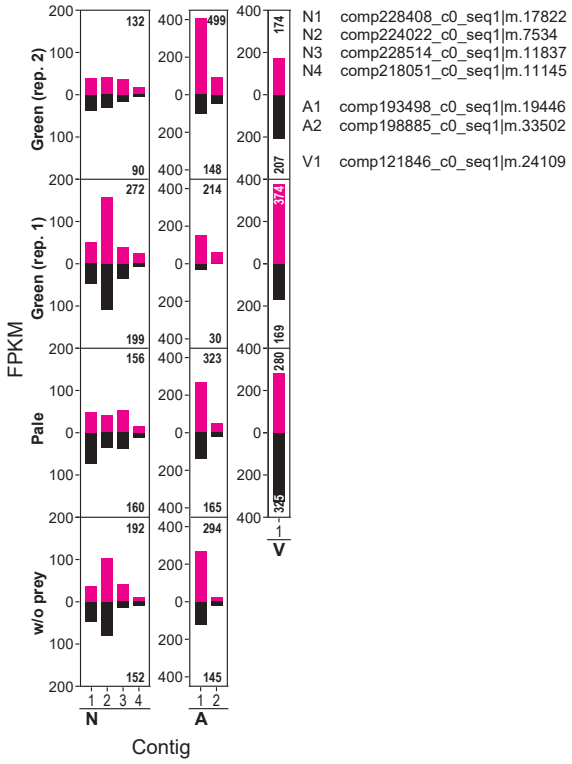

Squalene monooxygenase

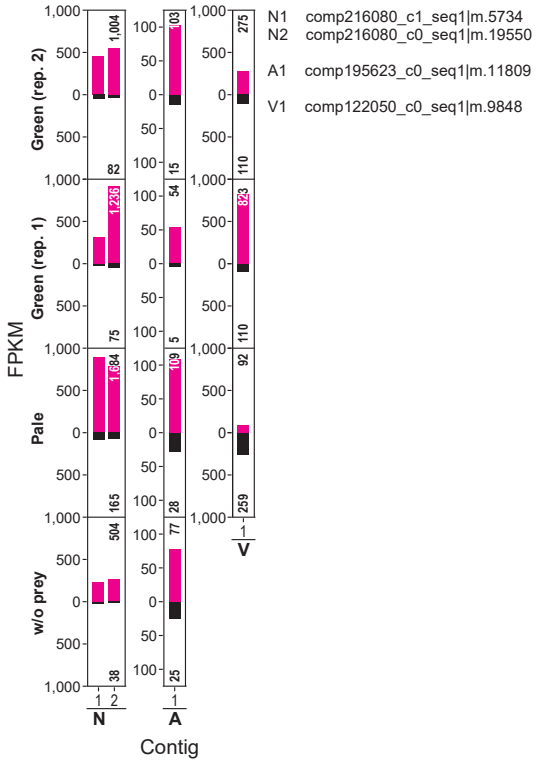

L-gulonolactone oxidase

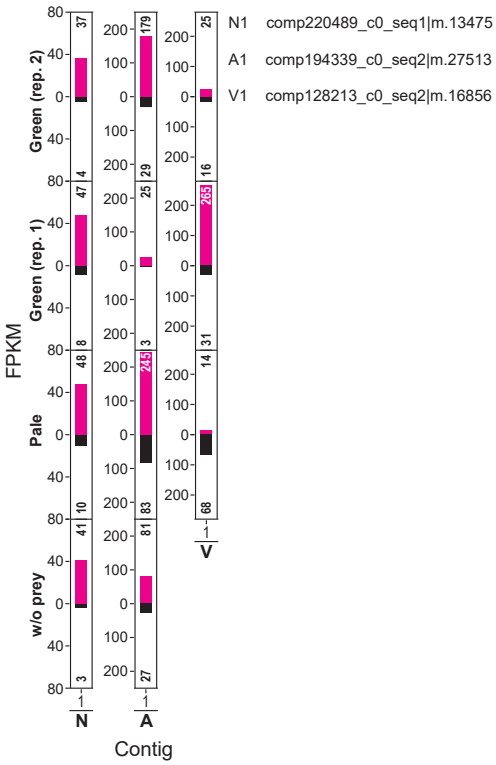

Myosin 1

Type I

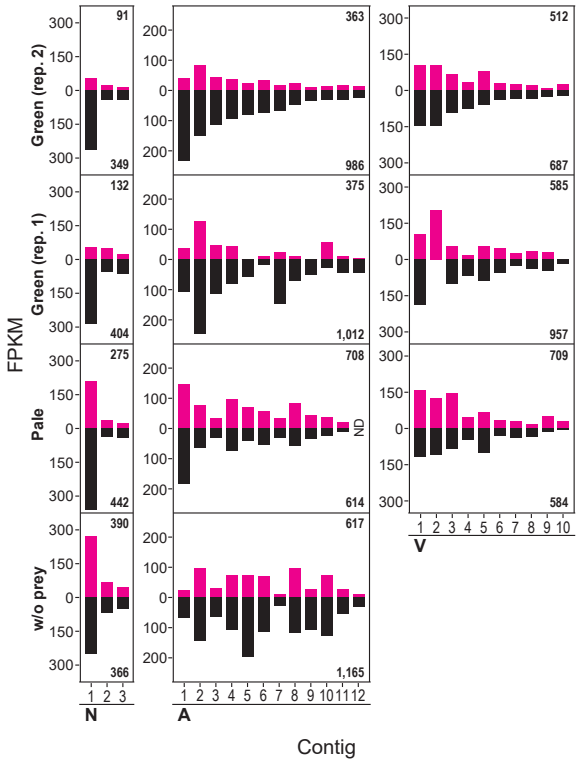

N1 comp221724_c0_seq1|m.7380
N2 comp228109_c0_seq1|m.3268
N3 comp222815_c1_seq1|m.8438

A1 comp195149_c2_seq1|m.48654
A2 comp198265_c0_seq3|m.5910
A3 comp194928_c1_seq2|m.24990
A4 comp197586_c5_seq3|m.6533
A5 comp197586_c1_seq1|m.53935
A6 comp197586_c0_seq1|m.46051
A7 comp195149_c0_seq1|m.30309
A8 comp197586_c4_seq1|m.45078
A9 comp197586_c2_seq1|m.43536
A10 comp188183_c0_seq1|m.44484
A11 comp195149_c1_seq2|m.47403
A12 comp194928_c0_seq1|m.39468

V1 comp126827_c3_seq1|m.4894
V2 comp127146_c0_seq1|m.4290
V3 comp127492_c0_seq1|m.28255
V4 comp128338_c0_seq6|m.2630
V5 comp126827_c1_seq1|m.30554
V6 comp127492_c3_seq1|m.2595
V7 comp127492_c2_seq1|m.29676
V8 comp127492_c1_seq1|m.26684
V9 comp126007_c1_seq1|m.21762
V10 comp120344_c0_seq1|m.31275

Type II

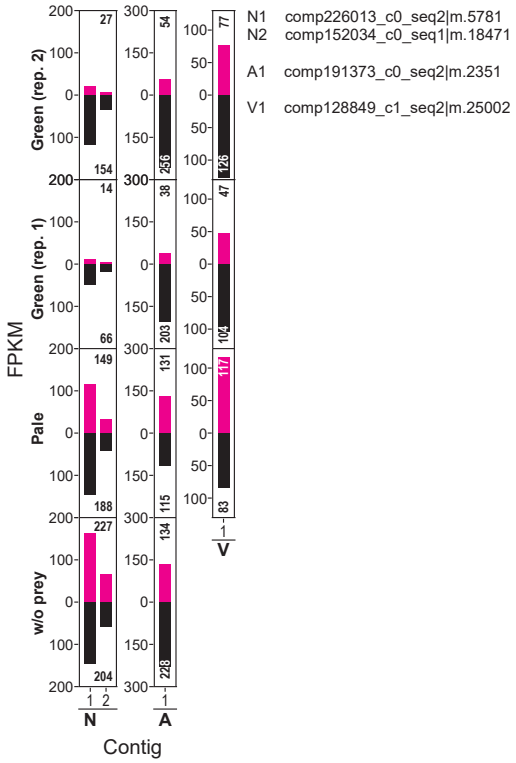

N1 comp226013_c0_seq2|m.5781
N2 comp152034_c0_seq1|m.18471

A1 comp191373_c0_seq2|m.2351

V1 comp128849_c1_seq2|m.25002

Type VII

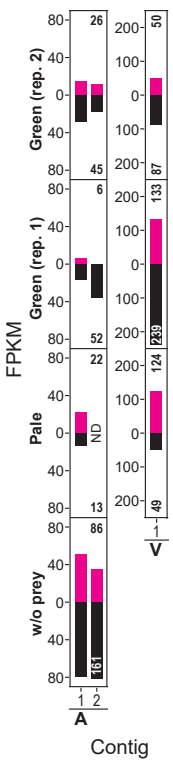

A1 comp198938_c1_seq1|m.14393
A2 comp198938_c2_seq2|m.44474

V1 comp128558_c4_seq1|m.2996

Myosin 2

Other types

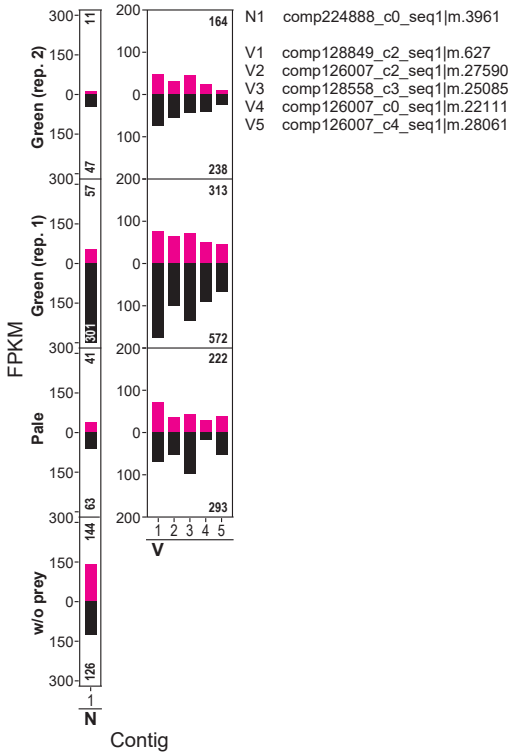

N1 comp224888_c0_seq1|m.3961

V1 comp128849_c2_seq1|m.627
V2 comp126007_c2_seq1|m.27590
V3 comp128558_c3_seq1|m.25085
V4 comp126007_c0_seq1|m.22111
V5 comp126007_c4_seq1|m.28061

Actin

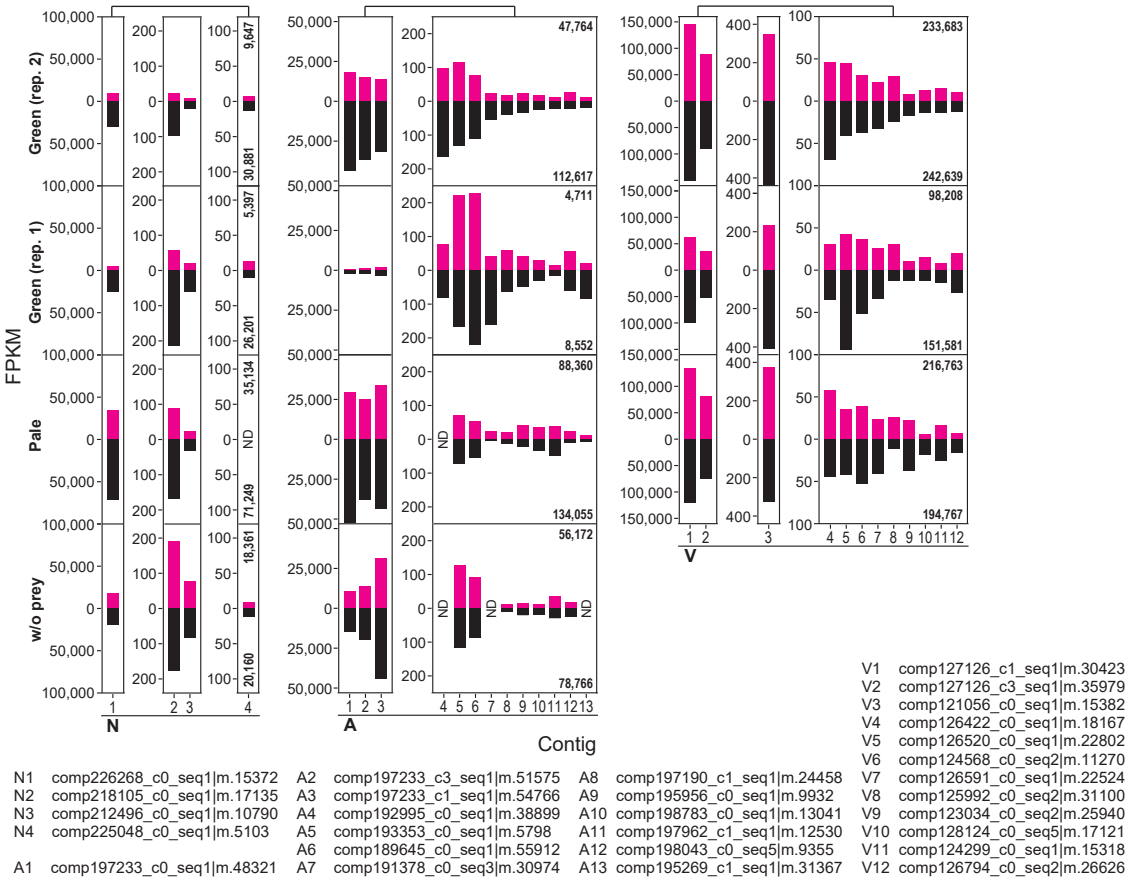

Figure 3.3. Comparison of the effect of the photosynthetic trait of bacterial prey on mRNA levels of selected genes among *Naegleria* sp., *Acanthamoeba* sp. and *Vannella* sp.

Respective amoebae were co-cultured with green or pale *S. elongatus* prey under dark and then transferred to light (200 µE m^{-2} s^{-1}). The cultures with green prey were performed twice independently and the both results (rep. 1 and rep. 2) are shown. To examine the effect of illumination that is independent of prey, respective amoebae were cultured in an organic growth medium without prey under dark and then transferred to light (w/o prey). Graphs show the mRNA levels (FPKM values) of contigs that are related to oxidative stress responses, carotenoid synthesis, DNA repair, respiration, v-type proton ATPase, proteolysis, oxygen reducing metabolisms, myosin, and actin under dark (black bar) and light (magenta bar) conditions. Each bar corresponds to one contig. For example, there are four, three, and three contigs encoding superoxide dismutase in *Naegleria* sp. (N), *Acanthamoeba* sp. (A), and *Vannella* sp. (V),

respectively. Numbers in the graph indicate total of the FPKM values in respective conditions. The FPKM values of respective contigs were compared only when the total of values of two comparative conditions were ≥20. Otherwise, the data were defied as not detected (ND). The contig IDs are shown beside each graph.

Oxidative stress responses 1

Superoxide dismutase

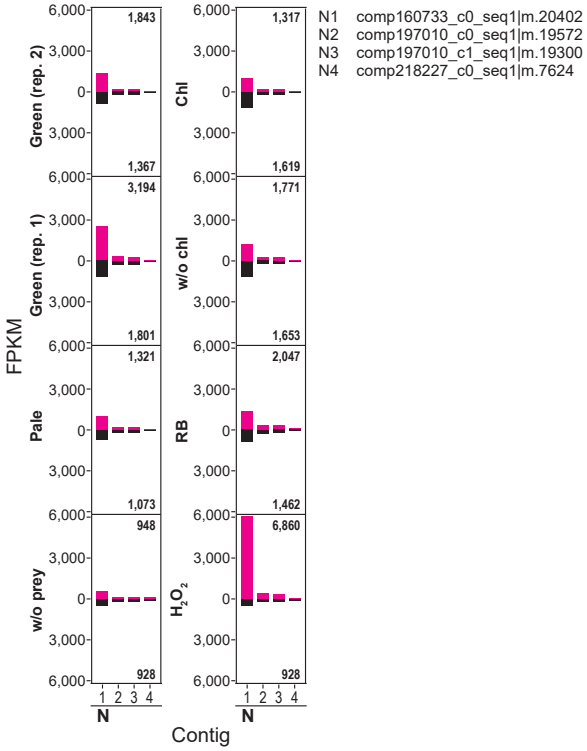

Catalase

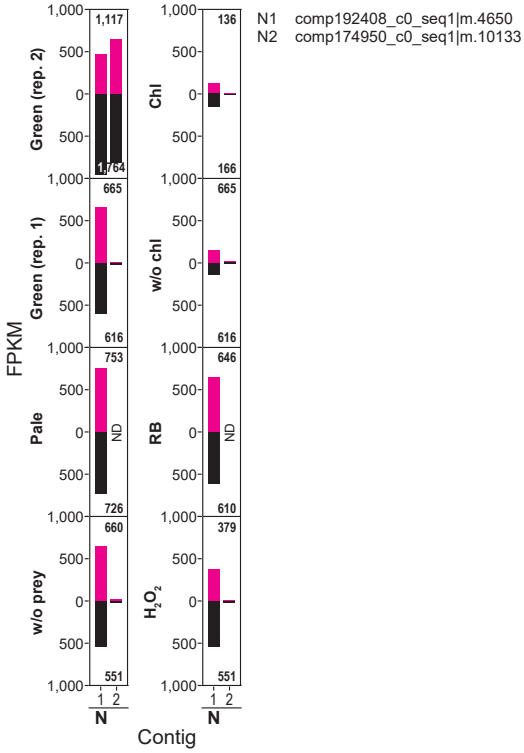

Peroxiredoxin

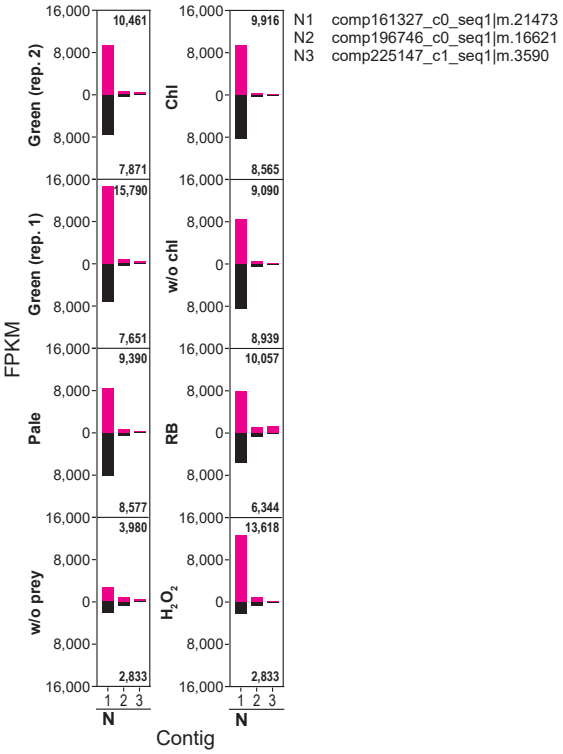

Glutaredoxin

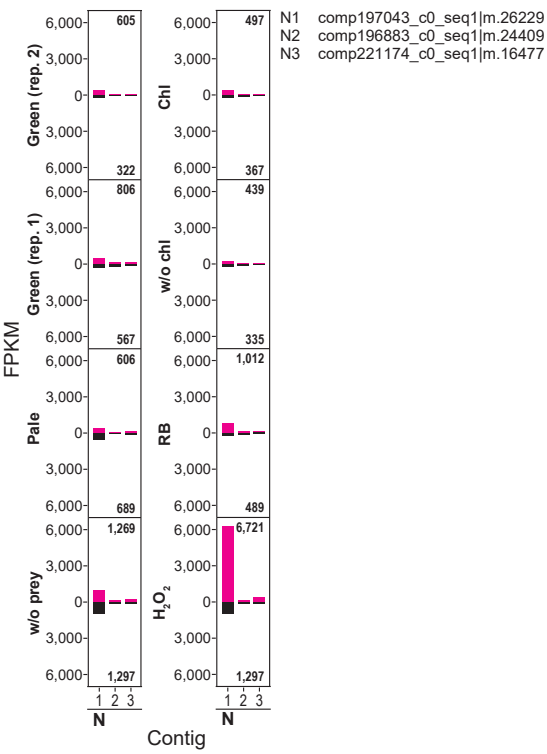

Oxidative stress responses 2

Thioredoxin

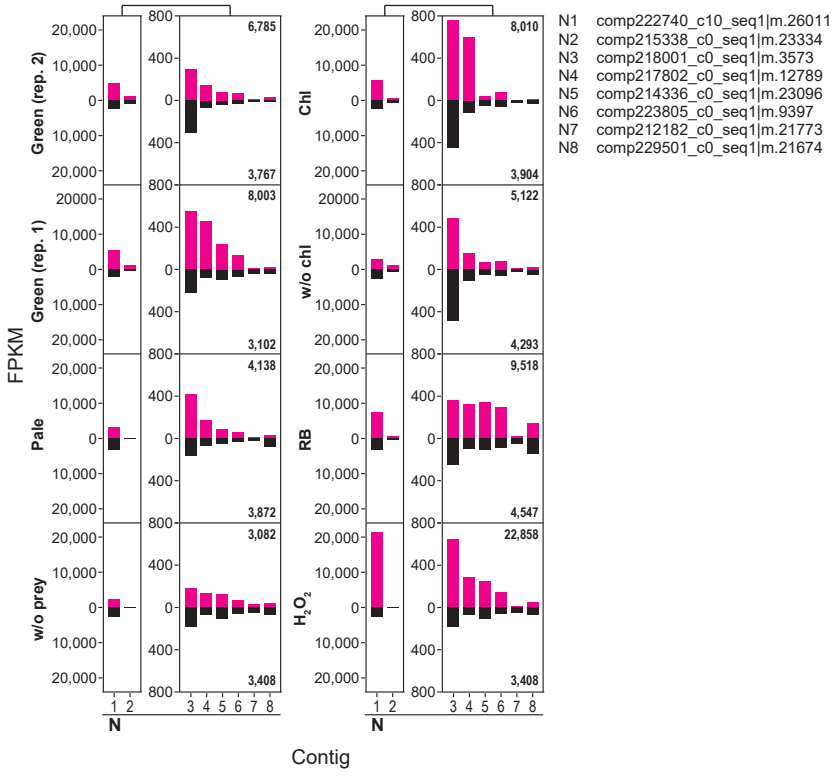

N1 comp222740_c10_seq1|m.26011
N2 comp215338_c0_seq1|m.23334
N3 comp218001_c0_seq1|m.3573
N4 comp217802_c0_seq1|m.12789
N5 comp214336_c0_seq1|m.23096
N6 comp223805_c0_seq1|m.9397
N7 comp212182_c0_seq1|m.21773
N8 comp229501_c0_seq1|m.21674

Glutathione synthetase

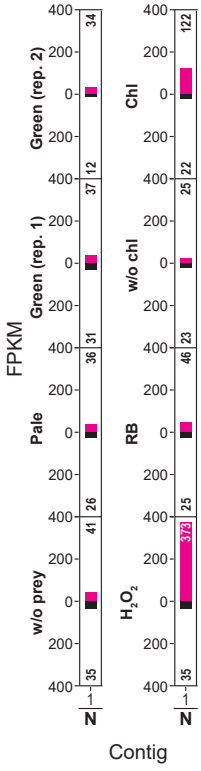

N1 comp170906_c0_seq1|m.12558

Glutathione peroxidase

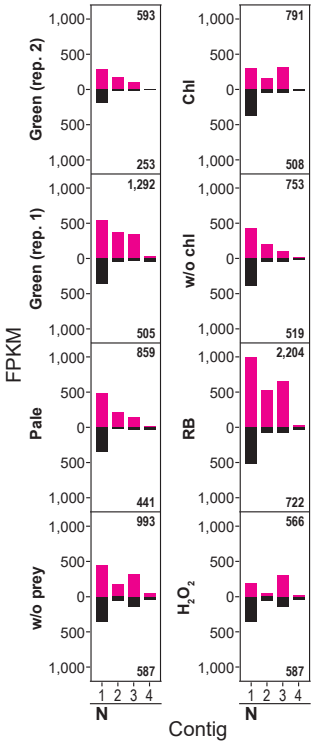

N1 comp197051_c1_seq2|m.22797
N2 comp227059_c0_seq3|m.1915
N3 comp226183_c1_seq1|m.3708
N4 comp230203_c0_seq1|m.20301

Glutathion S-transferase

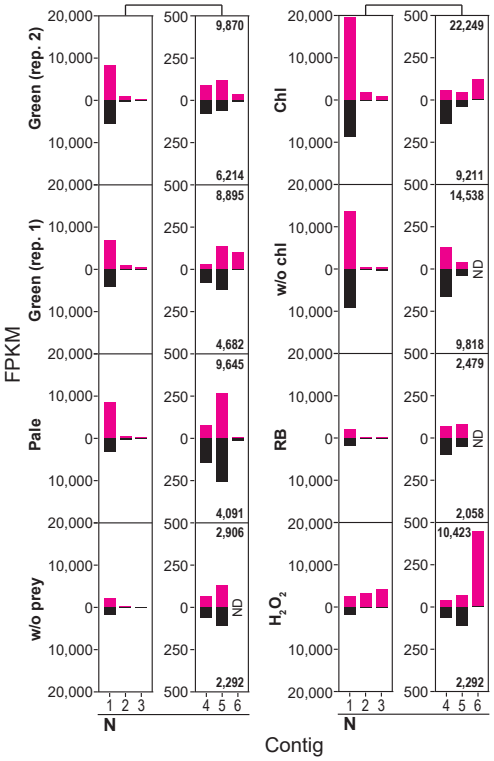

N1 comp222120_c0_seq1|m.19841
N2 comp215852_c0_seq1|m.19804
N3 comp220161_c1_seq1|m.17653
N4 comp219327_c0_seq1|m.18450
N5 comp171992_c0_seq1|m.19016
N6 comp219524_c0_seq1|m.20621

Oxidative stress responses 3

Carbonyl reductase

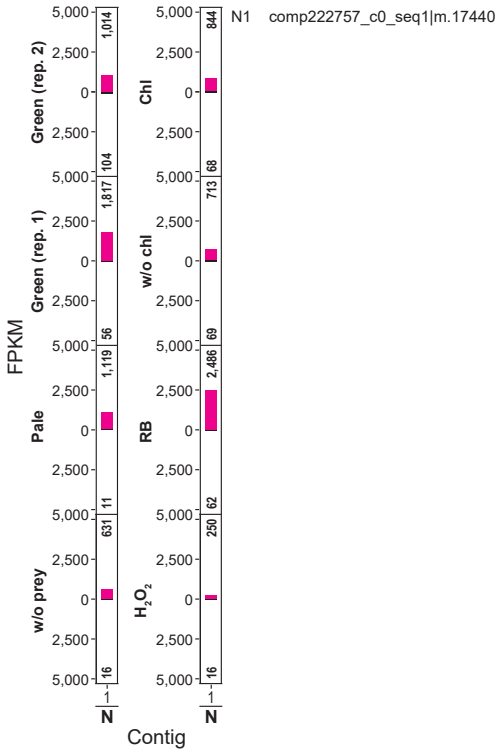

Peptide methionine sulfoxide reductase

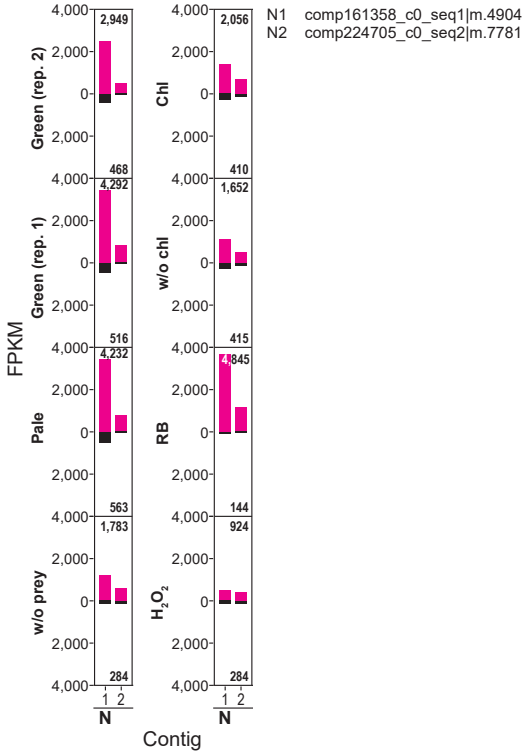

Apolipoprotein D

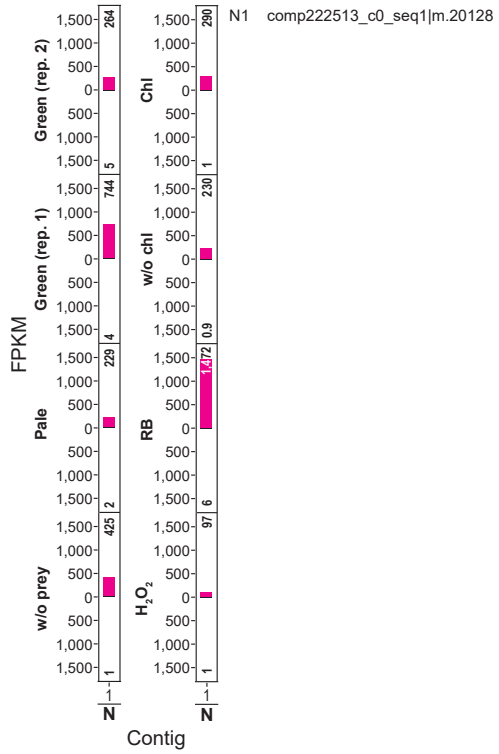

Cob(I)yrinic acid a,c-diamide adenosyltransferase

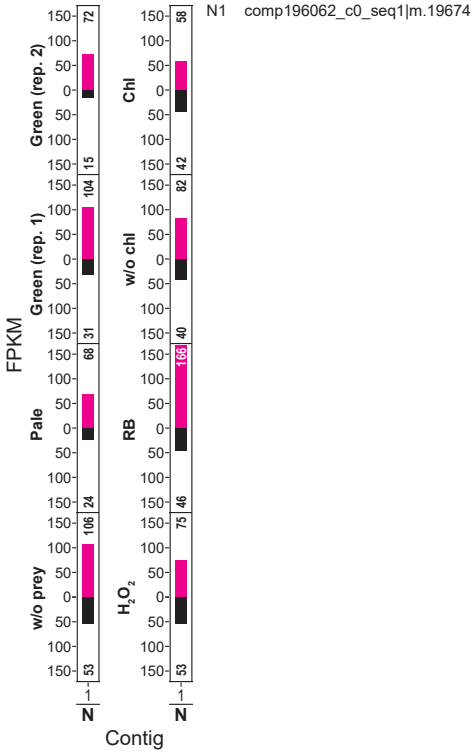

Carotenoid synthesis

Carotene epsilon-monooxygenase

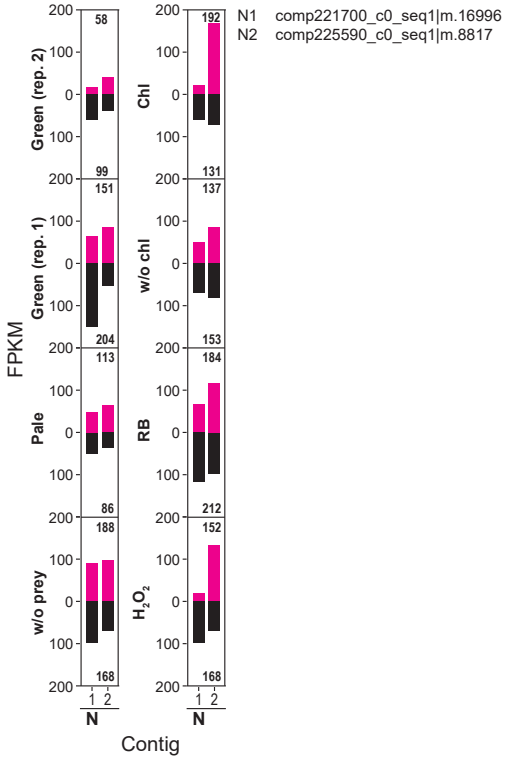

Phytoene desaturase

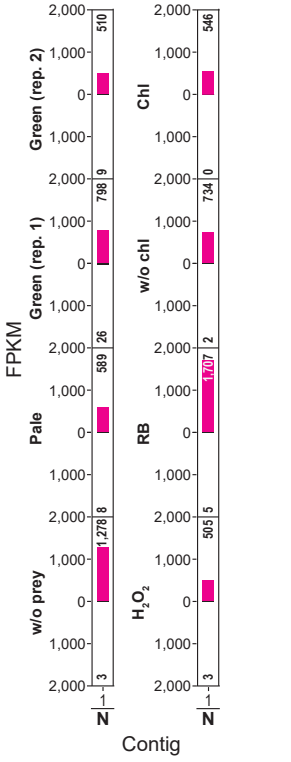

N1 comp217346_c0_seq1|m.11870

Geranylgeranyl pyrophosphate synthase

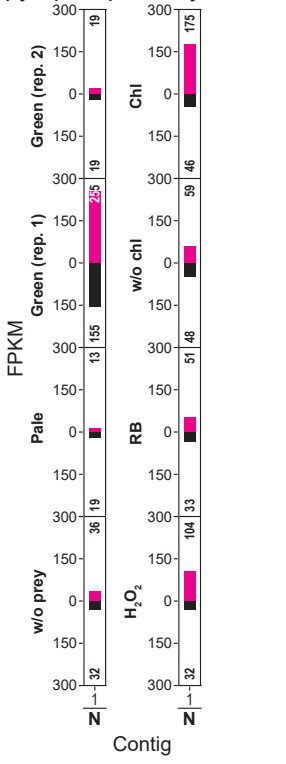

N1 comp213578_c0_seq1|m.14664

DNA repair

ALK B

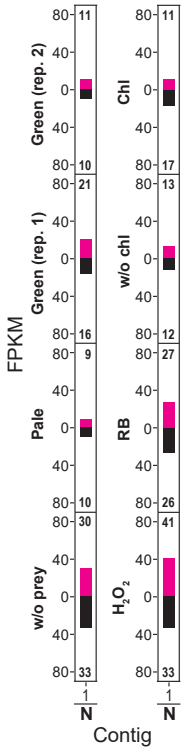

N1 comp220611_c0_seq1|m.15695

Deoxyribodipyrimidine photo-lyase

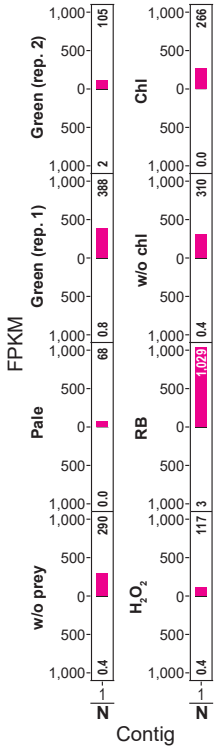

N1 comp222533_c0_seq1|m.15479

DNA-(apurinic or apyrimidinic site) lyase

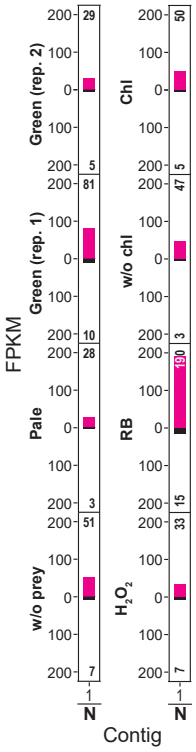

N1 comp225006_c0_seq1|m.7768

MSH2

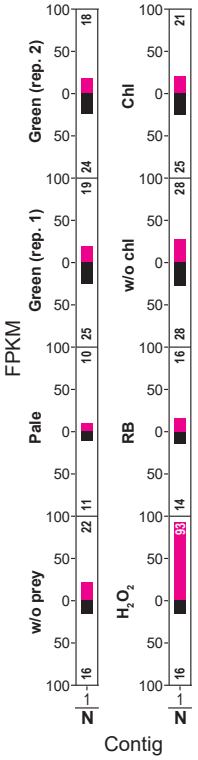

N1 comp225420_c0_seq1|m.4740

RAD5

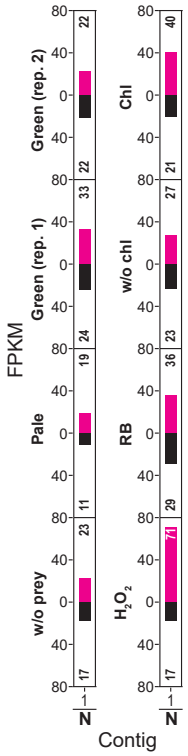

N1 comp218612_c0_seq1|m.4221

RAD51

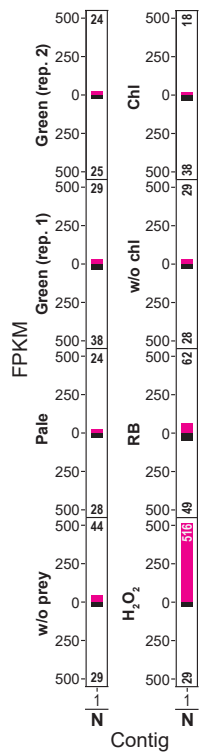

N1 comp196015_c0_seq1|m.15894

XRCC

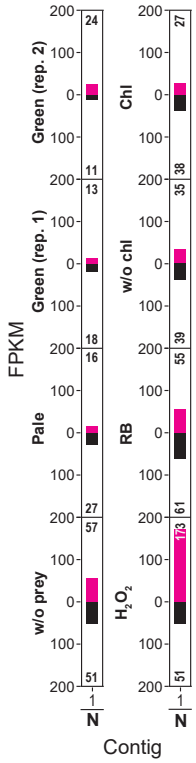

N1 comp221477_c2_seq1|m.17537

Respiration 1

ATP/ADP translocase

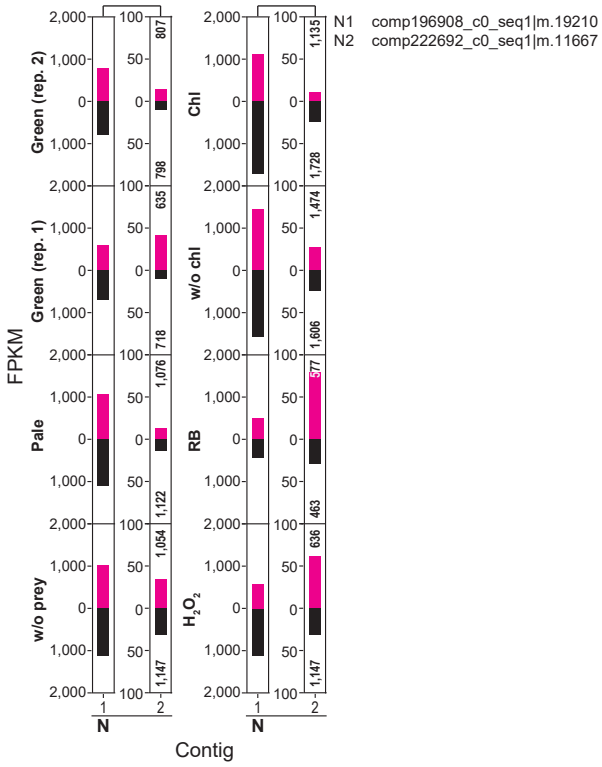

cox15

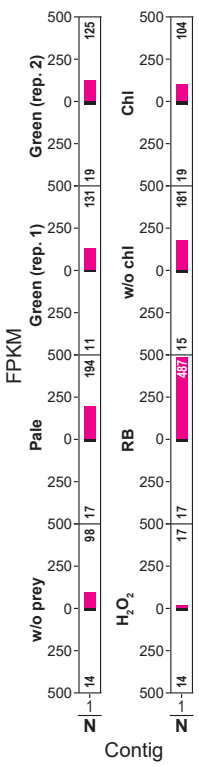

N1 comp228272_c0_seq1|m.12304

cox19

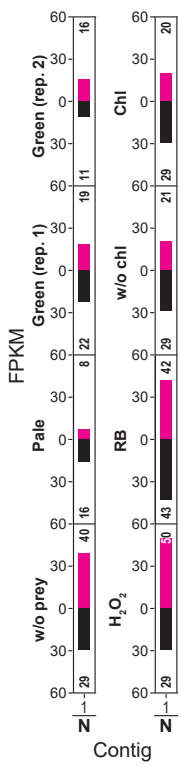

N1 comp169334_c0_seq1|m.12493

Prohibitin 1

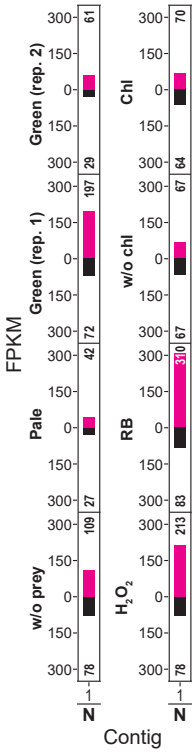

N1 comp228209_c0_seq1|m.19680

Prohibitin 2

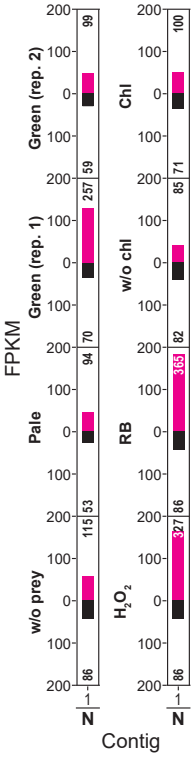

N1 comp227900_c0_seq1|m.15768

TIM14

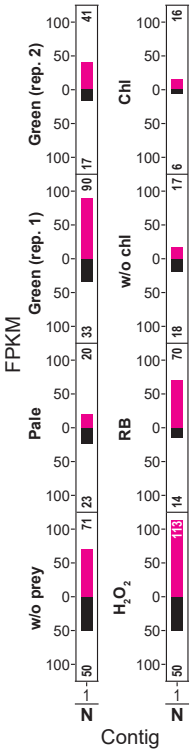

N1 comp220797_c0_seq1|m.5849

TIM17

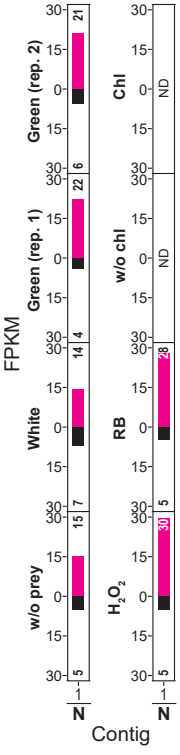

N1 comp186302_c0_seq1|m.19129

Respiration 2

TIM44

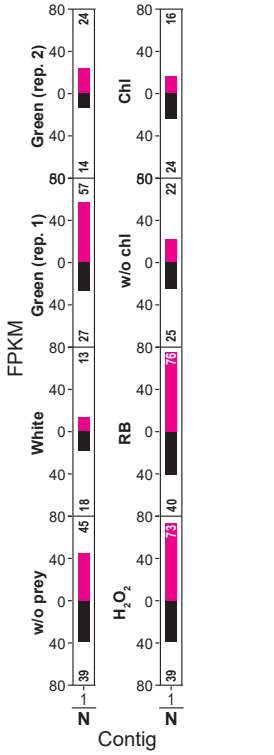

N1 comp182943_c0_seq1|m.12522

TIM50

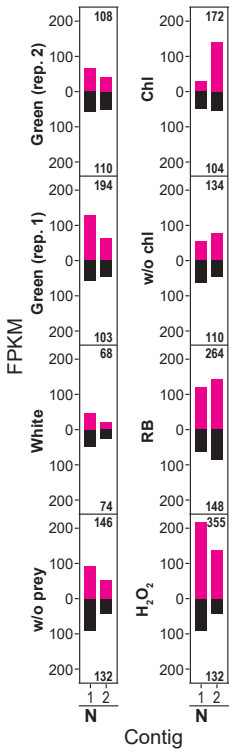

N1 comp168559_c0_seq1|m.14233
N2 comp221198_c0_seq1|m.14508

TOM40

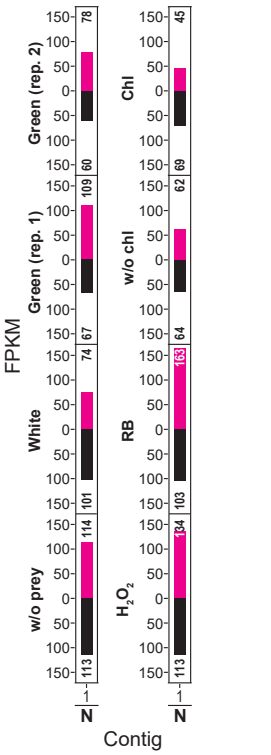

N1 comp227996_c0_seq1|m.16805

Vacuolar-type H⁺-ATPase

v-ATPase subunit A

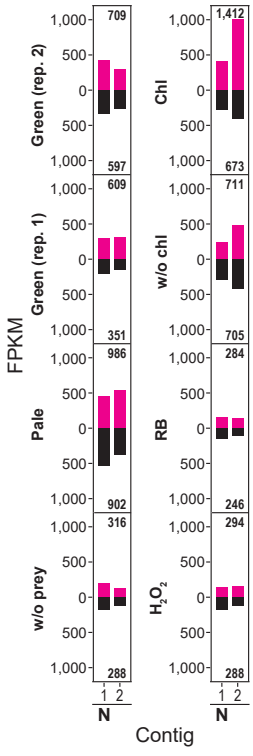

N1 comp227542_c0_seq1|m.10798
N2 comp221051_c0_seq1|m.7823

v-ATPase subunit B

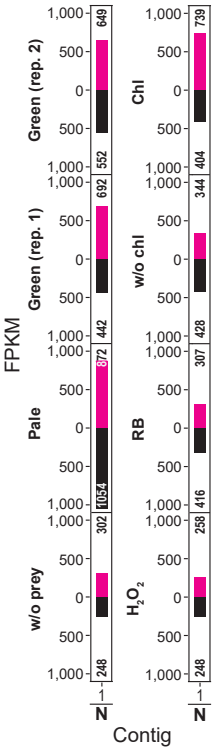

N1 comp196952_c0_seq1|m.13622

v-ATPase subunit C

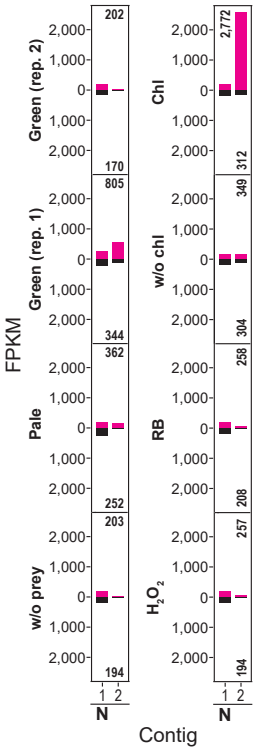

N1 comp196930_c0_seq1|m.11356
N2 comp196942_c0_seq1|m.21462

v-ATPase subunit D

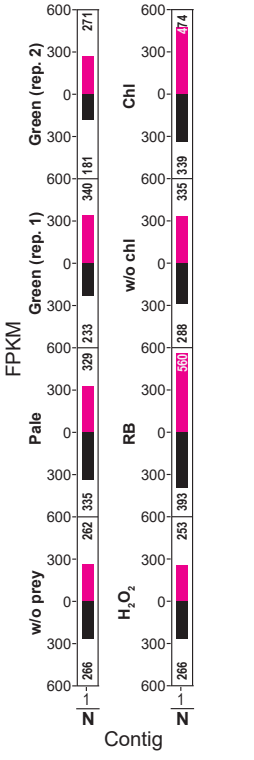

N1 comp196607_c0_seq1|m.18535

v-ATPase subunit E

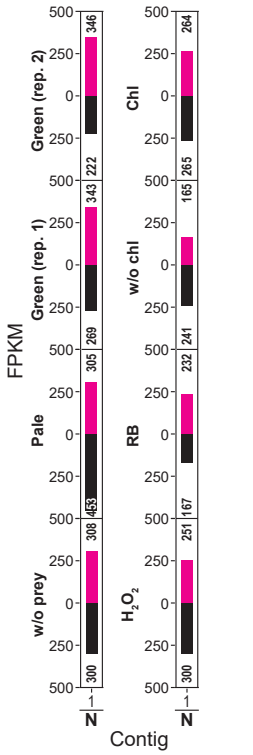

N1 comp227605_c0_seq1|m.19734

v-ATPase subunit F

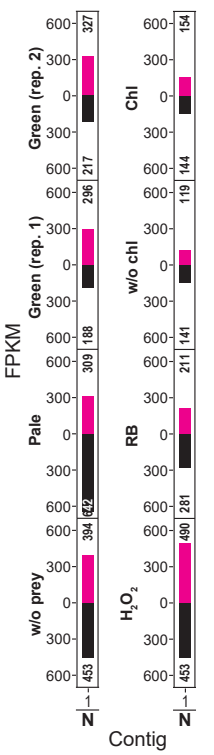

N1 comp227723_c0_seq1|m.25000

v-ATPase subunit H

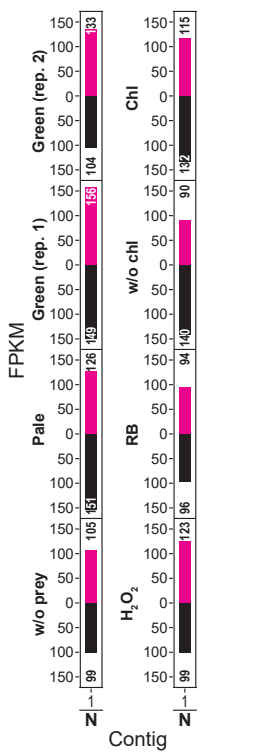

N1 comp158917_c0_seq1|m.13351

V-ATPase subunit c''

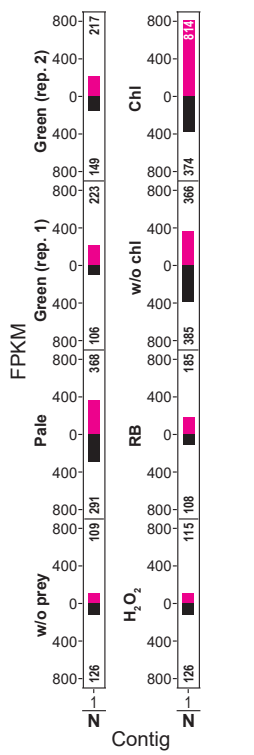

N1 comp227747_c0_seq1|m.19247

Proteolysis 1

Cathepsin A

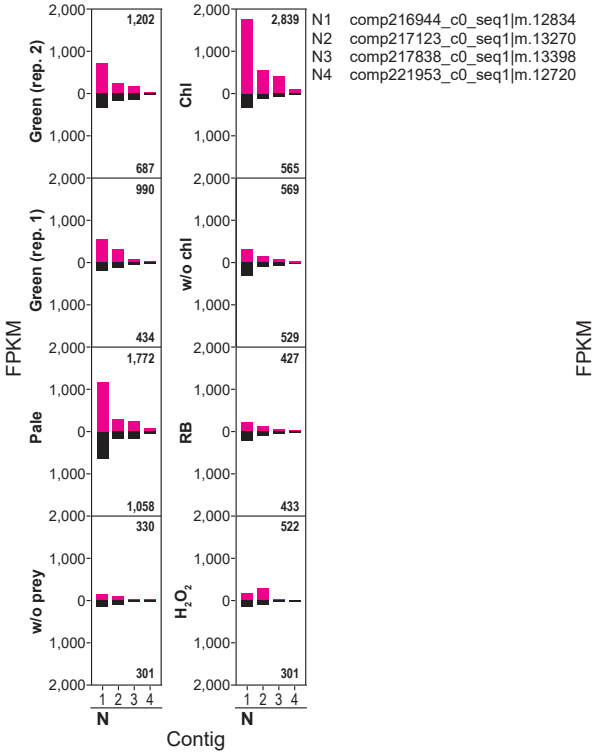

N1 comp216944_c0_seq1|m.12834
N2 comp217123_c0_seq1|m.13270
N3 comp217838_c0_seq1|m.13398
N4 comp221953_c0_seq1|m.12720

Cathepsin C

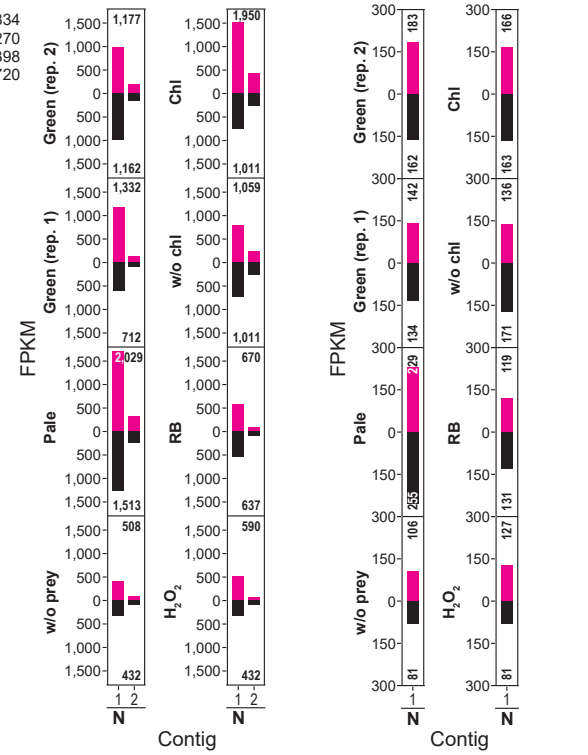

N1 comp214966_c0_seq1|m.12794
N2 comp221851_c2_seq3|m.12596

Cathepsin F

N1 comp221740_c0_seq1|m.7856

Cathepsin B

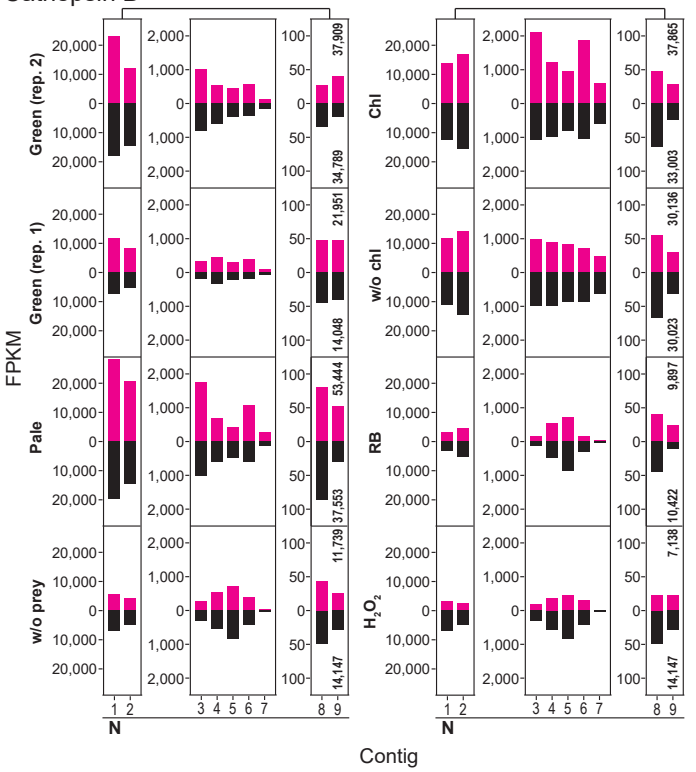

N1 comp222264_c1_seq2|m.24062
N2 comp222264_c0_seq2|m.18254
N3 comp161120_c0_seq1|m.21113
N4 comp196690_c1_seq1|m.20318
N5 comp196690_c0_seq1|m.25763
N6 comp161120_c1_seq1|m.24792
N7 comp222291_c0_seq1|m.19331
N8 comp219614_c1_seq1|m.18120
N9 comp224223_c0_seq1|m.11597

Proteolysis 2

Cathepsin L

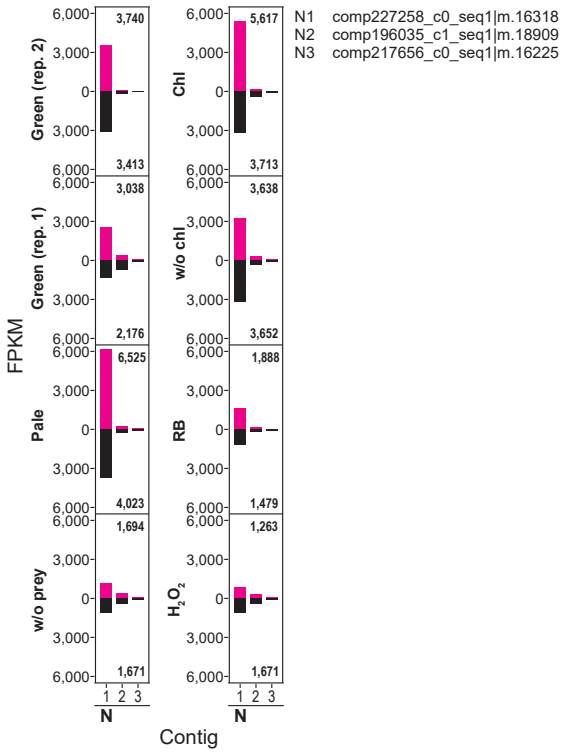

Cathepsin Z

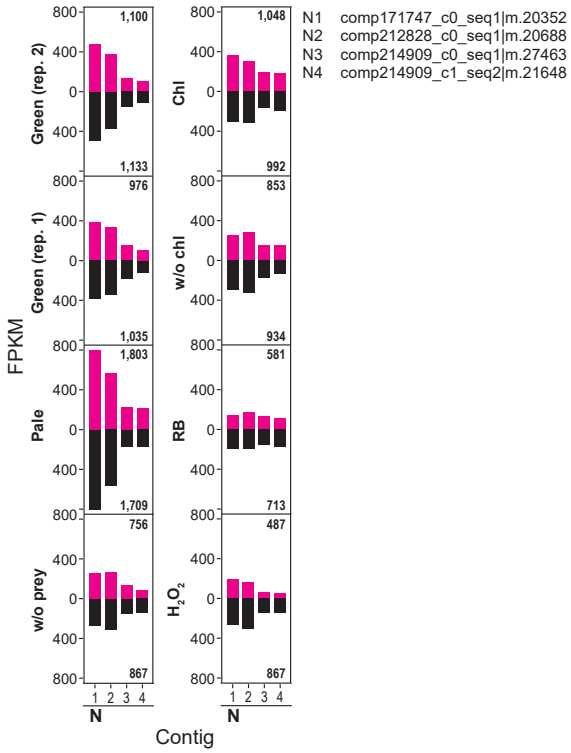

Chymotrypsin

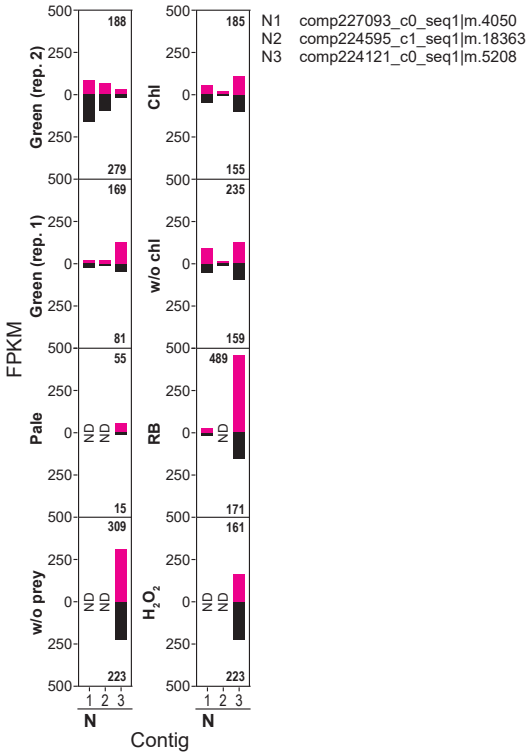

Oxygen reducing metabolism

Methylsterol monooxygenase

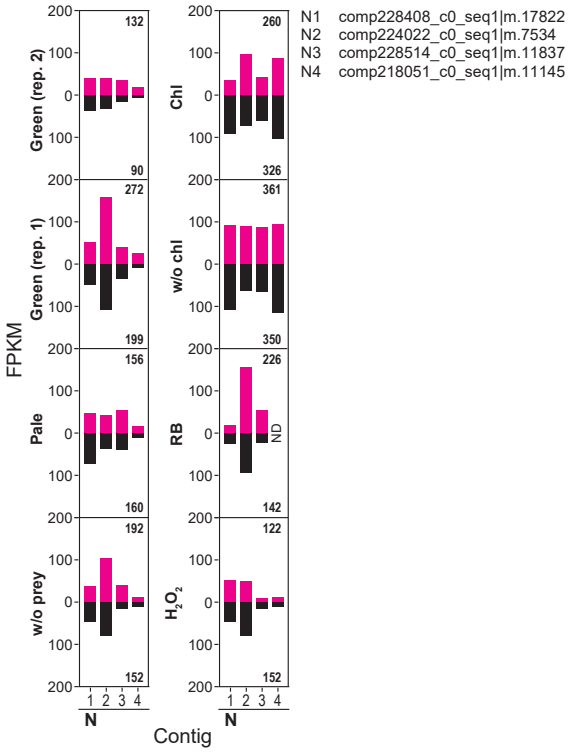

Squalene monooxygenase

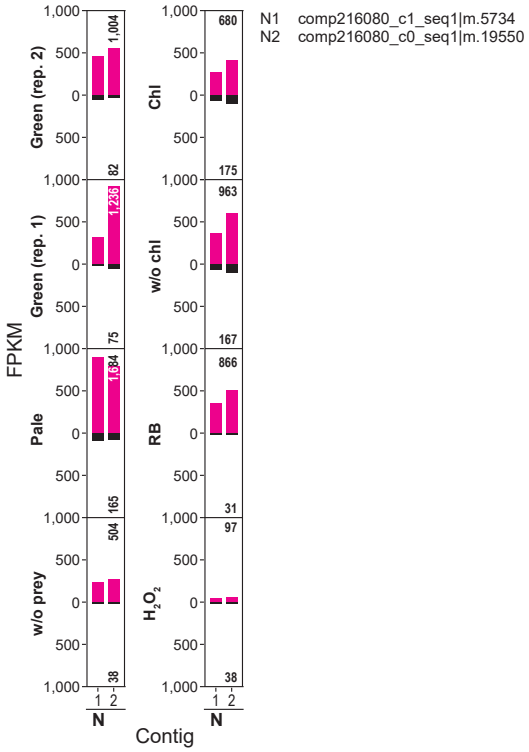

L-gulonolactone oxidase

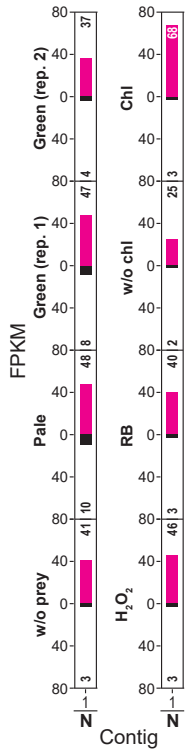

N1 comp220489_c0_seq1|m.13475

Myosin

Type I

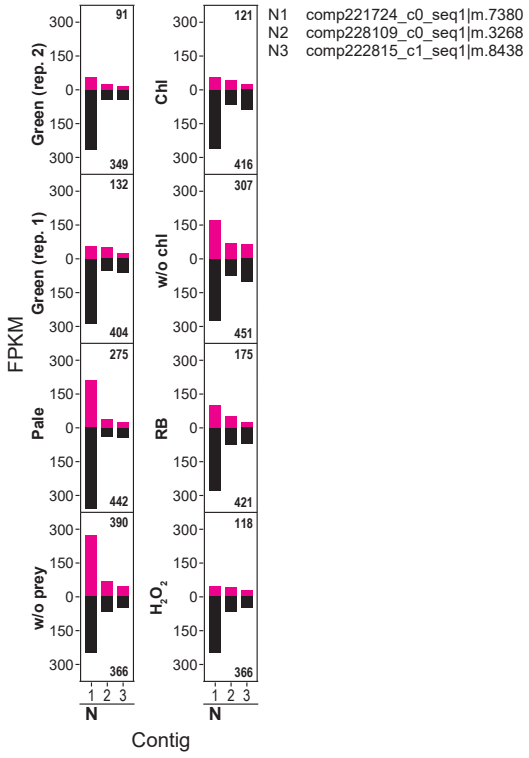

Type II

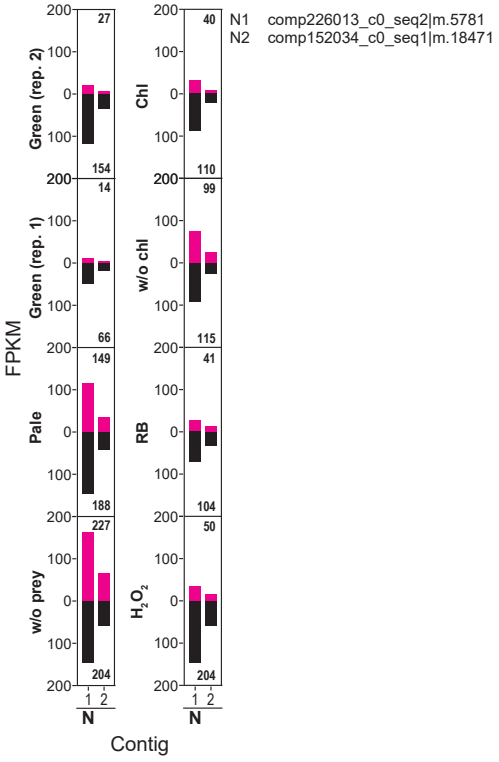

Other types

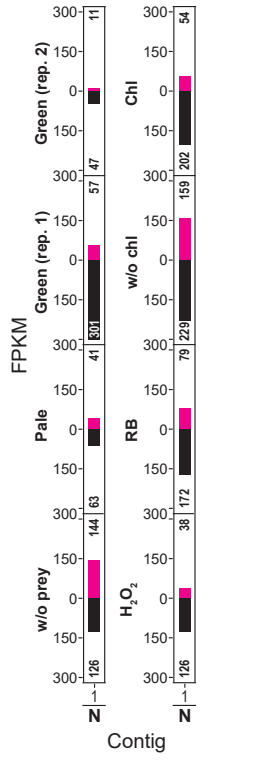

N1 comp224888_c0_seq1|m.3961

Actin

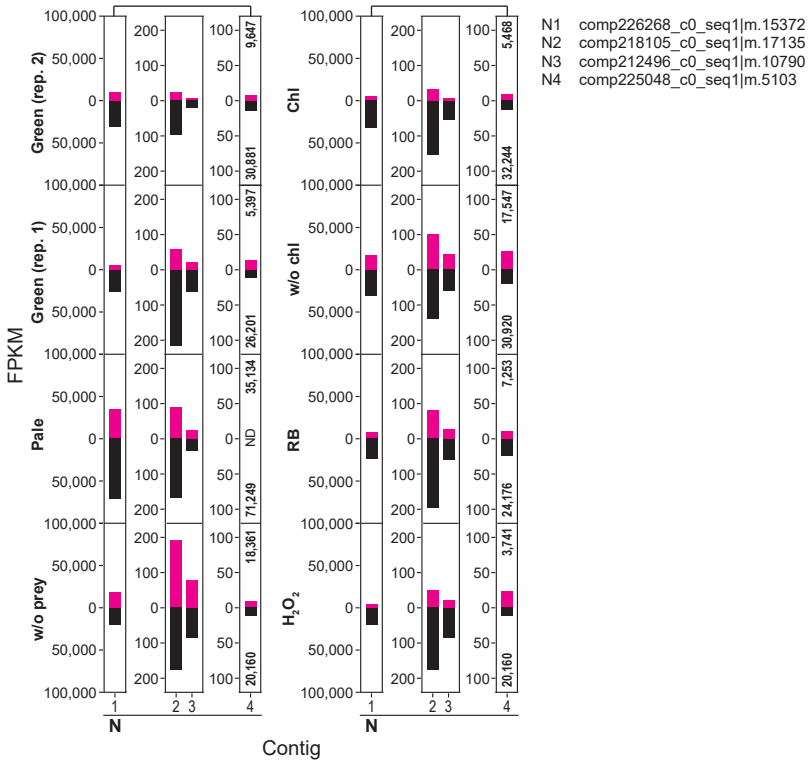

Figure 3.4. Effect of chlorophyll and ROS on mRNA levels of selected genes in *Naegleria* sp.

To examine effects of chlorophyll *a*, which produces singlet oxygen by illumination, *Naegleria* sp. was cultured with *E. coli* stained with/without chlorophyll *a* (Chl and w/o chl, respectively) under dark for 12 h (dark), and then transferred to light (200 µE m^{-2} s^{-1}) for 1 h (light). To examine the effects of singlet oxygen, *Naegleria* sp. was cultured without prey and with 30 nM Rose Bengal (RB), which produces singlet oxygen by illumination, under dark for 12 h (dark), and then transferred to light for 1 h (light). To examine the effects of H_2O_2, *Naegleria* sp. was cultured without prey for 12 h under dark (w/o H_2O_2), and then treated with 4 µM H_2O_2 under dark for 1 h (w/ H_2O_2). Graphs show the mRNA levels (FPKM values) of contigs that are related to oxidative stress response, carotenoid synthesis, DNA repair, respiration, v-type proton ATPase, proteolysis, oxygen reducing metabolisms, myosin, and actin under dark (black bar), light (magenta bar) or treatment of H_2O_2 under dark (magenta bar) conditions. Each bar corresponds to one contig. For example, there are four contigs encoding superoxide dismutase in *Naegleria* sp. (N). Numbers in the graph indicates the total of the FPKM

values in respective conditions. The FPKM values of respective contigs were compared only when the total of values of two comparative conditions were ≥20. Otherwise, the data were defied as not detected (ND). The contig IDs are shown beside each graph. For comparison, the effects of green (rep. 1 and rep. 2) or pale *S. elongatus* prey and illumination alone (w/o prey) (shown in Figure 3.3) are also regenerated.

Table 3.1. Gene ontology terms enriched in up-regulated genes (≥2 fold change) when *Naegleria* sp. co-cultured with green *S. elongatus* prey were transferred from dark to light (*P*-value ≤ 0.05).

Category	GO term		GO id	*P*-value
-	BP	methanogenesis	GO:0015948	0
-	MF	cobaltochelatase activity	GO:0051116	0
-	MF	4 iron, 4 sulfur cluster binding	GO:0051539	4.14E-38
-	MF	iron-sulfur cluster binding	GO:0051536	7.04E-38
-	BP	biosynthetic process	GO:0009058	6.70E-31
-	BP	oxidation-reduction process	GO:0055114	1.05E-26
-	BP	cobalamin biosynthetic process	GO:0009236	6.56E-19
-	MF	catalytic activity	GO:0003824	1.81E-18
-	BP	chlorophyll biosynthetic process	GO:0015995	7.62E-17
-	MF	oxidoreductase activity	GO:0016491	6.19E-16
-	MF	magnesium chelatase activity	GO:0016851	1.31E-15
-	MF	nickel cation binding	GO:0016151	1.30E-11
-	BP	methanogenesis, from carbon dioxide	GO:0019386	2.46E-10
-	MF	magnesium ion binding	GO:0000287	1.78E-09
-	BP	isoleucine biosynthetic process	GO:0009097	1.01E-08
-	MF	protein histidine kinase activity	GO:0004673	1.40E-08
-	MF	metal ion binding	GO:0046872	4.76E-08
-	BP	signal transduction by protein phosphorylation	GO:0023014	1.72E-07
-	MF	transferase activity, transferring glycosyl groups	GO:0016757	2.17E-07
-	BP	phosphorelay signal transduction system	GO:0000160	2.33E-07
Respiration	MF	FMN binding	GO:0010181	6.12E-07
-	BP	one-carbon metabolic process	GO:0006730	7.69E-07
Carotene	BP	carotenoid biosynthetic process	GO:0016117	9.78E-07
Respiration	MF	flavin adenine dinucleotide binding	GO:0050660	1.48E-06
-	BP	arginine biosynthetic process	GO:0006526	1.77E-06
-	MF	glutamate synthase activity	GO:0015930	2.56E-06
-	BP	polysaccharide biosynthetic process	GO:0000271	3.20E-06
-	MF	aminoacyl-tRNA ligase activity	GO:0004812	3.50E-06
-	BP	valine biosynthetic process	GO:0009099	3.92E-06
-	BP	aromatic amino acid family biosynthetic process	GO:0009073	4.66E-06
-	BP	threonine biosynthetic process	GO:0009088	4.68E-06
-	MF	coenzyme F420 hydrogenase activity	GO:0050454	4.68E-06
-	BP	tRNA aminoacylation for protein translation	GO:0006418	6.68E-06
-	BP	tRNA processing	GO:0008033	6.89E-06
-	BP	'de novo' IMP biosynthetic process	GO:0006189	9.64E-06
-	BP	DNA restriction-modification system	GO:0009307	1.74E-05
-	MF	helicase activity	GO:0004386	2.01E-05
-	MF	ferredoxin hydrogenase activity	GO:0008901	2.09E-05
-	BP	histidine biosynthetic process	GO:0000105	2.19E-05
-	BP	glutamate biosynthetic process	GO:0006537	2.55E-05
-	BP	leucine biosynthetic process	GO:0009098	2.58E-05
-	MF	oxidoreductase activity, acting on the CH-CH group of donors, NAD or NADP as acceptor	GO:0016628	2.61E-05
-	MF	oxidoreductase activity, acting on the CH-NH2 group of donors	GO:0016638	2.65E-05
-	MF	lyase activity	GO:0016829	5.25E-05
-	BP	membrane lipid biosynthetic process	GO:0046467	5.46E-05
-	MF	thiamine pyrophosphate binding	GO:0030976	5.55E-05
-	BP	thiamine biosynthetic process	GO:0009228	5.85E-05
-	BP	cell wall organization	GO:0071555	8.91E-05
-	BP	lysine biosynthetic process via diaminopimelate	GO:0009089	9.10E-05
-	BP	glutamine metabolic process	GO:0006541	9.89E-05
-	MF	oligosaccharyl transferase activity	GO:0004576	1.12E-04
-	BP	photosynthesis	GO:0015979	1.23E-04
-	MF	oxidoreductase activity, acting on paired donors, with incorporation or reduction of molecular oxygen	GO:0016705	1.39E-04
-	MF	pyridoxal phosphate binding	GO:0030170	1.47E-04
-	BP	mycothiol biosynthetic process	GO:0010125	1.62E-04
-	MF	formate dehydrogenase (NAD+) activity	GO:0008863	1.68E-04
-	BP	thiamine diphosphate biosynthetic process	GO:0009229	1.97E-04

Notes: Some GO terms were categorized into 10 categories which were based on their functions. Categories: Actomyosin, Carotene, Cytoskeleton, DNA repair, Motion, Oxidative stress responses, Phagocytosis, Proteolysis, Respiration, V-ATPase. GO, gene ontology; MF, molecular function; CC, cellular component; and BP, biological process. The results shown are based on reproduction by two independent cultures and experiments.

Table 3.1. Continued.

Category	GO term		GO id	*P*-value
-	MF	nitronate monooxygenase activity	GO:0018580	2.07E-04
-	MF	ATP binding	GO:0005524	2.11E-04
-	BP	carbohydrate biosynthetic process	GO:0016051	2.17E-04
-	MF	NAD binding	GO:0051287	2.33E-04
-	BP	transcription antitermination	GO:0031564	2.54E-04
-	MF	transferase activity, transferring alkyl or aryl (other than methyl) groups	GO:0016765	2.54E-04
-	MF	4-hydroxy-tetrahydrodipicolinate reductase	GO:0008839	2.54E-04
-	MF	NADP binding	GO:0050661	2.67E-04
-	BP	transport	GO:0006810	2.80E-04
-	BP	glycerophospholipid metabolic process	GO:0006650	2.99E-04
-	BP	cellular amino acid metabolic process	GO:0006520	3.26E-04
-	MF	cobalamin binding	GO:0031419	3.54E-04
-	BP	Mo-molybdopterin cofactor biosynthetic process	GO:0006777	3.83E-04
-	BP	intein-mediated protein splicing	GO:0016539	4.64E-04
-	MF	CoB--CoM heterodisulfide reductase activity	GO:0051912	5.58E-04
-	BP	isoprenoid biosynthetic process	GO:0008299	6.05E-04
DNA repair	MF	DNA photolyase activity	GO:0003913	6.06E-04
-	MF	tRNA (guanine-N2-)-methyltransferase activity	GO:0004809	6.17E-04
-	MF	coenzyme-B sulfoethylthiotransferase activity	GO:0050524	6.18E-04
-	MF	glutamate synthase (NADPH) activity	GO:0004355	6.29E-04
-	MF	formylmethanofuran dehydrogenase activity	GO:0018493	6.35E-04
Carotene	MF	geranylgeranyl reductase activity	GO:0045550	6.36E-04
-	BP	tetrapyrrole biosynthetic process	GO:0033014	6.36E-04
-	MF	coenzyme F420-dependent N5,N10-methenyltetrahydromethanopterin reductase activity	GO:0018537	6.36E-04
-	MF	N5,N10-methenyltetrahydromethanopterin hydrogenase activity	GO:0047068	6.36E-04
-	BP	coenzyme biosynthetic process	GO:0009108	6.56E-04
-	BP	protoporphyrinogen IX biosynthetic process	GO:0006782	7.01E-04
-	BP	cellular amino acid biosynthetic process	GO:0008652	7.12E-04
-	BP	DNA replication	GO:0006260	9.24E-04
-	MF	adenyl nucleotide binding	GO:0030554	9.91E-04
-	MF	nucleotidyltransferase activity	GO:0016779	1.05E-03
-	MF	nucleotide binding	GO:0000166	1.12E-03
-	MF	oxidoreductase activity, acting on the CH-OH group of donors, NAD or NADP as acceptor	GO:0016616	1.22E-03
-	BP	rRNA methylation	GO:0031167	1.25E-03
-	BP	growth	GO:0040007	1.33E-03
-	MF	DNA binding	GO:0003677	1.34E-03
-	BP	DNA catabolic process, exonucleolytic	GO:0000738	1.36E-03
-	MF	tRNA binding	GO:0000049	1.37E-03
-	MF	protein methyltransferase activity	GO:0008276	1.48E-03
-	BP	peptidoglycan biosynthetic process	GO:0009252	1.54E-03
Oxidative stress responses	MF	oxidoreductase activity, acting on the CH-CH group of donors	GO:0016627	1.57E-03
-	MF	3-beta-hydroxy-delta5-steroid dehydrogenase activity	GO:0003854	1.77E-03
-	MF	phosphorelay sensor kinase activity	GO:0000155	1.85E-03
-	MF	nuclease activity	GO:0004518	2.05E-03
-	MF	glutamine-fructose-6-phosphate transaminase (isomerizing) activity	GO:0004360	2.05E-03
-	BP	methionine biosynthetic process	GO:0009086	2.17E-03
-	BP	molybdopterin cofactor biosynthetic process	GO:0032324	2.37E-03
-	MF	phosphoglucosamine mutase activity	GO:0008966	2.38E-03
-	CC	molybdopterin synthase complex	GO:0019008	2.38E-03
-	MF	transferase activity	GO:0016740	2.48E-03
-	MF	asparagine synthase (glutamine-hydrolyzing) activity	GO:0004066	2.70E-03
-	BP	asparagine biosynthetic process	GO:0006529	2.70E-03
-	MF	ketol-acid reductoisomerase activity	GO:0004455	2.87E-03
-	CC	extrachromosomal circular DNA	GO:0005727	2.99E-03
-	CC	ATP-binding cassette (ABC) transporter complex	GO:0043190	3.15E-03
-	CC	S-layer	GO:0030115	3.15E-03
-	MF	acetylglucosaminyltransferase activity	GO:0008375	3.69E-03
-	BP	formate metabolic process	GO:0015942	4.15E-03
-	BP	steroid biosynthetic process	GO:0006694	4.49E-03

Table 3.1. Continued.

Category	GO term		GO id	*P*-value
-	BP	metabolic process	GO:0008152	4.89E-03
-	MF	aromatase activity	GO:0070330	5.26E-03
-	MF	N-methyltransferase activity	GO:0008170	5.40E-03
-	MF	pyruvate, water dikinase activity	GO:0008986	5.52E-03
-	MF	carbon-monoxide dehydrogenase (acceptor) activity	GO:0018492	5.87E-03
-	MF	ATPase activity	GO:0016887	5.94E-03
-	CC	chloroplast inner membrane	GO:0009706	5.97E-03
-	BP	'de novo' UMP biosynthetic process	GO:0044205	6.19E-03
-	MF	acetolactate synthase activity	GO:0003984	6.37E-03
-	MF	hydrolase activity, acting on acid anhydrides, catalyzing transmembrane movement of substances	GO:0016820	6.59E-03
-	MF	coenzyme binding	GO:0050662	6.80E-03
-	MF	lipid-transporting ATPase activity	GO:0034040	6.83E-03
Respiration	MF	proton-transporting ATP synthase activity, rotational mechanism	GO:0046933	7.11E-03
-	MF	oxidoreductase activity, acting on the aldehyde or oxo group of donors	GO:0016903	7.24E-03
-	BP	cation transport	GO:0006812	7.26E-03
-	MF	lysine-tRNA ligase activity	GO:0004824	7.26E-03
-	BP	lysyl-tRNA aminoacylation	GO:0006430	7.26E-03
-	MF	2-oxoglutarate synthase activity	GO:0047553	7.30E-03
-	MF	cobalamin-transporting ATPase activity	GO:0015420	7.31E-03
-	MF	chlorophyllide a oxygenase [overall] activity	GO:0010277	7.33E-03
-	MF	restriction endodeoxyribonuclease activity	GO:0015666	7.34E-03
-	MF	3-methyl-2-oxobutanoate dehydrogenase (ferredoxin) activity	GO:0043807	7.34E-03
-	BP	S-layer organization	GO:0045232	7.36E-03
-	BP	phenylacetate catabolic process	GO:0010124	7.38E-03
-	MF	phenylacetate-CoA ligase activity	GO:0047475	7.38E-03
-	MF	thiamine-phosphate kinase activity	GO:0009030	7.39E-03
-	BP	tryptophan biosynthetic process	GO:0000162	7.40E-03
-	BP	chorismate biosynthetic process	GO:0009423	7.40E-03
-	MF	oxidoreductase activity, acting on the CH-NH group of donors	GO:0016645	7.41E-03
-	MF	homoserine dehydrogenase activity	GO:0004412	7.41E-03
-	BP	lactate oxidation	GO:0019516	7.41E-03
-	MF	7,8-didemethyl-8-hydroxy-5-deazariboflavin synthase activity	GO:0044689	7.41E-03
-	MF	3-dehydroquinate synthase activity	GO:0003856	7.41E-03
-	MF	tRNA (guanine-N1-)-methyltransferase activity	GO:0009019	7.41E-03
-	MF	N-acetyl-gamma-glutamyl-phosphate reductase	GO:0003942	7.41E-03
-	BP	capsule polysaccharide biosynthetic process	GO:0045227	7.41E-03
-	MF	tetrahydromethanopterin S-methyltransferase activity	GO:0030269	7.41E-03
-	CC	phycobilisome	GO:0030089	7.41E-03
-	MF	molybdopterin synthase activity	GO:0030366	7.41E-03
-	MF	L-phenylalanine:2-oxoglutarate aminotransferase	GO:0080130	7.44E-03
-	BP	DNA catabolic process, endonucleolytic	GO:0000737	7.45E-03
-	BP	protein methylation	GO:0006479	8.16E-03
-	MF	carboxyl- or carbamoyltransferase activity	GO:0016743	8.26E-03
-	MF	iron ion binding	GO:0005506	8.97E-03
-	BP	sodium ion transport	GO:0006814	9.31E-03
-	BP	phospholipid biosynthetic process	GO:0008654	9.63E-03
-	BP	7-methylguanosine RNA capping	GO:0009452	9.87E-03
-	MF	L-aspartate:2-oxoglutarate aminotransferase activity	GO:0004069	1.03E-02
-	BP	SOS response	GO:0009432	1.04E-02
-	BP	O antigen biosynthetic process	GO:0009243	1.04E-02
-	MF	oxidoreductase activity, acting on NAD(P)H	GO:0016651	1.04E-02
-	BP	DNA methylation	GO:0006306	1.10E-02
-	MF	phosphogluconate dehydrogenase (decarboxylating) activity	GO:0004616	1.11E-02
-	MF	hydrolase activity	GO:0016787	1.11E-02
Proteolysis	MF	ATP-dependent peptidase activity	GO:0004176	1.12E-02
-	CC	plasma membrane	GO:0005886	1.21E-02
-	MF	methionine synthase activity	GO:0008705	1.23E-02
-	MF	molybdenum ion binding	GO:0030151	1.30E-02

Table 3.1. Continued.

Category	GO term		GO id	*P*-value
-	MF	dihydroorotate dehydrogenase activity	GO:0004152	1.35E-02
-	BP	UMP biosynthetic process	GO:0006222	1.35E-02
-	MF	DNA clamp loader activity	GO:0003689	1.39E-02
-	MF	cation transmembrane transporter activity	GO:0008324	1.54E-02
-	BP	lipid biosynthetic process	GO:0008610	1.71E-02
-	BP	phosphorylation	GO:0016310	1.72E-02
-	MF	aspartate-tRNA(Asn) ligase activity	GO:0050560	1.84E-02
-	MF	nucleic acid binding	GO:0003676	1.92E-02
-	MF	ligase activity, forming carbon-nitrogen bonds	GO:0016879	1.93E-02
-	MF	antiporter activity	GO:0015297	2.03E-02
-	MF	thioredoxin-disulfide reductase activity	GO:0004791	2.06E-02
-	MF	tRNA (guanine(37)-N(1))-methyltransferase activity	GO:0052906	2.07E-02
-	MF	2-isopropylmalate synthase activity	GO:0003852	2.08E-02
-	MF	all-trans-retinol 13,14-reductase activity	GO:0051786	2.08E-02
-	BP	purine nucleobase biosynthetic process	GO:0009113	2.09E-02
-	BP	glycerol-3-phosphate catabolic process	GO:0046168	2.09E-02
-	MF	very long-chain fatty acid-CoA ligase activity	GO:0031957	2.09E-02
Respiration	BP	galactose metabolic process	GO:0006012	2.09E-02
-	MF	cyclic pyranopterin monophosphate synthase activity	GO:0061597	2.09E-02
-	MF	dTDP-glucose 4,6-dehydratase activity	GO:0008460	2.09E-02
-	MF	phospho-N-acetylmuramoyl-pentapeptide-transferase activity	GO:0008963	2.09E-02
-	MF	3'-tRNA processing endoribonuclease activity	GO:0042781	2.09E-02
-	BP	cofactor metabolic process	GO:0051186	2.09E-02
-	BP	tetrahydrofolate biosynthetic process	GO:0046654	2.09E-02
-	BP	protein repair	GO:0030091	2.09E-02
V-ATPase	CC	proton-transporting V-type ATPase, V0 domain	GO:0033179	2.10E-02
-	MF	endonuclease activity	GO:0004519	2.25E-02
-	MF	DNA-directed DNA polymerase activity	GO:0003887	2.31E-02
-	MF	carbon-nitrogen ligase activity, with glutamine as amido-N-donor	GO:0016884	2.32E-02
-	MF	intramolecular transferase activity,	GO:0016868	2.40E-02
-	MF	hydrolase activity, acting on carbon-nitrogen (but not peptide) bonds	GO:0016810	2.42E-02
-	MF	phenylalanine-tRNA ligase activity	GO:0004826	2.43E-02
-	BP	phenylalanyl-tRNA aminoacylation	GO:0006432	2.43E-02
-	BP	tRNA pseudouridine synthesis	GO:0031119	2.48E-02
-	CC	magnesium chelatase complex	GO:0010007	2.49E-02
Oxidative stress responses	MF	peroxiredoxin activity	GO:0051920	2.56E-02
-	MF	calcium-transporting ATPase activity	GO:0005388	2.66E-02
-	BP	tRNA aminoacylation	GO:0043039	2.71E-02
-	BP	ommochrome biosynthetic process	GO:0006727	2.85E-02
-	BP	eye pigment precursor transport	GO:0006856	2.85E-02
-	MF	pigment binding	GO:0031409	2.85E-02
-	BP	gravitaxis	GO:0042332	2.85E-02
-	BP	cellular biogenic amine biosynthetic process	GO:0042401	2.85E-02
-	BP	eye pigment metabolic process	GO:0042441	2.85E-02
-	BP	cGMP transport	GO:0070731	2.85E-02
-	BP	transmembrane transport	GO:0055085	2.90E-02
-	MF	Type I site-specific deoxyribonuclease activity	GO:0009035	2.95E-02
-	MF	carbamoyl-phosphate synthase (glutamine-hydrolyzing) activity	GO:0004088	3.39E-02
-	MF	tRNA adenylyltransferase activity	GO:0004810	3.53E-02
-	BP	DNA topological change	GO:0006265	3.66E-02
-	BP	glutamyl-tRNA aminoacylation	GO:0006424	3.68E-02
-	BP	ATP hydrolysis coupled proton transport	GO:0015991	3.71E-02
-	MF	hydro-lyase activity	GO:0016836	3.86E-02
-	MF	DNA primase activity	GO:0003896	3.89E-02
-	BP	'de novo' AMP biosynthetic process	GO:0044208	3.92E-02
-	MF	histidine-tRNA ligase activity	GO:0004821	3.93E-02
-	BP	histidyl-tRNA aminoacylation	GO:0006427	3.93E-02
-	MF	phosphoglycerate mutase activity	GO:0004619	3.95E-02
-	MF	prenyltransferase activity	GO:0004659	3.95E-02
-	MF	tryptophan synthase activity	GO:0004834	3.95E-02
-	MF	UDP-glucose 4-epimerase activity	GO:0003978	3.95E-02

Table 3.1. Continued.

Category	GO term		GO id	*P*-value
-	MF	delta14-sterol reductase activity	GO:0050613	3.95E-02
-	BP	diaminopimelate biosynthetic process	GO:0019877	3.95E-02
-	MF	mannose-1-phosphate guanylyltransferase activity	GO:0004475	3.95E-02
Respiration	MF	NADPH dehydrogenase activity	GO:0003959	3.95E-02
-	MF	pentaerythritol trinitrate reductase activity	GO:0018548	3.95E-02
-	MF	trichloro-p-hydroquinone reductive dehalogenase	GO:0052690	3.95E-02
-	MF	deoxyhypusine synthase activity	GO:0034038	3.95E-02
-	BP	deoxyhypusine biosynthetic process from spermidine	GO:0050983	3.95E-02
-	MF	isopentenyl-diphosphate delta-isomerase activity	GO:0004452	3.95E-02
-	BP	dTDP-rhamnose biosynthetic process	GO:0019305	3.95E-02
-	MF	3'-5' exonuclease activity	GO:0008408	4.11E-02
-	BP	proteasomal ubiquitin-independent protein catabolic process	GO:0010499	4.40E-02
Proteolysis	BP	positive regulation of peptidase activity	GO:0010952	4.40E-02
Proteolysis	MF	peptidase activator activity	GO:0016504	4.40E-02
-	BP	spermatogenesis, exchange of chromosomal	GO:0035093	4.40E-02
-	CC	spermatoproteasome complex	GO:1990111	4.40E-02
-	BP	male courtship behavior	GO:0008049	4.52E-02
-	BP	peptidyl-lysine modification to peptidyl-hypusine	GO:0008612	4.82E-02
-	BP	compound eye pigmentation	GO:0048072	4.84E-02
Respiration	BP	pyruvate metabolic process	GO:0006090	4.97E-02

Table 3.2. Gene ontology terms enriched in down-regulated genes (≥2 fold change) when *Naegleria* sp. co-cultured with green *S. elongatus* prey were transferred from dark to light (*P*-value ≤ 0.05).

Category	GO term		GO id	*P*-value
-	BP	viral genome replication	GO:0019079	1.77E-04
-	BP	single organismal cell-cell adhesion	GO:0016337	6.60E-04
Actomyosin	MF	actin filament binding	GO:0051015	8.50E-04
Actomyosin	BP	actin filament bundle assembly	GO:0051017	1.65E-03
-	CC	synapse	GO:0045202	1.86E-03
-	CC	cell-cell junction	GO:0005911	2.15E-03
Actomyosin	CC	actin filament	GO:0005884	2.20E-03
-	MF	calcium ion binding	GO:0005509	2.34E-03
Actomyosin	CC	myosin complex	GO:0016459	2.45E-03
Cytoskeleton	MF	structural constituent of cytoskeleton	GO:0005200	3.02E-03
-	MF	acetoacetate-CoA ligase activity	GO:0030729	3.77E-03
-	MF	SH3/SH2 adaptor activity	GO:0005070	5.54E-03
-	BP	negative regulation of stress fiber assembly	GO:0051497	5.54E-03
-	BP	virion attachment to host cell pilus	GO:0039666	5.91E-03
-	BP	synaptic vesicle targeting	GO:0016080	5.93E-03
-	CC	external side of cell wall	GO:0010339	5.93E-03
-	BP	fungal-type cell wall polysaccharide metabolic	GO:0071966	5.93E-03
-	CC	cell leading edge	GO:0031252	6.88E-03
-	CC	cell junction	GO:0030054	7.04E-03
-	BP	tRNA modification	GO:0006400	7.18E-03
-	MF	RNA-directed RNA polymerase activity	GO:0003968	7.50E-03
-	BP	glomerular basement membrane development	GO:0032836	8.13E-03
-	BP	glomerular visceral epithelial cell development	GO:0072015	8.13E-03
-	MF	ferrous iron transmembrane transporter activity	GO:0015093	8.28E-03
-	BP	ferrous iron transport	GO:0015684	8.28E-03
-	BP	glomerular filtration	GO:0003094	8.73E-03
-	MF	hydrogen dehydrogenase (NADP+) activity	GO:0050583	9.74E-03
-	BP	heterophilic cell-cell adhesion via plasma membrane cell adhesion molecules	GO:0007157	9.97E-03
-	MF	cell adhesion molecule binding	GO:0050839	9.97E-03
-	BP	regulation of small GTPase mediated signal transduction	GO:0051056	1.05E-02
-	BP	calcium-mediated signaling using intracellular calcium source	GO:0035584	1.07E-02
-	MF	hydroxylamine reductase activity	GO:0050418	1.10E-02
-	NA	NA	GO:0005100	1.13E-02
-	BP	positive regulation of phospholipase activity	GO:0010518	1.14E-02
-	BP	regulation of GTPase activity	GO:0043087	1.14E-02
-	MF	phospholipase binding	GO:0043274	1.14E-02
-	BP	cell adhesion	GO:0007155	1.16E-02
-	MF	2-iminoacetate synthase activity	GO:0036355	1.16E-02
-	MF	terpene synthase activity	GO:0010333	1.18E-02
-	CC	fungal-type cell wall	GO:0009277	1.18E-02
Motion	MF	motor activity	GO:0003774	1.19E-02
-	BP	positive regulation of signal transduction	GO:0009967	1.30E-02
-	BP	termination of G-protein coupled receptor signaling pathway	GO:0038032	1.39E-02
-	MF	4 iron, 4 sulfur cluster binding	GO:0051539	1.42E-02
-	CC	dendritic spine	GO:0043197	1.49E-02
-	MF	transferase activity, transferring acyl groups other than amino-acyl groups	GO:0016747	1.55E-02
Actomyosin	BP	actin crosslink formation	GO:0051764	1.60E-02
-	BP	multicellular organismal development	GO:0007275	1.62E-02
-	CC	virion	GO:0019012	1.68E-02
-	BP	protein polymerization	GO:0051258	1.71E-02
-	MF	phospholipase activator activity	GO:0016004	1.73E-02
-	CC	growth cone	GO:0030426	1.73E-02
-	BP	phenylpropanoid metabolic process	GO:0009698	1.75E-02
-	MF	4-coumarate-CoA ligase activity	GO:0016207	1.75E-02
-	BP	mitotic centrosome separation	GO:0007100	1.76E-02

Notes: Some GO terms were categorized into 10 categories which were based on their functions. Categories: Actomyosin, Carotene, Cytoskeleton, DNA repair, Motion, Oxidative stress responses, Phagocytosis, Proteolysis, Respiration, V-ATPase. GO, gene ontology; MF, molecular function; CC, cellular component; and BP, biological process. The results shown are based on reproduction by two independent cultures and experiments.

Table 3.2. Continued.

Category	GO term		GO id	*P*-value
-	BP	imaginal disc development	GO:0007444	1.76E-02
-	BP	extracellular polysaccharide metabolic process	GO:0046379	1.77E-02
-	BP	focal adhesion assembly	GO:0048041	1.97E-02
-	BP	centrosome cycle	GO:0007098	1.98E-02
-	BP	spore germination	GO:0009847	2.06E-02
-	BP	swim bladder development	GO:0048794	2.08E-02
-	BP	regulation of canonical Wnt signaling pathway	GO:0060828	2.08E-02
-	CC	PML body	GO:0016605	2.10E-02
-	BP	microtubule-based process	GO:0007017	2.13E-02
Phagocytosis	CC	phagocytic vesicle	GO:0045335	2.16E-02
-	MF	short-chain carboxylesterase activity	GO:0034338	2.35E-02
-	BP	positive regulation of mitotic metaphase/anaphase transition	GO:0045842	2.43E-02
-	MF	receptor binding	GO:0005102	2.46E-02
-	CC	nuclear outer membrane-endoplasmic reticulum membrane network	GO:0042175	2.51E-02
Motion	CC	filopodium	GO:0030175	2.69E-02
-	BP	viral entry into host cell	GO:0046718	2.69E-02
-	MF	ATPase activity, coupled	GO:0042623	2.72E-02
-	MF	lyase activity	GO:0016829	2.77E-02
-	BP	fatty acid metabolic process	GO:0006631	2.81E-02
-	CC	postsynaptic membrane	GO:0045211	2.82E-02
Motion	BP	germ cell migration	GO:0008354	2.92E-02
Motion	BP	positive regulation of filopodium assembly	GO:0051491	3.18E-02
Proteolysis	BP	self proteolysis	GO:0097264	3.24E-02
-	MF	ferredoxin hydrogenase activity	GO:0008901	3.35E-02
-	BP	positive phototaxis	GO:0046956	3.36E-02
-	BP	activation of phospholipase C activity	GO:0007202	3.42E-02
-	BP	Rho protein signal transduction	GO:0007266	3.47E-02
-	CC	clathrin-coated vesicle	GO:0030136	3.59E-02
-	MF	protein binding	GO:0005515	3.65E-02
-	CC	contractile vacuole	GO:0000331	3.75E-02
-	CC	dendrite	GO:0030425	3.95E-02
-	CC	A band	GO:0031672	4.01E-02
-	BP	catabolic process	GO:0009056	4.03E-02
-	BP	thermotaxis	GO:0043052	4.11E-02
-	BP	negative regulation of focal adhesion assembly	GO:0051895	4.52E-02
-	BP	thiamine diphosphate biosynthetic process	GO:0009229	4.59E-02
-	MF	arginine transmembrane transporter activity	GO:0015181	4.65E-02
-	MF	L-lysine transmembrane transporter activity	GO:0015189	4.65E-02
-	BP	lysine transport	GO:0015819	4.65E-02
-	CC	integral component of organelle membrane	GO:0031301	4.65E-02
-	BP	amino acid homeostasis	GO:0080144	4.65E-02
-	BP	L-lysine transmembrane transport	GO:1903401	4.65E-02
-	MF	profilin binding	GO:0005522	4.74E-02

Table 3.3. Gene ontology terms enriched in up-regulated genes (≥2 fold change) when *Acanthamoeba* sp. co-cultured with green *S. elongatus* prey were transferred from dark to light (*P*-value ≤ 0.05).

Category	GO term		GO id	*P*-value
-	BP	oxidation-reduction process	GO:0055114	1.12E-10
Respiration	CC	mitochondrial inner membrane	GO:0005743	6.62E-10
-	CC	integral component of membrane	GO:0016021	1.68E-08
-	BP	transport	GO:0006810	1.41E-06
Respiration	CC	mitochondrion	GO:0005739	5.02E-06
Oxidative stress responses	MF	oxidoreductase activity, acting on the CH-CH group of donors	GO:0016627	5.32E-06
-	MF	ATPase activity	GO:0016887	1.96E-05
-	MF	oxidoreductase activity	GO:0016491	3.42E-05
Respiration	BP	riboflavin biosynthetic process	GO:0009231	1.17E-04
Respiration	BP	heme biosynthetic process	GO:0006783	2.20E-04
-	BP	steroid metabolic process	GO:0008202	4.03E-04
-	BP	transmembrane transport	GO:0055085	4.34E-04
-	MF	mannitol dehydrogenase activity	GO:0046029	4.47E-04
-	BP	sorocarp morphogenesis	GO:0031288	4.52E-04
-	BP	cholesterol biosynthetic process	GO:0006695	4.58E-04
-	BP	deoxyribonucleoside diphosphate metabolic process	GO:0009186	4.61E-04
-	BP	cholesterol metabolic process	GO:0008203	4.74E-04
-	BP	pyridoxal phosphate biosynthetic process	GO:0042823	5.25E-04
Respiration	CC	riboflavin synthase complex	GO:0009349	5.35E-04
-	BP	response to antibiotic	GO:0046677	5.55E-04
-	CC	HslUV protease complex	GO:0009376	5.82E-04
-	MF	oxidoreductase activity, acting on paired donors, with incorporation or reduction of molecular oxygen	GO:0016705	5.86E-04
-	MF	2-iminoacetate synthase activity	GO:0036355	5.86E-04
Proteolysis	MF	intramolecular lyase activity	GO:0016872	5.87E-04
Respiration	BP	heme a biosynthetic process	GO:0006784	5.97E-04
Respiration	BP	respiratory chain complex IV assembly	GO:0008535	5.97E-04
DNA repair	MF	DNA photolyase activity	GO:0003913	6.23E-04
Oxidative stress responses	BP	UV protection	GO:0009650	6.23E-04
-	MF	antibiotic transporter activity	GO:0042895	6.24E-04
-	BP	fatty acid metabolic process	GO:0006631	9.16E-04
-	BP	aromatic amino acid family biosynthetic process	GO:0009073	9.24E-04
-	MF	ATPase activity, coupled to transmembrane movement of substances	GO:0042626	1.10E-03
Respiration	MF	flavin adenine dinucleotide binding	GO:0050660	1.27E-03
-	MF	steroid dehydrogenase activity	GO:0016229	1.68E-03
-	MF	iron ion binding	GO:0005506	1.86E-03
-	MF	alkane 1-monooxygenase activity	GO:0018685	2.07E-03
-	BP	high-density lipoprotein particle remodeling	GO:0034375	2.89E-03
-	BP	reverse cholesterol transport	GO:0043691	2.89E-03
-	BP	carbon utilization	GO:0015976	3.05E-03
-	BP	pyridoxine biosynthetic process	GO:0008615	3.06E-03
-	MF	ionotropic glutamate receptor binding	GO:0035255	3.13E-03
-	BP	steroid biosynthetic process	GO:0006694	3.16E-03
-	BP	cellular iron ion homeostasis	GO:0006879	3.55E-03
-	CC	cytoplasmic side of endosome membrane	GO:0010009	3.60E-03
Respiration	MF	2 iron, 2 sulfur cluster binding	GO:0051537	3.76E-03
Respiration	CC	mitochondrial intermembrane space	GO:0005758	3.80E-03
-	MF	heme binding	GO:0020037	4.84E-03
Oxidative stress responses	MF	ribonucleoside-diphosphate reductase activity, thioredoxin disulfide as acceptor	GO:0004748	4.89E-03
-	BP	drug metabolic process	GO:0017144	5.03E-03
-	BP	anion transport	GO:0006820	5.16E-03
-	MF	transmembrane transporter activity	GO:0022857	6.26E-03
-	MF	antiporter activity	GO:0015297	6.52E-03
Respiration	CC	mitochondrial inner membrane presequence translocase complex	GO:0005744	6.72E-03
-	BP	pyrimidine ribonucleotide biosynthetic process	GO:0009220	7.92E-03
Carotene	BP	carotenoid biosynthetic process	GO:0016117	8.01E-03

Notes: Some GO terms were categorized into 10 categories which were based on their functions. Categories: Actomyosin, Carotene, Cytoskeleton, DNA repair, Motion, Oxidative stress responses, Phagocytosis, Proteolysis, Respiration, V-ATPase. GO, gene ontology; MF, molecular function; CC, cellular component; and BP, biological process. The results shown are based on reproduction by two independent cultures and experiments.

Table 3.3. Continued.

Category	GO term		GO id	*P*-value
DNA repair	MF	DNA-(apurinic or apyrimidinic site) lyase activity	GO:0003906	8.52E-03
-	MF	sterol 14-demethylase activity	GO:0008398	8.59E-03
-	BP	cobalamin biosynthetic process	GO:0009236	8.61E-03
-	BP	demethylation	GO:0070988	8.65E-03
-	BP	long-chain fatty acid metabolic process	GO:0001676	9.91E-03
-	BP	histidine biosynthetic process	GO:0000105	9.95E-03
-	BP	thiamine biosynthetic process	GO:0009228	1.00E-02
-	CC	ATP-binding cassette (ABC) transporter complex	GO:0043190	1.02E-02
-	MF	cholesterol binding	GO:0015485	1.05E-02
-	BP	androgen metabolic process	GO:0008209	1.09E-02
-	BP	endosomal lumen acidification	GO:0048388	1.15E-02
-	MF	ATP-dependent helicase activity	GO:0008026	1.17E-02
Respiration	BP	protein targeting to mitochondrion	GO:0006626	1.27E-02
-	MF	long-chain fatty acid-CoA ligase activity	GO:0004467	1.31E-02
-	BP	chorismate biosynthetic process	GO:0009423	1.33E-02
-	BP	cholesterol transport	GO:0030301	1.39E-02
-	BP	cellular response to starvation	GO:0009267	1.40E-02
-	MF	adenyl nucleotide binding	GO:0030554	1.48E-02
-	MF	acyl-CoA dehydrogenase activity	GO:0003995	1.56E-02
-	MF	carbonate dehydratase activity	GO:0004089	1.63E-02
-	CC	intracellular membrane-bounded organelle	GO:0043231	1.73E-02
-	BP	triglyceride catabolic process	GO:0019433	1.85E-02
-	NA	NA	GO:0005100	1.90E-02
-	MF	aromatase activity	GO:0070330	1.91E-02
-	MF	copper chaperone activity	GO:0016531	1.97E-02
-	BP	protein import into mitochondrial inner membrane	GO:0045039	1.97E-02
Oxidative stress responses	MF	sulfiredoxin activity	GO:0032542	2.06E-02
Oxidative stress responses	MF	peptide-methionine (S)-S-oxide reductase activity	GO:0008113	2.09E-02
-	MF	L-methionine-(S)-S-oxide reductase activity	GO:0036456	2.09E-02
-	BP	L-methionine biosynthetic process from methionine sulphoxide	GO:1990355	2.09E-02
-	MF	retinoic acid binding	GO:0001972	2.11E-02
-	BP	vitamin A metabolic process	GO:0006776	2.11E-02
-	MF	retinol binding	GO:0019841	2.11E-02
-	MF	phosphatidylcholine-retinol O-acyltransferase activity	GO:0047173	2.11E-02
-	BP	negative regulation of mitochondrial electron transport, NADH to ubiquinone	GO:1902957	2.11E-02
-	MF	methylmalonyl-CoA epimerase activity	GO:0004493	2.13E-02
-	BP	L-methylmalonyl-CoA metabolic process	GO:0046491	2.13E-02
Respiration	BP	protein-FAD linkage	GO:0018293	2.13E-02
Respiration	BP	mitochondrial unfolded protein response	GO:0034514	2.13E-02
-	MF	6,7-dimethyl-8-ribityllumazine synthase activity	GO:0000906	2.13E-02
-	MF	N1-acetylspermine:oxygen oxidoreductase (propane-1,3-diamine-forming) activity	GO:0052893	2.19E-02
-	MF	spermidine oxidase (propane-1,3-diamine-forming) activity	GO:0052896	2.19E-02
-	MF	N8-acetylspermidine:oxygen oxidoreductase (propane-1,3-diamine-forming) activity	GO:0052897	2.19E-02
-	MF	N1-acetylspermidine:oxygen oxidoreductase (propane-1,3-diamine-forming) activity	GO:0052898	2.19E-02
-	MF	spermine oxidase (propane-1,3-diamine-forming) activity	GO:0052900	2.19E-02
Proteolysis	BP	positive regulation of protein catabolic process	GO:0045732	2.21E-02
-	BP	negative regulation of platelet-derived growth factor receptor signaling pathway	GO:0010642	2.21E-02
-	BP	tissue regeneration	GO:0042246	2.21E-02
-	BP	negative regulation of protein import into nucleus	GO:0042308	2.21E-02
-	BP	negative regulation of smooth muscle cell	GO:0048662	2.21E-02
-	BP	negative regulation of lipoprotein lipid oxidation	GO:0060588	2.21E-02
-	BP	negative regulation of monocyte chemotactic protein-1 production	GO:0071638	2.21E-02
-	BP	negative regulation of cytokine production involved in inflammatory response	GO:1900016	2.21E-02
-	BP	negative regulation of smooth muscle cell-matrix adhesion	GO:2000098	2.21E-02

Table 3.3. Continued.

Category	GO term		GO id	*P*-value
Motion	BP	negative regulation of T cell migration	GO:2000405	2.21E-02
-	CC	NMDA selective glutamate receptor complex	GO:0017146	2.23E-02
-	MF	somatostatin receptor binding	GO:0031877	2.23E-02
-	BP	habituation	GO:0046959	2.23E-02
-	BP	determination of affect	GO:0050894	2.23E-02
-	BP	righting reflex	GO:0060013	2.23E-02
-	CC	excitatory synapse	GO:0060076	2.23E-02
-	MF	scaffold protein binding	GO:0097110	2.23E-02
-	BP	regulation of alpha-amino-3-hydroxy-5-methyl-4-isoxazole propionate selective glutamate receptor	GO:2000311	2.23E-02
-	MF	flavin-linked sulfhydryl oxidase activity	GO:0016971	2.23E-02
-	MF	thiol oxidase activity	GO:0016972	2.23E-02
Oxidative stress responses	BP	vitamin B6 biosynthetic process	GO:0042819	2.24E-02
-	BP	histone H2A monoubiquitination	GO:0035518	2.25E-02
DNA repair	BP	UV-damage excision repair	GO:0070914	2.25E-02
-	BP	positive regulation of G1/S transition of mitotic cell	GO:1900087	2.25E-02
Proteolysis	MF	ATP-dependent peptidase activity	GO:0004176	2.26E-02
-	BP	kidney development	GO:0001822	2.28E-02
-	MF	3-oxo-5-alpha-steroid 4-dehydrogenase activity	GO:0003865	2.29E-02
-	BP	androgen biosynthetic process	GO:0006702	2.29E-02
-	BP	response to muscle activity	GO:0014850	2.29E-02
-	BP	diterpenoid metabolic process	GO:0016101	2.29E-02
-	BP	thalamus development	GO:0021794	2.29E-02
-	BP	hypothalamus development	GO:0021854	2.29E-02
-	BP	pituitary gland development	GO:0021983	2.29E-02
-	BP	male genitalia development	GO:0030539	2.29E-02
-	BP	response to follicle-stimulating hormone	GO:0032354	2.29E-02
-	BP	progesterone metabolic process	GO:0042448	2.29E-02
-	BP	circadian sleep/wake cycle, REM sleep	GO:0042747	2.29E-02
-	MF	cholestenone 5-alpha-reductase activity	GO:0047751	2.29E-02
-	BP	response to growth hormone	GO:0060416	2.29E-02
-	BP	response to fungicide	GO:0060992	2.29E-02
-	BP	cellular response to testosterone stimulus	GO:0071394	2.29E-02
-	CC	glyoxysome	GO:0009514	2.29E-02
-	MF	FMN adenylyltransferase activity	GO:0003919	2.31E-02
-	BP	FAD biosynthetic process	GO:0006747	2.31E-02
-	BP	FMN metabolic process	GO:0046444	2.31E-02
-	MF	uroporphyrinogen decarboxylase activity	GO:0004853	2.32E-02
-	BP	arachidonic acid metabolic process	GO:0019369	2.32E-02
Carotene	BP	geranylgeranyl diphosphate biosynthetic process	GO:0033386	2.33E-02
-	BP	purine nucleotide biosynthetic process	GO:0006164	2.33E-02
-	BP	mitochondrial iron ion transport	GO:0048250	2.35E-02
-	MF	fatty acid binding	GO:0005504	2.35E-02
-	MF	chalcone isomerase activity	GO:0045430	2.35E-02
-	BP	response to karrikin	GO:0080167	2.38E-02
-	BP	lignin biosynthetic process	GO:0009809	2.39E-02
-	MF	cinnamoyl-CoA reductase activity	GO:0016621	2.39E-02
-	MF	protoheme IX farnesyltransferase activity	GO:0008495	2.40E-02
-	BP	heme O biosynthetic process	GO:0048034	2.40E-02
-	BP	regulation of synaptic transmission, glutamatergic	GO:0051966	2.42E-02
-	BP	negative regulation of proteasomal protein catabolic process	GO:1901799	2.42E-02
-	BP	regulation of systemic arterial blood pressure	GO:0003073	2.43E-02
-	BP	cardiac left ventricle morphogenesis	GO:0003214	2.43E-02
-	BP	epinephrine metabolic process	GO:0042414	2.43E-02
-	BP	norepinephrine metabolic process	GO:0042415	2.43E-02
-	BP	dopamine metabolic process	GO:0042417	2.43E-02
-	BP	phosphate ion homeostasis	GO:0055062	2.43E-02
-	BP	response to catecholamine	GO:0071869	2.43E-02
-	BP	response to epinephrine	GO:0071871	2.43E-02
-	BP	response to norepinephrine	GO:0071873	2.43E-02
-	BP	response to salt	GO:1902074	2.43E-02
-	BP	neutrophil activation	GO:0042119	2.44E-02
-	BP	aromatic compound biosynthetic process	GO:0019438	2.45E-02
Respiration	MF	ferrochelatase activity	GO:0004325	2.46E-02

Table 3.3. Continued.

Category	GO term		GO id	*P*-value
-	BP	D-amino acid biosynthetic process	GO:0046437	2.47E-02
-	MF	D-alanine:2-oxoglutarate aminotransferase activity	GO:0047810	2.47E-02
-	MF	trans-hexaprenyltranstransferase activity	GO:0000010	2.48E-02
-	MF	glutaryl-CoA dehydrogenase activity	GO:0004361	2.48E-02
-	MF	kynurenine 3-monooxygenase activity	GO:0004502	2.48E-02
-	MF	tRNA-intron endonuclease activity	GO:0000213	2.49E-02
-	CC	tRNA-intron endonuclease complex	GO:0000214	2.49E-02
Oxidative stress responses	MF	L-gulonolactone oxidase activity	GO:0050105	2.49E-02
-	MF	orotate phosphoribosyltransferase activity	GO:0004588	2.49E-02
-	BP	cholesterol biosynthetic process via 24,25-dihydrolanosterol	GO:0033488	2.49E-02
-	BP	type I interferon signaling pathway	GO:0060337	2.49E-02
-	MF	chlorophyllide a oxygenase [overall] activity	GO:0010277	2.49E-02
-	MF	IMP cyclohydrolase activity	GO:0003937	2.50E-02
-	MF	phosphoribosylaminoimidazolecarboxamide formyltransferase activity	GO:0004643	2.50E-02
-	MF	squalene monooxygenase activity	GO:0004506	2.50E-02
DNA repair	BP	photoreactive repair	GO:0000719	2.50E-02
DNA repair	MF	deoxyribodipyrimidine photo-lyase activity	GO:0003904	2.50E-02
-	MF	peptidase activity, acting on L-amino acid peptides	GO:0070011	2.50E-02
Motion	BP	fibroblast migration	GO:0010761	2.50E-02
-	BP	termination of RNA polymerase I transcription	GO:0006363	2.50E-02
-	MF	diaminohydroxyphosphoribosylaminopyrimidine deaminase activity	GO:0008835	2.50E-02
-	MF	hormone-sensitive lipase activity	GO:0033878	2.50E-02
-	MF	rRNA primary transcript binding	GO:0042134	2.50E-02
-	BP	ergothioneine biosynthesis from histidine via N-alpha,N-alpha,N-alpha-trimethyl-L-histidine	GO:0052704	2.50E-02
-	MF	ATP phosphoribosyltransferase activity	GO:0003879	2.50E-02
-	MF	histidinol dehydrogenase activity	GO:0004399	2.50E-02
-	MF	phosphoribosyl-AMP cyclohydrolase activity	GO:0004635	2.50E-02
-	MF	arachidonic acid monooxygenase activity	GO:0008391	2.50E-02
-	MF	3,4-dihydroxy-2-butanone-4-phosphate synthase	GO:0008686	2.50E-02
-	MF	indole-3-acetic acid amido synthetase activity	GO:0010279	2.50E-02
-	BP	heme transport	GO:0015886	2.50E-02
Carotene	BP	carotene biosynthetic process	GO:0016120	2.50E-02
-	MF	geranylgeranyl-diphosphate geranylgeranyltransferase activity	GO:0016767	2.50E-02
Carotene	MF	lycopene beta cyclase activity	GO:0045436	2.50E-02
-	BP	urate metabolic process	GO:0046415	2.50E-02
-	BP	icosanoid biosynthetic process	GO:0046456	2.50E-02
Carotene	MF	phytoene synthase activity	GO:0046905	2.50E-02
-	BP	regulation of neuronal synaptic plasticity	GO:0048168	2.50E-02
-	BP	lauric acid metabolic process	GO:0048252	2.50E-02
Oxidative stress responses	BP	programmed cell death in response to reactive oxygen species	GO:0097468	2.50E-02
Respiration	BP	ubiquinone biosynthetic process	GO:0006744	2.58E-02
-	BP	response to drug	GO:0042493	2.70E-02
-	CC	endosome membrane	GO:0010008	2.72E-02
-	BP	cell differentiation	GO:0030154	2.76E-02
-	BP	isoprenoid biosynthetic process	GO:0008299	3.04E-02
-	BP	cholesterol homeostasis	GO:0042632	3.16E-02
-	BP	protein ubiquitination involved in ubiquitin-dependent protein catabolic process	GO:0042787	3.47E-02
-	MF	benzodiazepine receptor activity	GO:0008503	4.13E-02
-	BP	regulation of cholesterol transport	GO:0032374	4.13E-02
-	CC	Cul4B-RING E3 ubiquitin ligase complex	GO:0031465	4.20E-02
-	BP	cellular response to cAMP	GO:0071320	4.21E-02
-	BP	positive regulation of protein processing	GO:0010954	4.21E-02
-	BP	membrane protein intracellular domain proteolysis	GO:0031293	4.21E-02
-	BP	cellular response to unfolded protein	GO:0034620	4.21E-02
-	CC	endoplasmic reticulum quality control compartment	GO:0044322	4.21E-02
-	BP	cellular response to estradiol stimulus	GO:0071392	4.28E-02
-	MF	amide binding	GO:0033218	4.28E-02
-	BP	eye pigment precursor transport	GO:0006856	4.34E-02

Table 3.3. Continued.

Category	GO term		GO id	*P*-value
-	BP	gravitaxis	GO:0042332	4.34E-02
-	BP	cellular biogenic amine biosynthetic process	GO:0042401	4.34E-02
-	BP	eye pigment metabolic process	GO:0042441	4.34E-02
-	BP	cGMP transport	GO:0070731	4.34E-02
-	MF	adenyl-nucleotide exchange factor activity	GO:0000774	4.35E-02
-	BP	heart contraction	GO:0060047	4.36E-02
Respiration	MF	NADH dehydrogenase (ubiquinone) activity	GO:0008137	4.38E-02
-	BP	stem vascular tissue pattern formation	GO:0010222	4.39E-02
-	BP	very-low-density lipoprotein particle remodeling	GO:0034372	4.40E-02
-	BP	lipoprotein biosynthetic process	GO:0042158	4.40E-02
-	BP	regulation of high-density lipoprotein particle	GO:0090107	4.40E-02
-	BP	response to axon injury	GO:0048678	4.41E-02
-	BP	negative regulation of macrophage derived foam cell differentiation	GO:0010745	4.43E-02
-	BP	regulation of cholesterol esterification	GO:0010872	4.43E-02
-	BP	positive regulation of cholesterol efflux	GO:0010875	4.43E-02
-	BP	negative regulation of lipid storage	GO:0010888	4.43E-02
-	MF	toxin transporter activity	GO:0019534	4.43E-02
-	BP	phospholipid efflux	GO:0033700	4.43E-02
-	MF	sterol-transporting ATPase activity	GO:0034041	4.43E-02
-	BP	low-density lipoprotein particle remodeling	GO:0034374	4.43E-02
-	MF	glycoprotein transporter activity	GO:0034437	4.43E-02
-	BP	amyloid precursor protein catabolic process	GO:0042987	4.43E-02
-	BP	response to high density lipoprotein particle	GO:0055099	4.43E-02
-	BP	vitamin K metabolic process	GO:0042373	4.45E-02
-	MF	15-hydroxyprostaglandin dehydrogenase (NADP+) activity	GO:0047021	4.45E-02
-	MF	prostaglandin-E2 9-reductase activity	GO:0050221	4.45E-02
-	MF	phosphoribosyl-ATP diphosphatase activity	GO:0004636	4.45E-02
-	MF	3-dehydroquinate synthase activity	GO:0003856	4.47E-02
-	MF	3-phosphoshikimate 1-carboxyvinyltransferase	GO:0003866	4.47E-02
-	MF	shikimate kinase activity	GO:0004765	4.47E-02
-	BP	leaf morphogenesis	GO:0009965	4.51E-02
-	CC	receptor complex	GO:0043235	4.54E-02
-	MF	23S rRNA (guanine(2445)-N(2))-methyltransferase activity	GO:0052915	4.55E-02
-	MF	rRNA (guanine-N7-)-methyltransferase activity	GO:0070043	4.55E-02
-	MF	oxygen transporter activity	GO:0005344	4.56E-02
-	BP	retinoic acid metabolic process	GO:0042573	4.56E-02
-	MF	hydrolase activity, acting on acid anhydrides, catalyzing transmembrane movement of substances	GO:0016820	4.59E-02
-	BP	negative regulation of actin filament bundle assembly	GO:0032232	4.62E-02
-	BP	cellular response to growth factor stimulus	GO:0071363	4.64E-02
-	BP	ferrous iron import	GO:0070627	4.64E-02
-	BP	manganese ion transmembrane transport	GO:0071421	4.64E-02
-	MF	5-amino-6-(5-phosphoribosylamino)uracil reductase activity	GO:0008703	4.64E-02
-	BP	lung alveolus development	GO:0048286	4.66E-02
-	BP	isoprenoid metabolic process	GO:0006720	4.67E-02
-	MF	GKAP/Homer scaffold activity	GO:0030160	4.68E-02
-	BP	protein localization to synapse	GO:0035418	4.68E-02
-	MF	dimethylallyltranstransferase activity	GO:0004161	4.68E-02
-	MF	geranyltranstransferase activity	GO:0004337	4.68E-02
-	BP	geranyl diphosphate biosynthetic process	GO:0033384	4.68E-02
-	BP	farnesyl diphosphate biosynthetic process	GO:0045337	4.68E-02
-	MF	methenyltetrahydrofolate cyclohydrolase activity	GO:0004477	4.70E-02
-	MF	methylenetetrahydrofolate dehydrogenase (NADP+) activity	GO:0004488	4.70E-02
-	MF	prenyltransferase activity	GO:0004659	4.70E-02
-	BP	male sex differentiation	GO:0046661	4.71E-02
-	MF	glyoxylate reductase activity	GO:0047964	4.71E-02
-	MF	farnesyltranstransferase activity	GO:0004311	4.72E-02
-	BP	cytochrome complex assembly	GO:0017004	4.73E-02
-	BP	urogenital system development	GO:0001655	4.74E-02
-	BP	response to testosterone	GO:0033574	4.74E-02

Table 3.3. Continued.

Category	GO term		GO id	*P*-value
-	BP	serotonin metabolic process	GO:0042428	4.74E-02
-	CC	palmitoyltransferase complex	GO:0002178	4.75E-02
-	CC	intrinsic component of Golgi membrane	GO:0031228	4.75E-02
-	MF	delta14-sterol reductase activity	GO:0050613	4.78E-02
-	MF	heme transporter activity	GO:0015232	4.83E-02
Respiration	BP	mitochondrial fission	GO:0000266	4.84E-02
-	BP	xenobiotic transport	GO:0042908	4.85E-02
-	MF	molybdate ion transmembrane transporter activity	GO:0015098	4.85E-02
-	BP	molybdate ion transport	GO:0015689	4.85E-02
-	MF	orotidine-5'-phosphate decarboxylase activity	GO:0004590	4.86E-02
-	BP	RNA 5'-end processing	GO:0000966	4.87E-02
-	BP	negative regulation of viral genome replication	GO:0045071	4.87E-02
DNA repair	CC	XPC complex	GO:0071942	4.88E-02
-	BP	negative regulation of photomorphogenesis	GO:0010100	4.89E-02
-	BP	short-day photoperiodism, flowering	GO:0048575	4.89E-02
-	BP	renal water homeostasis	GO:0003091	4.91E-02
-	BP	pressure natriuresis	GO:0003095	4.91E-02
-	MF	arachidonic acid epoxygenase activity	GO:0008392	4.91E-02
-	BP	epoxygenase P450 pathway	GO:0019373	4.91E-02
-	BP	negative regulation of blood coagulation	GO:0030195	4.91E-02
-	BP	leukotriene B4 catabolic process	GO:0036101	4.91E-02
Oxidative stress responses	BP	vitamin E metabolic process	GO:0042360	4.91E-02
-	BP	vitamin K biosynthetic process	GO:0042371	4.91E-02
-	MF	vitamin-K-epoxide reductase (warfarin-sensitive)	GO:0047057	4.91E-02
-	MF	leukotriene-B4 20-monooxygenase activity	GO:0050051	4.91E-02
-	BP	sodium ion homeostasis	GO:0055078	4.91E-02
-	MF	CDP-diacylglycerol-serine O-phosphatidyltransferase activity	GO:0003882	4.91E-02
-	MF	D-arabinono-1,4-lactone oxidase activity	GO:0003885	4.93E-02
-	MF	sphinganine-1-phosphate aldolase activity	GO:0008117	4.93E-02
-	BP	sphingolipid catabolic process	GO:0030149	4.93E-02
-	BP	execution phase of apoptosis	GO:0097194	4.94E-02
-	BP	transpiration	GO:0010148	4.94E-02
-	BP	protein unfolding	GO:0043335	4.94E-02
-	BP	transcription initiation from RNA polymerase I	GO:0006361	4.94E-02
-	BP	linoleic acid metabolic process	GO:0043651	4.94E-02
-	BP	detection of mechanical stimulus	GO:0050982	4.94E-02

Table 3.4. Gene ontology terms enriched in down-regulated genes (≥2 fold change) when *Acanthamoeba* sp. co-cultured with green *S. elongatus* prey were transferred from dark to light (*P*-value ≤ 0.05).

Category	GO term		GO id	*P*-value
-	BP	cyclic nucleotide biosynthetic process	GO:0009190	2.72E-12
-	MF	phosphorus-oxygen lyase activity	GO:0016849	2.72E-12
-	BP	intracellular signal transduction	GO:0035556	4.35E-12
-	MF	protein serine/threonine kinase activity	GO:0004674	2.04E-05
-	BP	cortical actin cytoskeleton stabilization	GO:0033109	5.14E-05
-	CC	macropinocytic cup	GO:0070685	5.14E-05
Motion	BP	positive regulation of cell motility	GO:2000147	5.14E-05
Phagocytosis	BP	digestion	GO:0007586	1.79E-04
-	BP	positive regulation of small GTPase mediated signal transduction	GO:0051057	6.20E-04
-	CC	integral component of membrane	GO:0016021	6.74E-04
Phagocytosis	BP	phagocytosis, engulfment	GO:0006911	8.17E-04
-	MF	Rho guanyl-nucleotide exchange factor activity	GO:0005089	1.11E-03
Actomyosin	CC	myosin complex	GO:0016459	1.23E-03
Phagocytosis	CC	phagocytic cup lip	GO:0097203	1.40E-03
Motion	MF	motor activity	GO:0003774	1.47E-03
Phagocytosis	BP	positive regulation of phagocytosis	GO:0050766	1.86E-03
Phagocytosis	CC	early phagosome	GO:0032009	4.39E-03
Phagocytosis	CC	phagocytic cup	GO:0001891	4.64E-03
-	CC	ruffle	GO:0001726	4.98E-03
Cytoskeleton	CC	cytoskeleton	GO:0005856	5.58E-03
-	CC	extracellular space	GO:0005615	5.93E-03
-	BP	cardioblast differentiation	GO:0010002	6.34E-03
-	CC	neuronal cell body	GO:0043025	7.05E-03
-	MF	profilin binding	GO:0005522	7.09E-03
-	MF	N-acyltransferase activity	GO:0016410	7.18E-03
-	MF	hydroxycinnamoyltransferase activity	GO:0050734	7.18E-03
-	MF	spermidine:sinapoyl CoA N-acyltransferase activity	GO:0080072	7.18E-03
-	MF	spermidine:coumaroyl CoA N-acyltransferase activity	GO:0080073	7.18E-03
-	MF	spermidine:caffeoyl CoA N-acyltransferase activity	GO:0080074	7.18E-03
-	MF	spermidine:feruloyl CoA N-acyltransferase activity	GO:0080075	7.18E-03
-	BP	spermidine hydroxycinnamate conjugate biosynthetic process	GO:0080088	7.18E-03
-	BP	mRNA transcription	GO:0009299	7.71E-03
-	MF	potassium-transporting ATPase activity	GO:0008556	7.74E-03
-	BP	potassium ion export across plasma membrane	GO:0097623	7.74E-03
-	BP	calcium ion import into cell	GO:1990035	7.74E-03
-	BP	cell migration involved in sprouting angiogenesis	GO:0002042	8.06E-03
-	BP	complement receptor mediated signaling pathway	GO:0002430	8.06E-03
-	MF	glycosylphosphatidylinositol phospholipase D activity	GO:0004621	8.06E-03
-	BP	GPI anchor release	GO:0006507	8.06E-03
-	BP	positive regulation of alkaline phosphatase activity	GO:0010694	8.06E-03
-	BP	negative regulation of triglyceride catabolic process	GO:0010897	8.06E-03
Respiration	BP	positive regulation of glucose metabolic process	GO:0010907	8.06E-03
-	BP	positive regulation of high-density lipoprotein particle clearance	GO:0010983	8.06E-03
-	MF	sodium channel regulator activity	GO:0017080	8.06E-03
-	BP	positive regulation of insulin secretion involved in cellular response to glucose stimulus	GO:0035774	8.06E-03
-	BP	positive regulation of cytolysis	GO:0045919	8.06E-03
-	BP	response to oxygen levels	GO:0070482	8.06E-03
-	BP	transepithelial transport	GO:0070633	8.06E-03
-	BP	cellular response to cholesterol	GO:0071397	8.06E-03
-	BP	cellular response to triglyceride	GO:0071401	8.06E-03
-	BP	regulation of cellular response to insulin stimulus	GO:1900076	8.06E-03
-	BP	neurotrophin TRK receptor signaling pathway	GO:0048011	9.25E-03
-	MF	ATP binding	GO:0005524	9.36E-03
-	CC	cell leading edge	GO:0031252	1.05E-02
-	MF	cysteine-type peptidase activity	GO:0008234	1.11E-02
Actomyosin	BP	actomyosin structure organization	GO:0031032	1.30E-02

Notes: Some GO terms were categorized into 10 categories which were based on their functions. Categories: Actomyosin, Carotene, Cytoskeleton, DNA repair, Motion, Oxidative stress responses, Phagocytosis, Proteolysis, Respiration, V-ATPase. GO, gene ontology; MF, molecular function; CC, cellular component; and BP, biological process. The results shown are based on reproduction by two independent cultures and experiments.

Table 3.4. Continued.

Category	GO term		GO id	*P*-value
Actomyosin	MF	actin filament binding	GO:0051015	1.34E-02
-	CC	muscle tendon junction	GO:0005927	1.35E-02
Phagocytosis	BP	feeding behavior	GO:0007631	1.48E-02
-	BP	trophectodermal cell proliferation	GO:0001834	1.49E-02
-	BP	axon development	GO:0061564	1.49E-02
-	BP	positive regulation of transcription involved in G1/S transition of mitotic cell cycle	GO:0071931	1.49E-02
-	BP	apoptotic process involved in development	GO:1902742	1.49E-02
Motion	BP	negative regulation of motor neuron apoptotic	GO:2000672	1.49E-02
-	BP	nucleobase-containing small molecule	GO:0015949	1.51E-02
-	BP	cellular response to pH	GO:0071467	1.54E-02
-	MF	oxygen sensor activity	GO:0019826	1.54E-02
-	BP	regulation of Rho protein signal transduction	GO:0035023	1.54E-02
-	MF	adiponectin binding	GO:0055100	1.56E-02
-	BP	regulation of calcium ion-dependent exocytosis	GO:0017158	1.60E-02
-	BP	regulation of T cell differentiation in thymus	GO:0033081	1.60E-02
-	BP	regulation of T cell proliferation	GO:0042129	1.60E-02
-	BP	chondrocyte differentiation	GO:0002062	1.60E-02
-	BP	positive regulation of membrane protein ectodomain proteolysis	GO:0051044	1.60E-02
-	BP	cellular calcium ion homeostasis	GO:0006874	1.87E-02
-	BP	choline metabolic process	GO:0019695	2.15E-02
-	BP	positive regulation of secretion	GO:0051047	2.16E-02
-	BP	neurotransmitter catabolic process	GO:0042135	2.17E-02
-	BP	pre-mRNA catabolic process	GO:1990261	2.20E-02
-	CC	high-density lipoprotein particle	GO:0034364	2.22E-02
-	BP	positive regulation of peptidyl-threonine	GO:0010800	2.26E-02
-	MF	NAD(P)+ transhydrogenase (AB-specific) activity	GO:0008750	2.26E-02
-	BP	regulation of pro-B cell differentiation	GO:2000973	2.29E-02
Motion	BP	positive regulation of endothelial cell migration	GO:0010595	2.31E-02
-	BP	lymphocyte homeostasis	GO:0002260	2.38E-02
-	BP	positive regulation of epidermal growth factor receptor signaling pathway	GO:0045742	2.40E-02
-	BP	nodulation	GO:0009877	2.81E-02
-	BP	synaptic transmission, cholinergic	GO:0007271	2.85E-02
-	MF	receptor tyrosine kinase binding	GO:0030971	2.90E-02
-	BP	salivary gland cell autophagic cell death	GO:0035071	2.92E-02
-	MF	methyltransferase activity	GO:0008168	2.95E-02
-	BP	Cajal body organization	GO:0030576	2.99E-02
-	MF	uridine nucleosidase activity	GO:0045437	3.03E-02
-	MF	cAMP-dependent protein kinase inhibitor activity	GO:0004862	3.03E-02
-	BP	regulation of fatty acid metabolic process	GO:0019217	3.03E-02
-	BP	regulation of small GTPase mediated signal transduction	GO:0051056	3.03E-02
-	BP	positive regulation of growth	GO:0045927	3.04E-02
-	MF	phosphorylase kinase regulator activity	GO:0008607	3.04E-02
-	BP	positive regulation of RNA splicing	GO:0033120	3.07E-02
-	MF	RNA-directed RNA polymerase activity	GO:0003968	3.07E-02
-	BP	adiponectin-activated signaling pathway	GO:0033211	3.09E-02
-	MF	hormone binding	GO:0042562	3.09E-02
-	BP	phosphatidylcholine metabolic process	GO:0046470	3.11E-02
-	MF	small GTPase binding	GO:0031267	3.13E-02
-	BP	B cell homeostasis	GO:0001782	3.18E-02
-	MF	cholinesterase activity	GO:0004104	3.25E-02
-	MF	sequence-specific DNA binding	GO:0043565	3.36E-02
-	MF	acetylcholinesterase activity	GO:0003990	3.48E-02
-	BP	positive regulation of triglyceride biosynthetic	GO:0010867	3.49E-02
-	CC	Gemini of coiled bodies	GO:0097504	3.52E-02
-	BP	pyrimidine nucleobase metabolic process	GO:0006206	3.66E-02
-	MF	guanyl-nucleotide exchange factor activity	GO:0005085	3.67E-02
-	CC	presynaptic membrane	GO:0042734	3.68E-02
-	BP	pollen exine formation	GO:0010584	3.76E-02
-	BP	collagen catabolic process	GO:0030574	3.76E-02
-	MF	transmembrane signaling receptor activity	GO:0004888	3.77E-02
Respiration	BP	positive regulation of glucose import	GO:0046326	3.88E-02

Table 3.4. Continued.

Category	GO term		GO id	*P*-value
-	BP	cellular response to drug	GO:0035690	3.90E-02
-	NA	NA	GO:0043088	3.91E-02
-	BP	sarcoplasmic reticulum calcium ion transport	GO:0070296	3.93E-02
-	BP	membrane depolarization during SA node cell action potential	GO:0086046	3.93E-02
-	MF	guanylate cyclase activity	GO:0004383	3.96E-02
-	BP	cGMP biosynthetic process	GO:0006182	3.96E-02
-	BP	heart development	GO:0007507	4.07E-02
-	BP	cellular aromatic compound metabolic process	GO:0006725	4.16E-02
-	BP	regulation of myelination	GO:0031641	4.29E-02
-	CC	SMN complex	GO:0032797	4.35E-02
-	MF	beta-amyloid binding	GO:0001540	4.36E-02
-	BP	regulation of aggregation involved in sorocarp development	GO:0060176	4.43E-02
-	BP	mesoderm development	GO:0007498	4.45E-02
-	BP	female pregnancy	GO:0007565	4.53E-02
-	MF	cAMP-dependent protein kinase regulator activity	GO:0008603	4.55E-02
-	CC	extracellular region	GO:0005576	4.64E-02
-	MF	calcium-dependent phospholipid binding	GO:0005544	4.68E-02
-	MF	sterol 14-demethylase activity	GO:0008398	4.69E-02
Motion	CC	lamellipodium	GO:0030027	4.70E-02
-	BP	demethylation	GO:0070988	4.71E-02
-	BP	positive regulation of apoptotic process	GO:0043065	4.83E-02
-	MF	ferric iron binding	GO:0008199	4.83E-02

Table 3.5. Gene ontology terms enriched in up-regulated genes (≥2 fold change) when *Vannella* sp. co-cultured with green *S. elongatus* prey were transferred from dark to light (*P*-value ≤ 0.05).

Category	GO term		GO id	*P*-value
-	BP	oxidation-reduction process	GO:0055114	1.82E-10
-	CC	integral component of membrane	GO:0016021	5.13E-10
Respiration	CC	mitochondrion	GO:0005739	1.72E-09
Respiration	CC	mitochondrial inner membrane	GO:0005743	2.39E-09
-	BP	transport	GO:0006810	3.77E-09
-	MF	oxidoreductase activity	GO:0016491	1.39E-08
-	MF	ATPase activity, coupled to transmembrane movement of substances	GO:0042626	2.41E-08
Respiration	MF	flavin adenine dinucleotide binding	GO:0050660	3.89E-06
DNA repair	MF	DNA photolyase activity	GO:0003913	2.57E-05
Oxidative stress responses	MF	antioxidant activity	GO:0016209	6.68E-05
Respiration	BP	respiratory chain complex IV assembly	GO:0008535	7.30E-05
Oxidative stress responses	MF	oxidoreductase activity, acting on the CH-CH group of donors	GO:0016627	9.05E-05
Respiration	CC	mitochondrial membrane	GO:0031966	1.59E-04
-	BP	transmembrane transport	GO:0055085	3.28E-04
Respiration	BP	heme biosynthetic process	GO:0006783	3.75E-04
Proteolysis	MF	ATP-dependent peptidase activity	GO:0004176	4.13E-04
-	MF	chlorophyllide a oxygenase [overall] activity	GO:0010277	4.31E-04
Respiration	BP	mitochondrial electron transport, succinate to ubiquinone	GO:0006121	4.96E-04
-	MF	cob(I)yrinic acid a,c-diamide adenosyltransferase	GO:0008817	5.63E-04
-	MF	ubiquitin activating enzyme activity	GO:0004839	6.06E-04
-	BP	modification-dependent protein catabolic process	GO:0019941	6.06E-04
-	MF	ATPase activity	GO:0016887	6.38E-04
Oxidative stress responses	MF	galactonolactone dehydrogenase activity	GO:0016633	6.39E-04
-	MF	L-gulono-1,4-lactone dehydrogenase activity	GO:0080049	6.39E-04
-	BP	ergothioneine biosynthesis from histidine via N-alpha,N-alpha,N-alpha-trimethyl-L-histidine	GO:0052704	7.95E-04
Proteolysis	BP	oxidation-dependent protein catabolic process	GO:0070407	8.00E-04
Respiration	BP	regulation of mitochondrial DNA replication	GO:0090296	8.00E-04
DNA repair	MF	deoxyribodipyrimidine photo-lyase activity	GO:0003904	8.81E-04
-	CC	chloroplast thylakoid	GO:0009534	8.81E-04
Proteolysis	BP	proteolysis	GO:0006508	9.19E-04
-	BP	protein-chromophore linkage	GO:0018298	9.55E-04
Proteolysis	MF	serine-type peptidase activity	GO:0008236	1.12E-03
-	BP	negative regulation of platelet-derived growth factor receptor signaling pathway	GO:0010642	1.13E-03
-	BP	negative regulation of protein import into nucleus	GO:0042308	1.13E-03
-	BP	negative regulation of lipoprotein lipid oxidation	GO:0060588	1.13E-03
-	BP	negative regulation of monocyte chemotactic protein-1 production	GO:0071638	1.13E-03
-	BP	negative regulation of cytokine production involved in inflammatory response	GO:1900016	1.13E-03
-	BP	negative regulation of smooth muscle cell-matrix adhesion	GO:2000098	1.13E-03
Motion	BP	negative regulation of T cell migration	GO:2000405	1.13E-03
-	MF	transporter activity	GO:0005215	1.34E-03
Oxidative stress responses	BP	response to oxidative stress	GO:0006979	1.57E-03
Respiration	MF	2 iron, 2 sulfur cluster binding	GO:0051537	1.70E-03
-	MF	sphinganine-1-phosphate aldolase activity	GO:0008117	1.87E-03
-	BP	sphingolipid catabolic process	GO:0030149	1.87E-03
-	CC	extracellular exosome	GO:0070062	2.07E-03
-	MF	D-arabinono-1,4-lactone oxidase activity	GO:0003885	2.11E-03
-	BP	protein repair	GO:0030091	2.22E-03
-	BP	negative regulation of smooth muscle cell	GO:0048662	2.29E-03
-	BP	aging	GO:0007568	2.43E-03
-	BP	tissue regeneration	GO:0042246	2.82E-03
-	MF	ribonuclease T2 activity	GO:0033897	2.91E-03
Respiration	MF	succinate dehydrogenase (ubiquinone) activity	GO:0008177	3.05E-03

Notes: Some GO terms were categorized into 10 categories which were based on their functions. Categories: Actomyosin, Carotene, Cytoskeleton, DNA repair, Motion, Oxidative stress responses, Phagocytosis, Proteolysis, Respiration, V-ATPase. GO, gene ontology; MF, molecular function; CC, cellular component; and BP, biological process. The results shown are based on reproduction by two independent cultures and experiments.

Table 3.5. Continued.

Category	GO term		GO id	*P*-value
Oxidative stress responses	BP	L-ascorbic acid biosynthetic process	GO:0019853	3.65E-03
-	MF	aminomethyltransferase activity	GO:0004047	3.80E-03
-	BP	cobalamin metabolic process	GO:0009235	4.03E-03
Respiration	CC	mitochondrial matrix	GO:0005759	4.07E-03
-	MF	cholesterol binding	GO:0015485	4.29E-03
-	BP	tryptophan catabolic process to kynurenine	GO:0019441	4.51E-03
-	MF	dioxygenase activity	GO:0051213	4.71E-03
-	MF	acyl-CoA dehydrogenase activity	GO:0003995	4.73E-03
-	BP	peripheral nervous system axon regeneration	GO:0014012	5.31E-03
-	BP	metabolic process	GO:0008152	5.74E-03
DNA repair	MF	DNA N-glycosylase activity	GO:0019104	5.88E-03
-	BP	chaperone-mediated protein complex assembly	GO:0051131	6.43E-03
-	MF	ferrous iron binding	GO:0008198	7.68E-03
-	BP	cobalamin biosynthetic process	GO:0009236	7.70E-03
Respiration	BP	glucose metabolic process	GO:0006006	7.77E-03
-	CC	chloroplast thylakoid membrane	GO:0009535	7.80E-03
-	BP	response to drug	GO:0042493	8.70E-03
-	BP	very long-chain fatty acid catabolic process	GO:0042760	9.03E-03
-	BP	nucleotide metabolic process	GO:0009117	1.17E-02
-	BP	cellular protein modification process	GO:0006464	1.18E-02
Oxidative stress responses	BP	response to UV-B	GO:0010224	1.18E-02
-	BP	iron ion homeostasis	GO:0055072	1.24E-02
-	BP	negative regulation of focal adhesion assembly	GO:0051895	1.27E-02
DNA repair	MF	DNA-(apurinic or apyrimidinic site) lyase activity	GO:0003906	1.29E-02
Oxidative stress responses	BP	response to reactive oxygen species	GO:0000302	1.32E-02
-	BP	negative regulation of mitochondrial membrane	GO:0010917	1.34E-02
-	BP	positive regulation of necrotic cell death	GO:0010940	1.34E-02
Respiration	BP	positive regulation of mitochondrial membrane permeability	GO:0035794	1.34E-02
-	BP	stem vascular tissue pattern formation	GO:0010222	1.38E-02
-	BP	cotyledon vascular tissue pattern formation	GO:0010588	1.38E-02
Oxidative stress responses	MF	peroxiredoxin activity	GO:0051920	1.38E-02
-	MF	acid phosphatase activity	GO:0003993	1.40E-02
-	BP	glycine catabolic process	GO:0006546	1.40E-02
-	BP	response to axon injury	GO:0048678	1.44E-02
-	BP	positive regulation of skeletal muscle contraction by regulation of release of sequestered calcium ion	GO:0014810	1.45E-02
Oxidative stress responses	MF	glutathione dehydrogenase (ascorbate) activity	GO:0045174	1.45E-02
-	MF	methylarsonate reductase activity	GO:0050610	1.45E-02
-	BP	positive regulation of ryanodine-sensitive calcium-release channel activity	GO:0060316	1.45E-02
Respiration	BP	protein-FAD linkage	GO:0018293	1.48E-02
-	BP	small molecule metabolic process	GO:0044281	1.49E-02
-	BP	positive phototaxis	GO:0046956	1.50E-02
-	MF	oxidoreductase activity, acting on the CH-OH group of donors, NAD or NADP as acceptor	GO:0016616	1.51E-02
DNA repair	BP	base-excision repair	GO:0006284	1.51E-02
-	MF	phosphatidylinositol transporter activity	GO:0008526	1.51E-02
-	MF	coenzyme binding	GO:0050662	1.52E-02
-	BP	drug metabolic process	GO:0017144	1.65E-02
-	MF	4 iron, 4 sulfur cluster binding	GO:0051539	1.75E-02
-	BP	secondary metabolite biosynthetic process	GO:0044550	1.78E-02
-	MF	insulin-like growth factor-activated receptor activity	GO:0005010	1.85E-02
-	MF	copper ion binding	GO:0005507	1.86E-02
DNA repair	BP	base-excision repair, AP site formation	GO:0006285	1.87E-02
-	MF	organic acid transmembrane transporter activity	GO:0005342	1.88E-02
-	BP	organic acid transport	GO:0015849	1.88E-02
Respiration	BP	NADH metabolic process	GO:0006734	1.89E-02
-	MF	diiodophenylpyruvate reductase activity	GO:0047860	1.89E-02
-	BP	embryonic placenta development	GO:0001892	1.96E-02
-	MF	vitamin E binding	GO:0008431	1.96E-02
-	BP	intermembrane transport	GO:0046909	1.96E-02
-	BP	vitamin transport	GO:0051180	1.96E-02
-	BP	intracellular pH reduction	GO:0051452	1.96E-02

Table 3.5. Continued.

Category	GO term		GO id	*P*-value
-	BP	negative regulation of establishment of blood-brain barrier	GO:0090212	1.96E-02
-	MF	amino acid binding	GO:0016597	2.02E-02
-	MF	sphingosine N-acyltransferase activity	GO:0050291	2.04E-02
-	BP	carboxylic acid metabolic process	GO:0019752	2.06E-02
Proteolysis	BP	misfolded or incompletely synthesized protein catabolic process	GO:0006515	2.06E-02
Respiration	BP	tricarboxylic acid cycle	GO:0006099	2.08E-02
-	MF	NAD binding	GO:0051287	2.09E-02
-	BP	short-chain fatty acid metabolic process	GO:0046459	2.12E-02
-	MF	GTP cyclohydrolase I activity	GO:0003934	2.15E-02
-	BP	7,8-dihydroneopterin 3'-triphosphate biosynthetic process	GO:0035998	2.15E-02
-	MF	phospholipid-translocating ATPase activity	GO:0004012	2.16E-02
-	BP	leaf morphogenesis	GO:0009965	2.19E-02
-	BP	alpha-amino acid metabolic process	GO:1901605	2.22E-02
-	BP	vitamin K metabolic process	GO:0042373	2.24E-02
-	MF	15-hydroxyprostaglandin dehydrogenase (NADP+) activity	GO:0047021	2.24E-02
-	MF	prostaglandin-E2 9-reductase activity	GO:0050221	2.24E-02
-	BP	NAD biosynthetic process	GO:0009435	2.30E-02
Oxidative stress responses	MF	biliverdin reductase activity	GO:0004074	2.37E-02
-	BP	heme catabolic process	GO:0042167	2.37E-02
-	MF	riboflavin reductase (NADPH) activity	GO:0042602	2.37E-02
-	CC	neuronal cell body	GO:0043025	2.37E-02
-	BP	thiamine transport	GO:0015888	2.40E-02
-	CC	plastid	GO:0009536	2.48E-02
Oxidative stress responses	MF	thioredoxin peroxidase activity	GO:0008379	2.52E-02
-	BP	sulfate transport	GO:0008272	2.57E-02
-	MF	sulfate transmembrane transporter activity	GO:0015116	2.57E-02
-	CC	chromosome passenger complex	GO:0032133	2.70E-02
-	MF	oxygen-dependent protoporphyrinogen oxidase	GO:0004729	2.71E-02
-	BP	sucrose transport	GO:0015770	2.74E-02
-	BP	light-independent bacteriochlorophyll biosynthetic process	GO:0036070	2.75E-02
-	BP	root development	GO:0048364	2.78E-02
-	MF	holocytochrome-c synthase activity	GO:0004408	2.78E-02
-	BP	negative regulation of exit from mitosis	GO:0001100	2.81E-02
-	MF	purine nucleosidase activity	GO:0008477	2.81E-02
-	BP	purine-containing compound salvage	GO:0043101	2.81E-02
-	MF	inosine nucleosidase activity	GO:0047724	2.81E-02
-	MF	branched-chain-amino-acid transaminase activity	GO:0004084	2.84E-02
-	BP	branched-chain amino acid biosynthetic process	GO:0009082	2.84E-02
-	MF	L-leucine transaminase activity	GO:0052654	2.84E-02
-	MF	L-valine transaminase activity	GO:0052655	2.84E-02
-	MF	L-isoleucine transaminase activity	GO:0052656	2.84E-02
Respiration	MF	ferrochelatase activity	GO:0004325	2.86E-02
-	BP	negative regulation of striated muscle tissue development	GO:0045843	2.87E-02
Respiration	BP	heme a biosynthetic process	GO:0006784	2.89E-02
-	BP	phototransduction	GO:0007602	2.90E-02
-	CC	subrhabdomeral cisterna	GO:0016029	2.90E-02
-	BP	rhodopsin mediated signaling pathway	GO:0016056	2.90E-02
-	BP	deactivation of rhodopsin mediated signaling	GO:0016059	2.90E-02
-	MF	sarcosine oxidase activity	GO:0008115	2.90E-02
-	BP	L-lysine catabolic process to acetyl-CoA via L-	GO:0033514	2.90E-02
-	MF	L-pipecolate oxidase activity	GO:0050031	2.90E-02
-	MF	carboxy-lyase activity	GO:0016831	2.92E-02
-	MF	L-tyrosine:2-oxoglutarate aminotransferase activity	GO:0004838	2.93E-02
-	BP	cell wall pectin metabolic process	GO:0052546	2.94E-02
DNA repair	MF	DNA (6-4) photolyase activity	GO:0003914	2.94E-02
-	BP	lysine catabolic process	GO:0006554	2.94E-02
-	BP	fatty-acyl-CoA biosynthetic process	GO:0046949	2.94E-02
-	MF	transferase activity, transferring selenium-containing groups	GO:0016785	2.96E-02

Table 3.5. Continued.

Category	GO term		GO id	*P*-value
-	MF	kynurenine 3-monooxygenase activity	GO:0004502	2.97E-02
-	BP	lipopolysaccharide core region biosynthetic process	GO:0009244	2.97E-02
Oxidative stress responses	BP	response to oxygen radical	GO:0000305	2.97E-02
-	BP	response to selenium ion	GO:0010269	2.97E-02
-	MF	chitin synthase activity	GO:0004100	2.98E-02
-	MF	squalene monooxygenase activity	GO:0004506	2.98E-02
-	MF	proline dehydrogenase activity	GO:0004657	2.98E-02
Respiration	CC	mitochondrial respiratory chain complex II, succinate dehydrogenase complex (ubiquinone)	GO:0005749	2.98E-02
-	BP	chitin biosynthetic process	GO:0006031	2.98E-02
-	BP	activation of JNKK activity	GO:0007256	2.98E-02
Oxidative stress responses	MF	L-ascorbate oxidase activity	GO:0008447	2.98E-02
-	BP	procambium histogenesis	GO:0010067	2.98E-02
-	BP	regulation of chlorophyll biosynthetic process	GO:0010380	2.98E-02
-	MF	protein tyrosine kinase activator activity	GO:0030296	2.98E-02
-	MF	trimethylamine monooxygenase activity	GO:0034899	2.98E-02
-	MF	thiamine phosphate phosphatase activity	GO:0042131	2.98E-02
-	BP	adenosine metabolic process	GO:0046085	2.98E-02
-	MF	lysophosphatidic acid phosphatase activity	GO:0052642	2.98E-02
-	BP	positive regulation of adenosine receptor signaling pathway	GO:0060168	2.98E-02
-	BP	positive regulation of protein tyrosine kinase activity	GO:0061098	2.98E-02
-	BP	cell septum assembly	GO:0090529	2.98E-02
-	MF	UDP-glucuronate 5'-epimerase activity	GO:0050379	2.98E-02
Oxidative stress responses	BP	response to UV	GO:0009411	3.02E-02
-	BP	aromatic amino acid family biosynthetic process	GO:0009073	3.04E-02
-	CC	chloroplast	GO:0009507	3.08E-02
Proteolysis	MF	serine-type carboxypeptidase activity	GO:0004185	3.09E-02
-	BP	phospholipid transport	GO:0015914	3.11E-02
-	CC	ATP-binding cassette (ABC) transporter complex	GO:0043190	3.16E-02
-	BP	negative regulation of ryanodine-sensitive calcium-release channel activity	GO:0060315	3.28E-02
-	BP	Golgi vesicle budding	GO:0048194	3.28E-02
-	BP	response to toxic substance	GO:0009636	3.45E-02
-	CC	chloroplast membrane	GO:0031969	3.46E-02
-	BP	cellular nitrogen compound metabolic process	GO:0034641	3.48E-02
-	MF	iron ion binding	GO:0005506	3.51E-02
-	BP	sorocarp morphogenesis	GO:0031288	3.53E-02
-	BP	valine catabolic process	GO:0006574	3.54E-02
Oxidative stress responses	BP	response to redox state	GO:0051775	3.73E-02
Oxidative stress responses	MF	peptide-methionine (S)-S-oxide reductase activity	GO:0008113	3.79E-02
Oxidative stress responses	MF	peroxidase activity	GO:0004601	3.84E-02
-	MF	small protein activating enzyme activity	GO:0008641	3.91E-02
Oxidative stress responses	MF	peptide-methionine (R)-S-oxide reductase activity	GO:0033743	3.95E-02
-	BP	regulation of release of sequestered calcium ion into cytosol by sarcoplasmic reticulum	GO:0010880	3.99E-02
-	MF	2-polyprenyl-6-methoxy-1,4-benzoquinone methyltransferase activity	GO:0008425	4.03E-02
-	MF	3-demethylubiquinone-9 3-O-methyltransferase	GO:0008689	4.03E-02
-	MF	UDP-N-acetylmuramate dehydrogenase activity	GO:0008762	4.05E-02
-	BP	shoot system development	GO:0048367	4.10E-02
-	MF	NADP binding	GO:0050661	4.11E-02
-	CC	cellular bud tip	GO:0005934	4.22E-02
-	CC	cellular bud neck	GO:0005935	4.22E-02
-	CC	mating projection tip	GO:0043332	4.22E-02
-	MF	methylmalonyl-CoA mutase activity	GO:0004494	4.23E-02
-	MF	intramolecular transferase activity	GO:0016866	4.23E-02
-	BP	positive regulation of DNA-templated transcription, elongation	GO:0032786	4.24E-02
-	MF	steroid dehydrogenase activity	GO:0016229	4.31E-02
-	MF	pyridoxal phosphate binding	GO:0030170	4.34E-02
Oxidative stress responses	BP	L-ascorbic acid metabolic process	GO:0019852	4.38E-02
-	BP	chlorophyll biosynthetic process	GO:0015995	4.38E-02
-	BP	oxaloacetate metabolic process	GO:0006107	4.40E-02
-	BP	tetrahydrofolate metabolic process	GO:0046653	4.43E-02

Table 3.5. Continued.

Category	GO term		GO id	*P*-value
Respiration	BP	sucrose metabolic process	GO:0005985	4.44E-02
Respiration	MF	sucrose transmembrane transporter activity	GO:0008515	4.44E-02
-	MF	secondary active sulfate transmembrane transporter activity	GO:0008271	4.46E-02
-	BP	visual perception	GO:0007601	4.54E-02
-	BP	response to retinoic acid	GO:0032526	4.56E-02
-	MF	NAD(P)H oxidase activity	GO:0016174	4.63E-02
-	MF	N-acetylglucosaminyldiphosphodolichol N-acetylglucosaminyltransferase activity	GO:0004577	4.64E-02
-	BP	negative regulation of synaptic transmission, glutamatergic	GO:0051967	4.66E-02
Oxidative stress responses	BP	cellular response to oxidative stress	GO:0034599	4.71E-02
-	BP	ameboidal-type cell migration	GO:0001667	4.73E-02
-	BP	leukotriene metabolic process	GO:0006691	4.74E-02
-	MF	retinoic acid binding	GO:0001972	4.77E-02
-	BP	glomerular basement membrane development	GO:0032836	4.85E-02
-	BP	glomerular visceral epithelial cell development	GO:0072015	4.85E-02
Respiration	MF	glyceraldehyde-3-phosphate dehydrogenase (NADP+) (non-phosphorylating) activity	GO:0008886	4.85E-02
-	BP	response to pH	GO:0009268	4.88E-02
-	MF	phospholipid transporter activity	GO:0005548	4.89E-02
-	BP	phosphate-containing compound metabolic process	GO:0006796	4.93E-02

Table 3.6. Gene ontology terms enriched in down-regulated genes (≥2 fold change) when *Vannella* sp. co-cultured with green *S. elongatus* prey were transferred from dark to light (*P*-value ≤ 0.05).

Category	GO term		GO id	*P*-value
-	BP	peptidyl-lysine demalonylation	GO:0036047	1.34E-03
-	BP	protein desuccinylation	GO:0036048	1.34E-03
-	BP	peptidyl-lysine desuccinylation	GO:0036049	1.34E-03
-	MF	2-hydroxyglutarate dehydrogenase activity	GO:0047545	1.82E-03
Oxidative stress responses	BP	negative regulation of reactive oxygen species metabolic process	GO:2000378	2.78E-03
-	MF	inositol-polyphosphate 5-phosphatase activity	GO:0004445	2.99E-03
-	MF	protein-malonyllysine demalonylase activity	GO:0036054	3.81E-03
-	MF	protein-succinyllysine desuccinylase activity	GO:0036055	3.81E-03
-	MF	inositol-1,4,5-trisphosphate 5-phosphatase activity	GO:0052658	3.89E-03
-	BP	regulation of protein processing	GO:0070613	3.89E-03
-	BP	ribonucleoprotein complex assembly	GO:0022618	3.92E-03
-	BP	protein deacetylation	GO:0006476	4.28E-03
-	BP	poly(A)+ mRNA export from nucleus	GO:0016973	4.75E-03
-	MF	phosphatidylinositol-4,5-bisphosphate 5-phosphatase activity	GO:0004439	5.07E-03
-	BP	sperm motility	GO:0030317	6.87E-03
-	BP	response to other organism	GO:0051707	1.58E-02
-	MF	double-stranded DNA binding	GO:0003690	1.59E-02
-	MF	NAD+ binding	GO:0070403	1.60E-02
Actomyosin	BP	negative regulation of actin filament	GO:0030835	2.16E-02
-	CC	endoplasmic reticulum-Golgi intermediate	GO:0005793	2.25E-02
Respiration	CC	mitochondrial intermembrane space	GO:0005758	2.30E-02
Cytoskeleton	CC	microtubule cytoskeleton	GO:0015630	2.52E-02
Actomyosin	CC	myosin complex	GO:0016459	3.03E-02
Actomyosin	CC	cortical actin cytoskeleton	GO:0030864	3.24E-02
-	BP	phosphatidylinositol dephosphorylation	GO:0046856	3.34E-02
Motion	MF	motor activity	GO:0003774	3.67E-02
-	CC	Golgi apparatus	GO:0005794	4.05E-02
Phagocytosis	CC	phagocytic cup	GO:0001891	4.17E-02
Motion	CC	pseudopodium	GO:0031143	4.55E-02
-	CC	cell leading edge	GO:0031252	4.78E-02
-	MF	RNA binding	GO:0003723	4.83E-02
Phagocytosis	CC	early endosome membrane	GO:0031901	4.96E-02

Notes: Some GO terms were categorized into 10 categories which were based on their functions. Categories: Actomyosin, Carotene, Cytoskeleton, DNA repair, Motion, Oxidative stress responses, Phagocytosis, Proteolysis, Respiration, V-ATPase. GO, gene ontology; MF, molecular function; CC, cellular component; and BP, biological process. The results shown are based on reproduction by two independent cultures and experiments.

Chapter 4. General discussion

Establishment of an experimental system to examine the effect of photosynthetic traits of prey on herbivorous unicellular organisms

Chloroplasts in algae and plants were established by endosymbiotic events in which a cyanobacterium or unicellular eukaryotic algae were integrated into previously non-photosynthetic eukaryotes (Rodriguez-Ezpeleta and Philippe 2006; Gould *et al.* 2008). The acquisition of chloroplasts has enabled the eukaryotic cells to proliferate autotrophically by performing photosynthesis. However, excitation of photosynthetic pigments (e.g. chlorophylls) and electron flow in the photosystems inevitably generate ROS which damage the cells (Asada 2006; Pospisil 2009). Thus, algae and plants have developed various mechanisms to reduce ROS generation, quench ROS, and repair biomolecules damaged by the photosynthetic oxidative stress (Pospíšil 2012; Sharma *et al.* 2012). It is well believed that existence of such mechanisms to cope with the photosynthetic oxidative stress were prerequisites for eukaryotic cells to perform photosynthesis. However, I thought that this is probably also the case for non-photosynthetic eukaryotes that accommodate temporal/facultative photosynthetic endosymbionts and further unicellular transparent eukaryotes that feed on photosynthetic preys. When such unicellular organisms engulf photosynthetic preys in the daytime, the engulfed preys are illuminated and thus photosystems probably operate. In particular, unregulated photosynthetic electron transfer and excitation of photosynthetic pigments detached from photosystems probably occur during digestion, which in turn produce higher levels of ROS inside the predator cells.

Based on the assumption, the aim of this study was to examine whether feeding on photosynthetic preys under illumination exposes unicellular predators to oxidative stress, and if that is the case, how the predators cope with the photosynthetic oxidative

stress. It is generally believed that chloroplasts have been established through phagotrophy and temporary (kleptoplasty) retention of photosynthetic prey and then facultative and ultimately obligate endosymbiotic relationship with photosynthetic preys by unicellular eukaryotes (Rodriguez-Ezpeleta and Philippe 2006). Thus, results of this study should yield important insights into the understanding of the evolutionary course in the establishment of photosynthetic eukaryotes as well as understanding of impacts of photosynthesis in microbial communities in ecosystems.

Because there have been no studies to examine the effects of photosynthesis of prey on predators, I newly established an experimental system. As unicellular predators, three species of amoebae (*Naegleria* sp., *Acanthamoeba* sp. and *Vannella* sp.) feeding on algae were isolated from a marsh (Figure 2.1A-C). Because these species are evolutionally distantly related, examination of them contributes to understanding of generality and diversity in effects of photosynthetic preys and mechanisms to cope with the photosynthetic oxidative stress. In addition, these three amoebae are able to feed on both photosynthetic and non-photosynthetic preys, comparison of behaviors between amoebae feeding on photosynthetic prey and non-photosynthetic prey is feasible. These characteristics facilitate determining whether respective responses are specific to photosynthetic traits of preys. As preys, I prepared the normal cyanobacterium *S. elongatus* (green) and pale *S. elongatus*, in which photosynthetic pigments were reduced, to examine the effect of photosynthetic traits of prey on predators. To examine the effect of free chlorophylls, *E. coli* stained with chlorophyll *a* was also prepared. In addition, to distinguish the responses by amoebae to the light stimulus itself and phototoxicity of the prey and to examine the effects of exogenous ROS on amoebae, I developed a procedure to grow amoebae in an organic medium without preys. All of these traits of

amoebae and experimental setups efficiently facilitated this study as a first step to address the effects of photosynthetic preys on unicellular predators and response by predators to the effects. With modifications, the experimental systems will be applicable to many other predators such as amoebae that thrive in other environments (e.g. seawater), ciliates and heterotrophic dinoflagellates.

Phototoxicity of photosynthetic prey and responses of amoebae to the photosynthetic oxidative stress

The first question of the study was whether feeding on photosynthetic preys under illumination exposes unicellular predators to oxidative stress. The results of this study showed that photosynthetic preys are phototoxic as expected and this toxicity is at least based on photosynthetic oxidative stress as below. *Naegleria* sp. feeding on the green *S. elongatus* prey, but not the pale prey, under high light condition (500 μE m^{-2} s^{-1}) exhibited cell death (Figure 2.2A, D). In addition, genes related to oxidative stress responses (Figure 3.3, Oxidative stress response) and DNA-repair (Figure 3.3, DNA repair) were upregulated upon illumination in all the three species of amoebae feeding on the photosynthetic prey. Majority of these genes were upregulated in amoebae feeding on the green prey but not in amoebae feeding on the pale prey.

The responses by amoebae to the photosynthetic oxidative stress that is given by prey revealed two phenomena that probably reduce the level of stress. When the three species of amoebae feeding on the green prey was illuminated, genes related to phagocytosis, including actin and myosin, were downregulated (Figure 3.3, myosin, actin; Table 3.2, *Naegleria* sp.; Table 3.4, *Acanthamoeba* sp.; Table 3.6, *Vannella* sp.). In addition, mRNA of type II myosin, which is involved in phagocytosis (Olazabal *et al.*

2002; Chandrasekar *et al.* 2014), was downregulated when *Naegleria* sp. fed on *E. coli* stained with chlorophyll *a* or they were treated with RB (under illumination) or H_2O_2 (under dark) (Figure 3.1D), suggesting that the downregulation was triggered by photosynthetic oxidative stress. Further, reduction of phagocytic activity upon illumination was observed in *Naegleria* sp. feeding on the green prey but not pale prey (Figure 3.2A and B). In addition to the down-regulation of phagocytic uptake of prey, acceleration of digestion of already engulfed prey upon illumination was observed in *Naegleria* sp. (Figure 3.2C and D). Both of these responses result in reduction of photosynthetic prey in the amoeba cells and thus reduction of photosynthetic oxidative stress under light condition (Figure 4).

In this regard, in a similar manner to the amoebae, it has been shown that green paramecium (*Paramecium bursaria*) starts to excrete endosymbiotic *Chlorella* spp. (green algae) when they are exposed to high light or treated with methyl viologen (Paraquat) which induces production of high level of ROS from photosystems under illumination (Kawano *et al.* 2010; Lowe *et al.* 2016) (Figure 4). In addition, in several species of corals, it is thought that the host cnidarian cells expel endosymbiotic dinoflagellate algae, and results in coral bleaching when they are exposed to high light or high temperature, which probably elevates oxidative stress (Weis 2008) (Figure 4). Thus, it is suggested that the cancellation of endosymbiotic relationships observed in organisms that accommodate facultative photosynthetic endosymbionts would have been already developed in their heterotrophic ancestors that fed on algae.

Such strategies to get rid of photosynthetic preys from the cells are impossible in the case of obligate endosymbiotic associations such as the chloroplast in algae and plants. However, it is known that some algae possess abilities to escape from high light

by swimming (Witman 1993) or gliding (Trojánková and Přibyl 2006) and that sessile land plants are able to relocate their chloroplasts in the cells to minimize light absorption by photosystems under high light condition (Wada *et al.* 2003) (Figure 4). In addition, algae and plants reduce chlorophylls in the chloroplast under high light condition to reduce absorption of excess light energy (Smith *et al.* 1990). Thus, although the mechanisms are different between obligate endosymbiotic relationships and other relationships, reduction of light absorption by photosystems is common strategy to reduce photosynthetic oxidative stress in obligate and facultative endosymbiotic associations and the relationship between unicellular predators and photosynthetic prey. In addition, it is suggested that the mechanisms escaping from high light and relocating chloroplasts were important for emergence and evolution of eukaryotic algae, which always possess chloroplasts, and sessile land plants.

In addition to the reduction of uptake of prey and acceleration of digestion of already engulfed prey, three species of amoebae feeding on the green prey exhibited several similar changes in the transcriptome upon illumination (Figure 3.3; Table 3.1, *Naegleria* sp.; Table 3.3, *Acanthamoeba* sp.; Table 3.5, *Vannella* sp.). As already known in algae (Huang *et al.* 2006) and plants (Rossel *et al.* 2002; Zhao *et al.* 2016) when they were exposed to high light, mRNA encoding proteins involved in oxidative stress responses (e.g. several “redoxin” proteins, proteins related to glutathione oxidation/reduction), DNA repair and carotenoid synthesis were upregulated. Carotenoids are known to dissipate ROS in algae and plants (Ramel *et al.* 2012) but further studies will be required in the case of amoebae, such as quantification of carotenoids and examination of their functions in amoebae.

Besides these responses, several other changes in the transcriptome upon illumination were observed as follows. Although the exact significance of these changes is unclear at this point, these changes were commonly observed in the three species of amoebae. Thus further studies on them will give further insights into the responses of predators to photosynthetic traits of prey. Genes related to respiration and genes encoding several monooxygenases, which consume oxygen in metabolisms, were upregulated upon illumination in all the three species of amoebae feeding on the green prey (Figure 3.3, oxygen reducing metabolism; Table 3.1, *Naegleria* sp.; Table 3.3, *Acanthamoeba* sp.; Table 3.5, *Vannella* sp.). These responses likely result in reduction of oxygen that is generated by photosystems and thus reduction of ROS generation in amoeba cells. Genes encoding components of v-ATPase, which acidify lysosomes and phagosomes, are upregulated raising the possibility that the acidification of phagosomes is related to the acceleration of digestion of the green prey upon illumination.

Although not addressed in this study, existence of the detoxification system of chlorophyll *a* was proposed in aquatic ecosystems. This proposal is based on the accumulation of the non-phototoxic chlorophyll *a* catabolite (13^2,17^3-cyclopheophorbide *a* enol) in cultures of a variety of herbivorous protists or in various types of aquatic environments (Kashiyama *et al.* 2012). The chlorophyll *a* detoxification system is suggested to be independent from the already known degradation process of chlorophylls in land plants (Hörtensteiner and Kräutler 2011) based on a predicted metabolic process (Kashiyama *et al.* 2013). However, the exact detoxification process and enzymes that are involved in the process are still not known. In this regard, the co-cultivation system developed in this study and the transcriptome data will give hints to address the mechanisms.

Future perspectives

Based on this study, I propose that the low uptake and rapid digestion of photosynthetic prey is one of the strategies to cope with the phototoxicity of photosynthetic prey and that this removal strategy was shifted to escaping strategy when eukaryotic cells started to accommodate photosynthesis (chloroplasts or obligate photosynthetic endosymbiont) permanently. In addition, several other possible responses to photosynthetic oxidative stress were suggested based on the transcriptome changes and these changes were common to all the three species of amoebae examined. These three species of amoebae are evolutionally distantly related thus suggesting the importance of these mechanisms for predators to feed on photosynthetic preys. However, the three species of amoebae were isolated from the same environment and thus it is still possible that the similarity in the responses to photosynthetic prey resulted from convergent adaptation of these amoebae to that environment. In order to further assess the generality in the evolution of predators to herbivorous ones and evolution of endosymbiotic relationships, studies of other organisms are required. These will be herbivorous seawater amoebae and herbivorous unicellular organisms other than amoebae such as ciliates and heterotrophic dinoflagellates. In addition, studies on predators that feed only on specific algal species and comparison of evolutionally closely related predators and the cells accommodating photosynthetic endosymbionts are also desired. In this regard, studies of the green amoeba (*Mayorella* sp., Amoebozoa) will be one candidate for comparison to the results of this study.

As far as I know, this study is the first to show that phototoxicity of photosynthesis affects on other non-photosynthetic organisms. In this study, I focused on the relationship between the predators and preys inside them. However, the

photosynthesis in microorganisms likely affects on adjacent non-photosynthetic microorganisms in nature especially in biofilms in which several kinds of microorganisms exist at high density. Thus, the results of this and further studies will be also important to understanding of ecosystems of microorganisms in future.

Figure

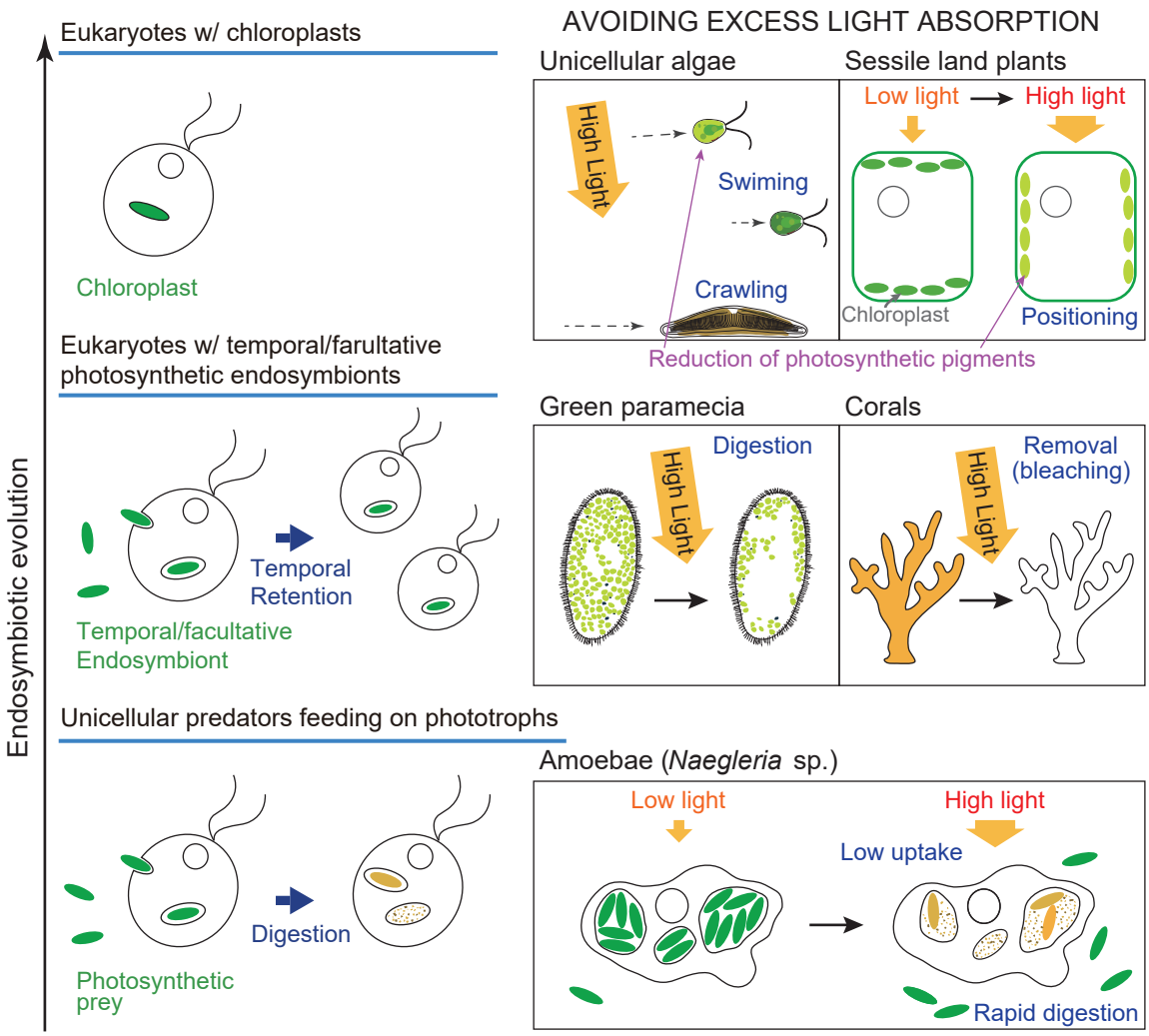

Figure 4. Comparison of mechanisms to reduce light absorption by photosystems in predators, facultative phototrophs, and algae and plants.

When the photosystems absorb excess light energy, ROS production is elevated. When eukaryotic algae are exposed to high light, they escape form light by swimming or crawling to reduce absorption of excess light energy by photosystems. When land plants are exposed to high light, the leaf cell changes the positioning of chloroplasts to reduce light absorption by photosystems. Reduction of photosynthetic pigments also occurs in algae and plants to reduce light absorption. Regarding facultative phototrophs, when the green paramecium is exposed to high light or reactive oxygen species, they digest endosymbionts. When the coral is exposed to high light, it removes the photosynthetic endosymbionts from the cells. Regarding herbivorous predators, my study showed that amoebae reduces uptake of photosynthetic prey whereas accelerates digestion of photosynthetic prey that have been engulfed under illumination.

Acknowledgements

First of all, I would like to express my sincere gratitude to Dr. Shin-ya Miyagishima (National Institute of Genetics, SOKENDAI) for his encouragements, suggestions, giving me the opportunity to study in his laboratory and for all aspects as my supervisor during this study.

I am extremely grateful to Dr. Tetsuji Kakutani (National Institute of Genetics, SOKENDAI, University of Tokyo), Dr. Takuji Iwasato (National Institute of Genetics, SOKENDAI), Dr. Tatsumi Hirata (National Institute of Genetics, SOKENDAI) and Dr. Yasukazu Nakamura (National Institute of Genetics, SOKENDAI) for many suggestions and encouragements as the progress report committee members for D4 and D5.

I am also extremely grateful to Dr. Takayuki Fujiwara (National Institute of Genetics, SOKENDAI) for supporting isolation of amoebae, kind suggestions and many encouragements, Dr. Shunsuke Hirooka (National Institute of Genetics) for technical guidance for extraction of mRNA of amoebae, and kind instruction for analyses of RNA-seq data and many encouragements, Dr. Yu Kanesaki (Tokyo University of Agriculture), and Dr. Hirofumi Yoshikawa (Tokyo University of Agriculture) for sequencing of all RNA samples, Dr. Yuichiro Kashiyama (Fukui University of Technology) for kind advices and encouragements, the current members of our laboratory, Dr. Ryo Onuma (National Institute of Genetics), Dr. Ryudo Ohbayashi (National Institute of Genetics), Dr. Yusuke Kobayashi (National Institute of Genetics), Ms. Jong Lin Wei (National Institute of Genetics), Ms. Kiyomi Hashimoto (National Institute of Genetics), Ms. Yoshiko Tanaka (National Institute of Genetics) for helpful advises, many encouragements, and their kind supports, Dr. Masato Kanemaki (National Institute of Genetics, SOKENDAI) and Dr. Toyoaki Natsume (National Institute of Genetics, SOKENDAI) for their kind guidance about cell sorter and

encouragements, Dr. Emiko Suzuki (National Institute of Genetics, SOKENDAI), Dr. Naruya Saitou (National Institute of Genetics, SOKENDAI, University of Tokyo) and Dr. Ryu Ueda (National Institute of Genetics, SOKENDAI) for many suggestions and encouragements as the former progress report committee members for D2. I also thank the former members of our laboratory, Dr. Yukihiro Kabeya, Dr. Nobuko Sumiya, Dr. Atsuko Era, Ms. Mami Nakamura, Ms. Akiko Yamashita, Ms. Tomomi Nakayama, and Dr. Chiharu Nagai for kind encouragements and their supports. Finally, I really thank to my family for their supports and encouragements.

A part of this research was performed using “DDBJ Read Annotation Pipeline". This study was supported by Japan Society for the Promotion of Science (JSPS) KAKENHI (JP17J08575 to A. U.).

References

Abramoff M.D., Magalhães P. J., Ram S. J. 2004. Image processing with ImageJ. *BIOPHOTONICS*. 11: 36-43.

Ahmad P., Jaleel C. A., Salem M. A., Nabi G., Sharma S. 2010. Roles of enzymatic and nonenzymatic antioxidants in plants during abiotic stress. *Crit. Rev. Biotechnol.* 30: 161-175.

Allen M. B. 1959. Studies with *Cyanidium caldarium*, an anomalously pigmented chlorophyte. *Archiv für Mikrobiologie*. 32: 270-277.

Allen M. M. 1968. Simple conditions for growth of unicellular blue-green algae on plates1, 2. *J. Phycol.* 4: 1-4.

Arnon D. I., McSwain B. D., Tsujimoto H. Y., Wada K. 1974. Photochemical activity and components of membrane preparations from blue-green algae. I. Coexistence of two photosystems in relation to chlorophyll *a* and removal of phycocyanin. *Biochim. Biophys. Acta.* 357: 231-245.

Artal-Sanz M., Tavernarakis N. 2009. Prohibitin and mitochondrial biology. *Trends Endocrinol. Metab.* 20: 394-401.

Arthur J. R. 2000. The glutathione peroxidases. *Cell. Mol. Life Sci.* 57: 1825-1835.

Asada K. 2006. Production and scavenging of reactive oxygen species in chloroplasts and their functions. *Plant Physiol.* 141: 391-396.

Barros M. H., Carlson C. G., Glerum D. M., Tzagoloff A. 2001. Involvement of mitochondrial ferredoxin and Cox15p in hydroxylation of heme O. *FEBS Letters*. 492: 133-138.

Bartley G. E., Scolnik P. A. 1995. Plant carotenoids: pigments for photoprotection, visual attraction, and human health. *Plant Cell*. 7: 1027-1038.

Bartley G. E., Scolnik P. A., Beyer P. 1999. Two *Arabidopsis thaliana* carotene desaturases, phytoene desaturase and zeta-carotene desaturase, expressed in *Escherichia coli*, catalyze a poly-*cis* pathway to yield pro-lycopene. *Eur. J. Biochem.* 259: 396-403.

Bohley P., Seglen P. O. 1992. Proteases and proteolysis in the lysosome. *Experientia*. 48: 151-157.

Buss F., Luzio J. P., Kendrick-Jones J. 2002. Myosin VI, an actin motor for membrane traffic and cell migration. *Traffic*. 3: 851-858.

Chandrasekar I., Goeckeler Z. M., Turney S. G., Wang P., Wysolmerski R. B., Adelstein R. S., Bridgman P. C. 2014. Nonmuscle myosin II is a critical regulator of clathrin-mediated endocytosis. *Traffic*. 15: 418-432.

Darie S., Gunsalus R. P. 1994. Effect of heme and oxygen availability on *hemA* gene expression in *Escherichia coli*: role of the *fnr*, *arcA*, and *himA* gene products. *J. Bacteriol.* 176: 5270-5276.

DellaPenna D., Pogson B. J. 2006. Vitamin synthesis in plants: Tocopherols and carotenoids. *Annu. Rev. Plant Biol.* 57: 711-738.

Fields S. D., Rhodes R. G. 1991. Ingestion and retention of *Chroomonas* spp. (Cryptophyceae) by *Gymnodinium acidotum* (Dinophyceae). *J. Phycol.* 27: 525-529.

Gorl M., Sauer J., Baier T., Forchhammer K. 1998. Nitrogen-starvation-induced chlorosis in *Synechococcus* PCC 7942: adaptation to long-term survival. *Microbiol.* 144: 2449-2458.

Goss R., Lepetit B. 2015. Biodiversity of NPQ. *J. Plant Physiol.* 172: 13-32.

Gould S. B., Waller R. F., McFadden G. I. 2008. Plastid evolution. *Annu. Rev. Plant. Biol.* 59: 491-517.

Grabherr M. G., Haas B. J., Yassour M., Levin J. Z., Thompson D. A., Amit I., Adiconis X., Fan L., Raychowdhury R., Zeng Q., Chen Z., Mauceli E., Hacohen N., Gnirke A., Rhind N., di Palma F., Birren B. W., Nusbaum C., Lindblad-Toh K., Friedman N., Regev A. 2011. Full-length transcriptome assembly from RNA-seq data without a reference genome. *Nat. Biotechnol.* 29: 644-652.

Grimme L. H., Boardman N. K. 1972. Photochemical activities of a particle fraction P 1 obtained from the green alga *Chlorella fusca*. *Biochem. Biophys. Res. Commun.* 49: 1617-1623.

Guha S., Padh H. 2008. Cathepsins: fundamental effectors of endolysosomal proteolysis. *Indian J. Biochem. Biophys.* 45: 75-90.

Halliwell B., Gutteridge John M. C. 1990. [1] Role of free radicals and catalytic metal ions in human disease: An overview. *Methods in Enzymology* (Academic Press).

Hasson T. 2003. Myosin VI: two distinct roles in endocytosis. *J. Cell Sci.* 116: 3453-3461.

Hörtensteiner S., Kräutler B. 2011. Chlorophyll breakdown in higher plants. *BBA - Bioenergetics*. 1807: 977-988.

Huang J. C., Chen F., Sandmann G. 2006. Stress-related differential expression of multiple beta-carotene ketolase genes in the unicellular green alga *Haematococcus pluvialis*. *J. Biotechnol.* 122: 176-185.

Johnson M. D., Tengs T., Oldach D., Stoecker D. K. 2006. Sequestration, performance, and functional control of cryptophyte plastids in the ciliate *Myrionecta rubra* (Ciliophora). *J. Phycol.* 42: 1235-1246.

Johnson M. P. 2016. Photosynthesis. *Essays in Biochemistry*. 60: 255-273.

Kaminuma E., Mashima J., Kodama Y., Gojobori T., Ogasawara O., Okubo K., Takagi T., Nakamura Y. 2010. DDBJ launches a new archive database with analytical tools for next-generation sequence data. *Nucleic Acids Res.* 38: D33-38.

Kashiyama Y., Yokoyama A., Kinoshita Y., Shoji S., Miyashiya H., Shiratori T., Suga H., Ishikawa K., Ishikawa A., Inouye I., Ishida K., Fujinuma D., Aoki K., Kobayashi M., Nomoto S., Mizoguchi T., Tamiaki H. 2012. Ubiquity and quantitative significance of detoxification catabolism of chlorophyll associated with protistan herbivory. *PNAS*. 109: 17328-17335.

Kashiyama Y., Yokoyama A., Shiratori T., Inouye I., Kinoshita Y., Mizoguchi T., Tamiaki H. 2013. 13^2,17^3-Cyclopheophorbide *b* enol as a catabolite of chlorophyll *b* in phycophagy by protists. *FEBS Letters*. 587: 2578-2583.

Kawano T., Irie K., Kadono T. 2010. Oxidative stress-mediated development of symbiosis in green paramecia. Joseph Seckbach and Martin Grube (eds.), *Symbioses and Stress: Joint Ventures in Biology* (Springer Netherlands: Dordrecht).

Keeling P. J. 2010. The endosymbiotic origin, diversification and fate of plastids. *Phil. Trans. R. Soc. B*. 365: 729-748.

Kochevar I. E., Redmond R. W. 2000. [2] Photosensitized production of singlet oxygen. *Methods in Enzymology* (Academic Press).

Krieger-Liszkay A. 2005. Singlet oxygen production in photosynthesis. *J. Exp. Bot.* 56: 337-346.

Langmead B., Salzberg S. L. 2012. Fast gapped-read alignment with Bowtie 2. *Nat. meth.* 9: 357-359.

Lewitus A. J., Glasgow H. B., Burkholder J. M. 1999. Kleptoplastidy in the toxic dinoflagellate *Pfiesteria piscicida* (Dinophyceae). *J. Phycol.* 35: 303-312.

Li B., Dewey C. N. 2011. RSEM: accurate transcript quantification from RNA-seq data with or without a reference genome. *BMC Bioinform.* 12: 323.

Lowe C. D., Minter E. J., Cameron D. D., Brockhurst M. A. 2016. Shining a light on exploitative host control in a photosynthetic endosymbiosis. *Curr. Biol.* 26: 207-211.

Marin B., Nowack E. C., Melkonian M. 2005. A plastid in the making: evidence for a second primary endosymbiosis. *Protist*. 156: 425-432.

Miao Q., Sun Y., Wei T., Zhao X., Zhao K., Yan L., Zhang X., Shu H., Yang F. 2008. Chymotrypsin B cached in rat liver lysosomes and involved in apoptotic regulation through a mitochondrial pathway. *J. Biol. Chem.* 283: 8218-8228.

Mokranjac D., Sichting M., Neupert W., Hell K. 2003. Tim14, a novel key component of the import motor of the TIM23 protein translocase of mitochondria. *EMBO*. 22: 4945-4956.

Moon-van der Staay S. Yeo, van der Staay G. W. M., Guillou L., Vaulot D., Claustre H., Medlin L. K. 2000. Abundance and diversity of prymnesiophytes in the picoplankton community from the equatorial Pacific Ocean inferred from 18S rDNA sequences. *Limnol. Oceanogr.* 45: 98-109.

Mooren O. L., Galletta B. J., Cooper J. A. 2012. Roles for actin assembly in endocytosis. *Annu. Rev. Biochem.* 81: 661-686.

Nagasaki H., Mochizuki T., Kodama Y., Saruhashi S., Morizaki S., Sugawara H., Ohyanagi H., Kurata N., Okubo K., Takagi T., Kaminuma E., Nakamura Y. 2013. DDBJ read annotation pipeline: a cloud computing-based pipeline for high-throughput analysis of next-generation sequencing data. *DNA Res.* 20: 383-390.

Niyogi K. K. 2000. Safety valves for photosynthesis. *Curr. Opin. Plant Biol.* 3: 455-460.

Olazabal I. M., Caron E., May R. C., Schilling K., Knecht D. A., Machesky L. M. 2002. Rho-kinase and myosin-II control phagocytic cup formation during CR, but not FcγR, phagocytosis. *Curr. Biol.* 12: 1413-1418.

Pospíšil P. 2012. Molecular mechanisms of production and scavenging of reactive oxygen species by photosystem II. *BBA - Bioenergetics*. 1817: 218-231.

Pospisil P. 2009. Production of reactive oxygen species by photosystem II. *Biochim. Biophys. Acta.* 1787: 1151-1160.

Ramel F., Birtic S., Cuiné S., Triantaphylidès C., Ravanat J., Havaux M. 2012. Chemical quenching of singlet oxygen by carotenoids in plants. *Plant Physiol.* 158: 1267-1278.

Rippka R., Deruelles J., Waterbury J. B., Herdman M., Stanier R. Y. 1979. Generic assignments, strain histories and properties of pure cultures of cyanobacteria. *Microbiol.* 111: 1-61.

Robinson M. D., McCarthy D. J., Smyth G. K. 2010. edgeR: a Bioconductor package for differential expression analysis of digital gene expression data. *Bioinformatics*. 26: 139-140.

Rodriguez-Ezpeleta N., Brinkmann H., Burey S. C., Roure B., Burger G., Loffelhardt W., Bohnert H. J., Philippe H., Lang B. F. 2005. Monophyly of primary photosynthetic eukaryotes: green plants, red algae, and glaucophytes. *Curr. Biol.* 15: 1325-1330.

Rodriguez-Ezpeleta N., Philippe H. 2006. Plastid Origin: Replaying the Tape. *Curr. Biol.* 16: R53-56.

Rossel J. B., Wilson I. W., Pogson B. J. 2002. Global changes in gene expression in response to high light in Arabidopsis. *Plant Physiol.* 130: 1109-1120.

Ruban A. V. 2012. *The photosynthetic membrane: molecular mechanisms and biophysics of light harvesting* (Wiley-Blackwell: Chichester).

Schiller D., Cheng Y. C., Liu Q., Walter W., Craig E. A. 2008. Residues of Tim44 Involved in both association with the translocon of the Inner mitochondrial membrane and regulation of mitochondrial Hsp70 tethering. *Mol. Cell. Biol.* 28: 4424-4433.

Sharma P., Jha A. B., Dubey R. S., Pessarakli M. 2012. Reactive oxygen species, oxidative damage, and antioxidative defense mechanism in plants under stressful conditions. *Journal of Botany*. 2012: 1-26.

Smith B. M., Morrissey P. J., Guenther J. E., Nemson J. A., Harrison M. A., Allen J. F., Melis A. 1990. Response of the photosynthetic apparatus in *Dunaliella salina* (green algae) to irradiance stress. *Plant Physiol.* 93: 1433-1440.

Smythe E., Ayscough K. R. 2006. Actin regulation in endocytosis. *J. Cell Sci.* 119: 4589-4598.

Stoecker D. K. 1999. Mixotrophy among dinoflagellates. *J. Eukaryot. Microbiol.* 46: 397-401.

Szymanska R., Strzalka K. 2010. Reactive oxygen species in plants--production, deactivation and role in signal transduction. *Postepy Biochem.* 56: 182-190.

Tanabe A. S. 2011. Kakusan4 and Aminosan: two programs for comparing nonpartitioned, proportional and separate models for combined molecular phylogenetic analyses of multilocus sequence data. *Mol. Ecol. Resour.* 11: 914-921.

Toei M., Saum R., Forgac M. 2010. Regulation and isoform function of the v-ATPases. *Biochemistry*. 49: 4715-4723.

Triantaphylides C., Havaux M. 2009. Singlet oxygen in plants: production, detoxification and signaling. *Trends Plant Sci*. 14: 219-228.

Trojánková K., Přibyl P. 2006. Negative photomovements of desmid *Micrasterias rotata* as response to strong light. *Czech Phycol.* 6: 135-142.

Velayos A., Eslava A. P., Iturriaga E. A. 2000. A bifunctional enzyme with lycopene cyclase and phytoene synthase activities is encoded by the *carRP* gene of *Mucor circinelloides*. *Eur. J. Biochem.* 267: 5509-5519.

Wada M., Kagawa T., Y. Sato. 2003. Chloroplast movement. *Annu. Rev. Plant Biol.* 54: 455-468.

Wakabayashi K., Misawa Y., Mochiji S., Kamiya R. 2011. Reduction-oxidation poise regulates the sign of phototaxis in *Chlamydomonas reinhardtii*. *PNAS*. 108: 11280-11284.

Weis V. M. 2008. Cellular mechanisms of cnidarian bleaching: stress causes the collapse of symbiosis. *J. Exp. Biol.* 211: 3059-3066.

Witman G. B. 1993. Chlamydomonas phototaxis. *Trends Cell Biol.* 3: 403-408.

Yoon O. K., Brem R. B. 2010. Noncanonical transcript forms in yeast and their regulation during environmental stress. *Rna*. 16: 1256-1267.

Young M. D., Wakefield M. J., Smyth G. K., Oshlack A. 2010. Gene ontology analysis for RNA-seq: accounting for selection bias. *Genome Biol.* 11: R14.

Zhao H., Lou Y., Sun H., Li L., Wang L., Dong L., Gao Z. 2016. Transcriptome and comparative gene expression analysis of *Phyllostachys edulis* in response to high light. *BMC Plant Biology*. 16: 34.